UNIVERSITÀ
DEGLI STUDI
DI BRESCIA

UNIVERSITÀ DEGLI STUDI DI BRESCIA

DOTTORADO DI RICERCA IN

SCIENZE BIOMEDICHE E MEDICINA TRASLAZIONALE

CICLO: XXXIV

ANTI-INFLAMMATORY PROPERTIES OF PDE4 INHIBITION IN SARS-COV-2-ACTIVATED HUMAN DENDRITIC CELLS

DOTTORANDA
NGUYEN HOANG OANH

RELATORE
Prof.ssa DANIELA BOSISIO

NOME DEL COORDINATORE DEL DOTTORATO
Chiar.ma Prof. MARIACRISTINA MISSALE

ABSTRACT

Dysfunctional immune response and hyper-inflammation with subsequent cytokine storm were shown to play a key role in the development of severe and fatal forms of Coronavirus disease 2019 (COVID-19). This clinical condition suggests that an overactive innate immune response may unleash virus-dependent immune pathology. Here, we described a novel mechanism of SARS-CoV-2-dependent activation of dendritic cells (DCs), based on the recognition of sequences of viral genomic ssRNA (SCV2-RNA) by endosomal pattern recognition receptors, namely TLR7 and TLR8. Importantly, SCV2-RNA recapitulated potent lung inflammation in vivo as shown by accumulation of proinflammatory mediators and immune cell infiltration; and induced a strong release of pro-inflammatory cytokines and Th1 polarization in vitro.

Tanimilast is a novel and selective inhaled inhibitor of phosphodiesterases 4 that is in advanced clinical development for the treatment of chronic obstructive pulmonary disease and could prove beneficial in severe COVID-19 pneumonia. In our experimental setting, the potent activation of DCs by SCV2-RNA was severely blunted by Tanimilast, which decreased the release of pro-inflammatory cytokines (TNF-α and IL-6), chemokines (CCL3, CXCL9, and CXCL10) and of Th1-polarizing cytokines (IL-12, type I IFNs). However, Tanimilast did not impair the acquisition of the maturation markers CD83, CD86, HLA-DR and CCR7. Consistent with this, Tanimilast did not reduce the capability of activated DCs to activate $CD4^+$ T cells but skewed their polarization towards a Th2 phenotype. In addition, Tanimilast blocked the increase of HLA class I molecules and restrained the proliferation and activation of cytotoxic $CD8^+$ T cells accordingly. The immune-modulatory effects of Tanimilast were further demonstrated by its capacity to enhance cAMP-dependent immunosuppressive molecules such as IDO1, TSP1, VEGFA and Amphiregulin in LPS-stimulated DCs. These cells also strongly upregulated CD141 and displayed increased uptake of dead cells.

Altogether, our results indicate that Tanimilast induce mature DCs to acquire immunomodulatory properties as well as a distinct semi-mature phenotype, associated with the prominent expression of CD141, thus proposing Tanimilast as a promising immunomodulatory drug for the treatment in inflammatory or immune-mediated diseases, possibly including severe COVID-19 pneumonia.

INDEX

INTRODUCTION

1. Severe acute respiratory syndrome coronavirus 2 (SARS-CoV-2) infection

1.1 Overview of SARS-CoV-2 infection

SARS-CoV-2 is enveloped, positive-sense, ssRNA virus, belonging the subfamily Coronavirinae in the family Coronaviridae of the order Nidovirales (1). It was first identified as the causative pathogen of the pneumonia outbreak in Wuhan China in December 2019. World Health Organization (WHO) designated COVID-19 as SARS-CoV-2 infection and later announced the pandemic in March 2020. As of now, COVID-19 has spread over 200 countries with more than 200 million infected cases and 5 million deaths, making it become one of the deadliest diseases of our time. Indeed, SARS-CoV-2 is highly contagious due to its easy and rapid modes of transmission through fomites and droplets during a close contact with an infected person (2) (Figure 1). Other transmission occurs via aerosols and possibly fecal-oral route, and mother to child. The incubation period of COVID-19 is rather large ranging from 2 to 14 days. However, longer incubation time up to 21 days was also reported (3). Much of evidence revealed that nearly half of SARS-CoV-2 infection was alternatively caused by asymptomatic persons who can transmit the virus for an extended period, even more than 14 days (4,5). In addition, the high mutagenic capacity renders SARS-CoV-2 more infectious and virulent to the host and attributes to the continual outbreaks in many countries.

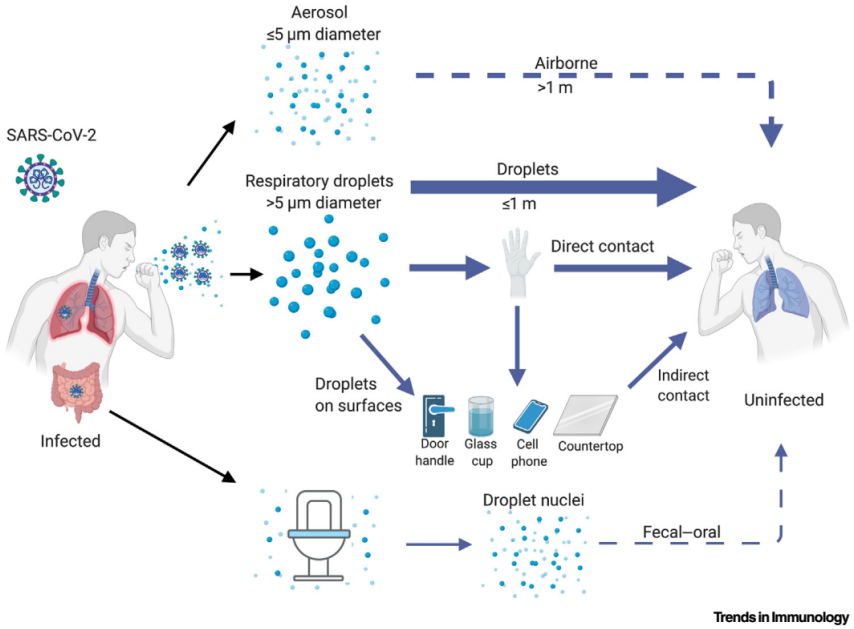

Figure 1. Proposed SARS-CoV-2 transmission routes (2)

Clinical presentation

The clinical presentation of COVID-19 is widely varied ranging from non to life threatening conditions (2) (Figure 2). The most common manifestations are fever, fatigue, and dry cough. Less common symptoms comprise headache, diarrhea, anorexia, sore throat, chest pain, chills, nausea, and vomiting. With the lung being the preferential target of the virus, the majority of patients show bilateral pneumonia on admission to healthcare facilities. Among them, one fifth will progress to acute lung injury (ALI) or acute respiratory distress syndrome (ARDS) which requires critical care and ventilation support. In a subgroup of patients, COVID-19 also presents severe extrapulmonary symptoms such as disseminated thrombosis, neurological disorders, or multiple organ dysfunction (6). In general, all ages are susceptible to SARS-CoV-2 infection. However, males aged above 60 with co-morbidities are prone to severe forms and worse outcomes compared to young people and children (7). Pregnant women are classified in moderate risk group as a precaution.

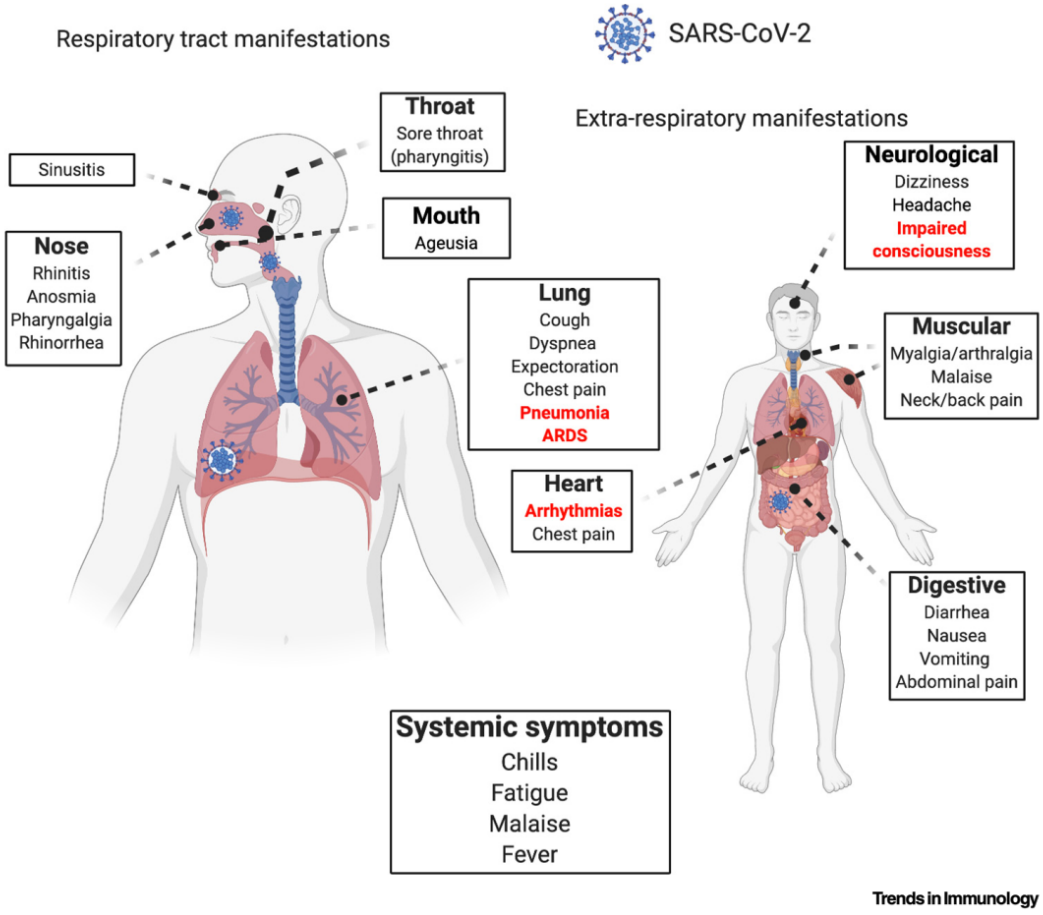

Figure 2. Clinical Symptoms of Coronavirus Infectious Disease 2019 (COVID-19) (2)

In the past year, myriad pharmacological candidates spanning from the known antiviral drugs to immunomodulatory agents have been put forward into clinical trials (8). Nevertheless, there are not yet therapies proven effective for the management of COVID-19. Therefore, preventive measures such as active testing, containment of infected individuals, social distancing and sanitation have been strictly implemented in the communities to restrict the spread of SARS-CoV-2 infection (9). In parallel, immunization campaigns have been globally launched since the approval of the first vaccine in December 2020. Today, more than 7.8 billion shots have been given around the world and half of the population was reported to receive the first dose. However, unequal vaccine distribution, vaccine hesitancy and refusal together with the emergence of new variants are formidable hurdles to achieve the high coverage of COVID-19 vaccines (9,10).

1.2 Pathogenesis of SARS-CoV-2 infection

SARS-CoV-2 entry and tropism

SARS-CoV-2 invades the host cells by binding its Spike proteins to the membrane bound form of angiotensin-converting enzyme (ACE)-2 which is abundantly expressed on nasal epithelial cells, tracheal and bronchial epithelia and alveolar epithelia (11,12). Hence, the respiratory tract is considered as the main viral reservoir and spread. The high expression of ACE-2 on endothelial cells, kidney, gastrointestinal tracts, especially the brush border of intestinal enterocyte also predispose these locations to become potential sites of infection, thus explaining for the involvement of multiple organs reported in many cases (13). Alternative receptors such as neuropilin (NRP)-1, dendritic cell-specific intercellular adhesion molecule-3-grabbing non-integrin (DC-SIGN), homolog dendritic cell-specific intercellular adhesion molecule-3-grabbing non-integrin related (L-SIGN), and macrophage galactose-type lectin (MGL) were also found facilitating the entry of SARS-CoV-2 (14–16). To access to the cytosol, SARS-CoV-2 employs the host serin protease TMPRSS2 to cleave the Spike proteins into two fragments of binding domains S1 and S2, enabling the membrane fusion and host cell penetration. Once inside the cells, SARS-CoV-2 exposes its genetic materials and starts the replication process. Viral particles by cellular exocytosis are exported to the extracellular space and efficiently spread along with the airway to lower part of the respiratory tract (Figure 3) (17). Concurrently, host cells are induced to apoptosis or pyroptosis when they fail to maintain proper cellular homeostasis. Importantly, the massive cytopathic effects induced by SARS-CoV-2 infection were shown to contribute to focal lung injuries (12,18). Additionally, the disruption of

bradykinin degradation by SARS-CoV-2-mediated downregulation of ACE-2 in the lung may lead to local angioedema, worsening the outcomes of COVID-19 pneumonia (19).

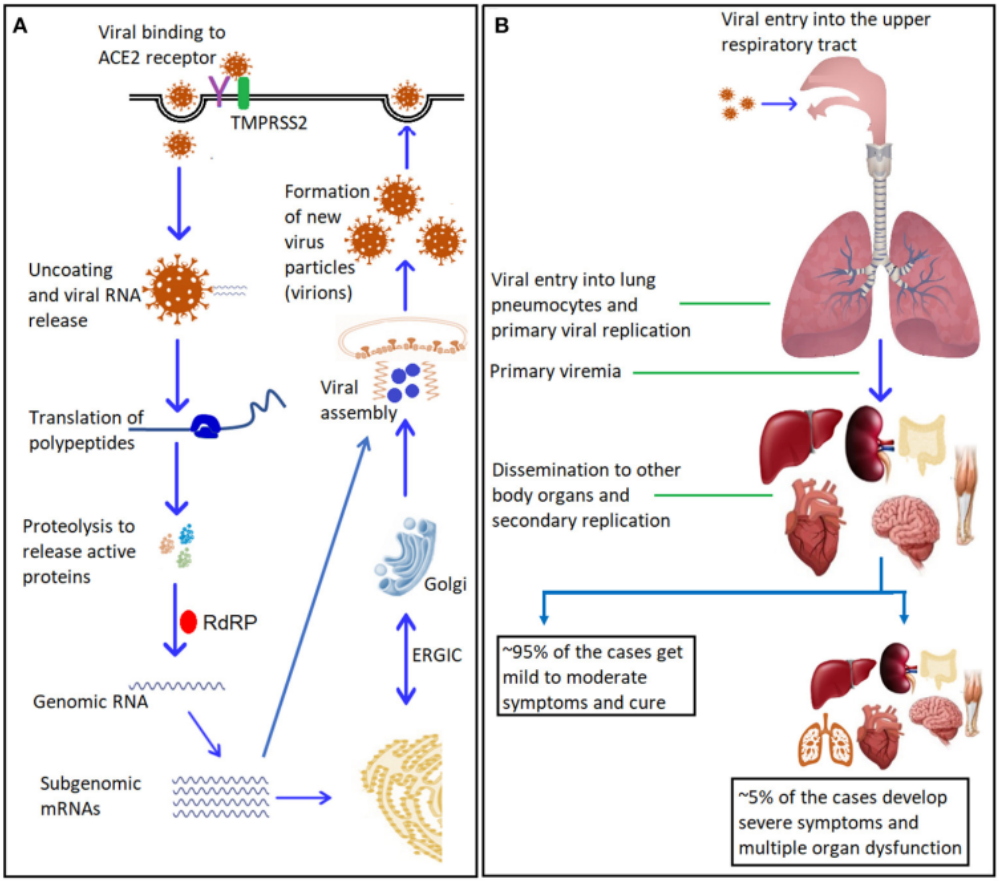

Figure 3. SARS-CoV-2: mechanism of entry, replication, and dissemination (17). (A) Entry and replication of SARS-CoV-2 inside the host cells. (B) Viremia and dissemination into body organs.

Clinical course of disease

The course of COVID-19 has been proposed to undergo three stages, corresponding to the increasing severity of the disease (Figure 4) (20). Stage I is characterized by non-specific or mild manifestations, occurring from the initial entry to the establishment of the viruses in the host. Simultaneously, infected cells trigger the signal of innate immunity through various pattern recognition receptors (PRRs) and damage-associated molecular patterns (DAMPs), promoting the production of type I interferons (IFNs) and the activation of adaptive immunity to halt the infection (21). At this stage, the infection is limited to the upper and conducting airway and can be detected with nasal swab. However, around 20% of the infected cases will progress to stage II featuring viral pneumonia and/or hypoxia. The infection is further spread to alveolar epithelial

cells, particularly type II pneumonocytes, an essential component for surfactant synthesis and secretion (22). Damaging type II pneumocytes by SARS-CoV-2 leads to lung collapse and irreversible long-term complications. Clinically, chest imaging presents bilateral infiltrates or ground glass opacity. Lymphopenia, along with high level of inflammatory markers are notable in this stage (23). Finally, the third stage is associated with the status of hyperinflammation followed by exuberant cytokine production and excessive tissue damage. Accordingly, patients develop detrimental conditions such as ARDS and multiple organ disorders. Histopathology in the lung revealed three types of injuries including diffuse alveolar damage during ARDS, diffuse thrombotic alveolar microvascular occlusion, and inflammatory mediator-associated airway inflammation (24,25). These injuries impair alveolar gas exchange and oxygenation, respiratory acidosis base balance, resulting in permanent lung lesions or death due to respiratory failure.

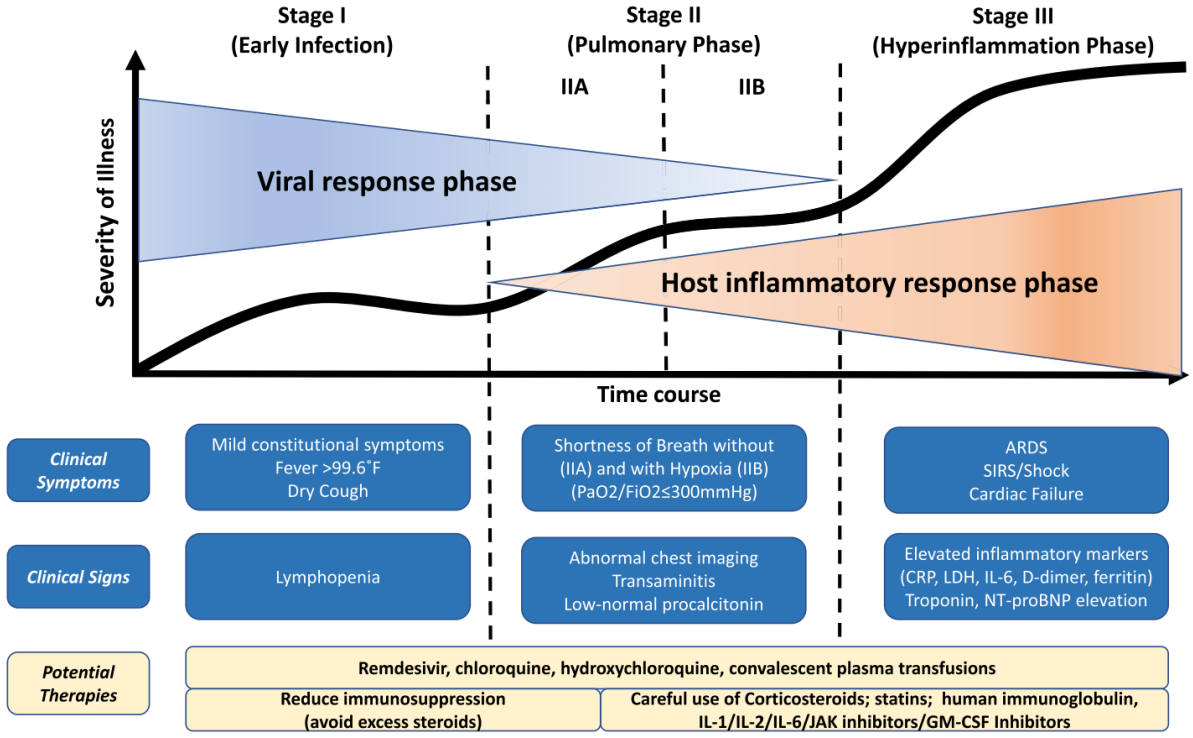

Figure 4. Classification of COVID-19 disease states and potential therapeutic targets (20)

1.3 Immunopathology of SARS-CoV-2 infection

A growing body of evidence have suggested that the host immune responses determine the grade as well as phenotypes of the disease. Immune dysregulations comprising aberrant type I IFNs production, cytopenia, overactivation or exhaustion of immune cells, hypercytokinemia and increased antibodies were extensively reported in severe and critical cases (Figure 5) (26).

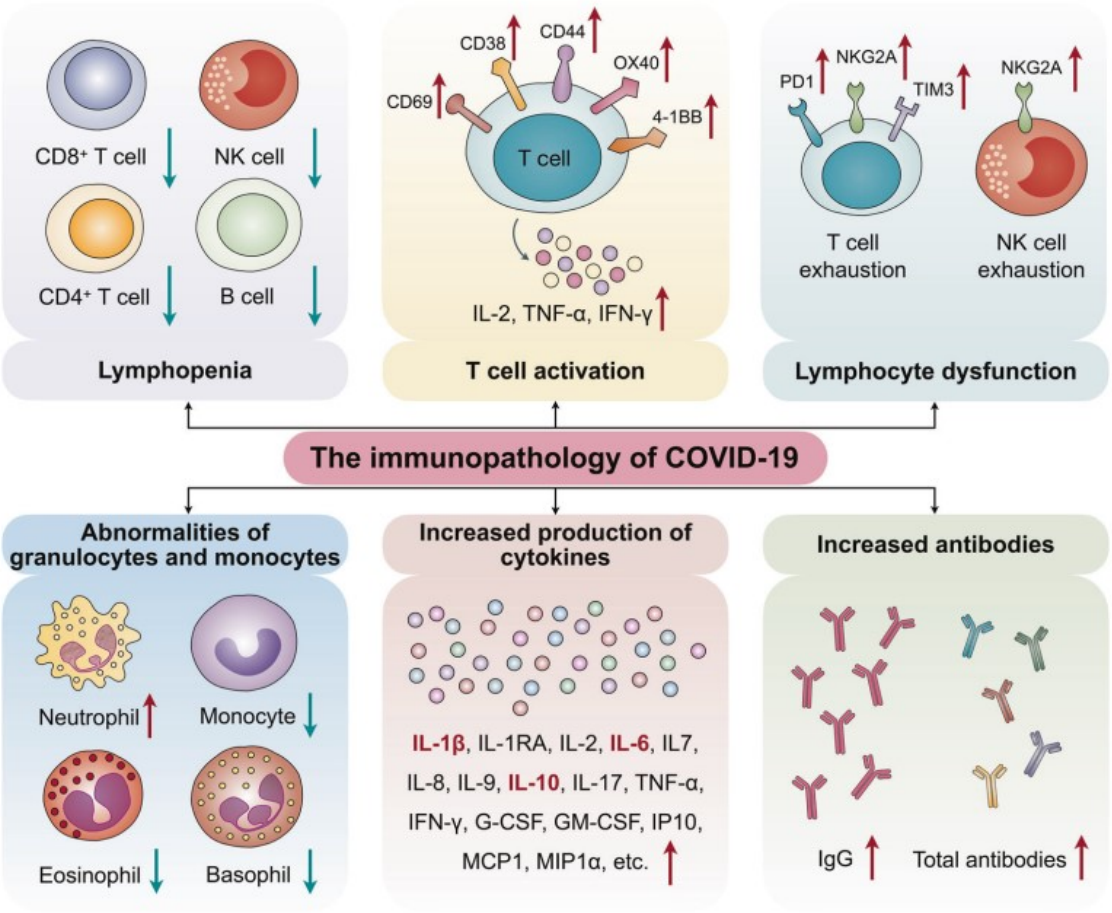

Figure 5. The immunopathology of COVID-19 (26)

Defective type I IFN production

Type I IFNs are produced after viral infection, resulting from the activation of TLR7/8 signaling, RIG-I, and MDA5 pathway in innate immune cells. These cytokines exhibit anti-viral properties by stimulating various interferon stimulated genes (ISGs), thus preventing viral replication within the cells (27). Indeed, patients with inborn errors of type I responses was associated with unfavorable outcomes (28,29). In COVID-19, the dynamics of type I IFNs response was found to reflect the severity of the disease. Indeed, a strong and early type I IFNs response associated with effective viral clearance and antiviral response was observed in mild cases. (30). Conversely, there was a lack of this type of cytokines at early phase in severe cases, but a delayed induction in later phase which coincided with hyperinflammatory status of the disease (31). Single-cell RNA analysis on human PBMCs of severe COVID-19 revealed that the upregulation of type I IFNs activities together with TNF/IL-1β signaling further aggravated the

intense inflammatory responses (32). Nonetheless, type I IFN response critically depends on the host immune response as the level of these cytokines were also undetectable in some cases of mild or severe presentations (32,33). It was shown that SARS-CoV-2 employed some evasion mechanisms to antagonize the activation of IRF3 by mediating the PRR signaling, thereby repressing the binding of this transcription factor to the promoter of IFN-β (34). In addition, SARS-CoV-2 expresses restriction factors of type I IFN such as NPS1 and ORF3a that can suppress IFN gene expression and BST-2 inhibition of viral release (35).

Abnormalities of immune cells

Lymphopenia is a key immunological disorder in severe COVID-19. The low proportion of lymphocytes (T cells, B cells and NK cells) has been shown to be a reliable predictor of disease prognosis, strongly correlated with the severity and mortality rates (23). Tan et al suggested that patients that have the percentage of lymphocytes lower than 20% can be classified as severe type. Lower than 5% is associated with high mortality rate and requires critical intervention. So far, some hypotheses have been proposed according to clinical observations. The increase level of p53, a key pro-apoptotic gene, in PBMC of COVID-19 patients implied that SARS-CoV-2 infected lymphocytes can undergo apoptotic process (36). Moreover, the elevation of the downstream signaling of pyroptosis IL-1β can partly explain for the loss of lymphocytes after infection (37). Many studies also confirmed that high level of pro-inflammatory cytokines could induce lymphocyte deficiency by repressing the development of hematopoietic precursors as well as $CD4^+$ $CD8^+$ thymocytes (38). Lastly, the infiltration of abundant immune cells into the infected area observed in postmortem studies can account for low number of lymphocytes in the peripheral blood. Indeed, numerous studies certified the infiltration of both $CD4^+$ and $CD8^+$ T cells in the lung parenchyma with a predominance of $CD4^+$ T cells (39–41).

Besides lymphopenia, SARS-CoV-2 infection disturbed other components of the immune branch. A significant reduction of eosinophils, basophils, dendritic cells, and monocytes were also reported in severe cases. In contrast, neutrophils and especially the neutrophils to lymphocyte ratio (NLR), an independent risk factor for severe disease and organ failure (42), were higher in severe COVID-19 compared to mild patients or healthy donors. Altogether, SARS-CoV-2 infection leads to major immunological perturbations which may be useful for patient stratification and management.

Lymphocyte overactivation and dysfunction

The patterns of lymphocyte activities are diverse depending on the course of the illness. Indeed, patients with severe clinical presentation display either marked lymphocyte activation or exhaustion. Phenotyping analysis on PBMCs revealed high profile of T cell activation markers such as HLA-DR and CD38 (43). By contrast, upregulation of PD-1 and CD244, together with decreased serum of perforin and granzyme A, signifying an exhausted state of cytotoxic lymphocytes were also observed in severe COVID-19 (44,45). Other than that, T cell compartment such as effector cells during SARS-CoV-2 infection was strikingly altered. Increasing evidence have highlighted the involvement of excessiveTh-1/Th-17 responses during SARS-CoV-2 infection (31,46–49). Particularly, the Th-17 effector cells have emerged as a critical factor in promoting exacerbations of the disease (47,50). On the other hand, some studies revealed a subgroup of severe patients presented the Th-2 signature in parallel with eosinophilia in the inflamed area of the lung (51–53). Nevertheless, several reports show that SARS-CoV-2 specific Th cells do not express Th-2 traits (54–56). Postmortem studies reveal that an immune profile defined by ISG expression and viral load, with limited lung damage can precede a stage with low ISG, low viral load and abundant infiltration of activated $CD8^+$ T cells (57). In addition, Kang and colleagues also observe a continual proliferation and overactivation of $CD8^+$ T cells in severe cases at later stage; and such a prolonged response may contribute to disease aggravation in COVID-19 (49). Despite the fact that cytotoxic $CD8^+$ T cells are critical in eradicating the viruses, excessive response can induce diffuse lung damage which is more lethal than viral replication (58–60).

Hypercytokinemia

The elevation of multiple pro-inflammatory mediators defined as cytokine storm is prominent event in the pathology of the disease (61). In COVID-19, robust production of cytokines may lead to endothelial dysfunction, vascular damage, metabolism disorders and consequently multiple organ failure (62). The level of IL-1β, IL-6, TNF-α, CXCL-10 is highly elevated compared to other pro-inflammatory mediators and correlated with the severity and mortality rate of the disease (63–65). Particularly, the increase of acute inflammatory cytokines IL-1β and TNF-α along with chemokines retain a sustained level of IL-6. Additionally, SARS-CoV-2 mediated ACE-2 downregulation may promote IL-6 production via the accumulation of Angiotensin II (66). IL-6 by forming with its receptors induces the activation of cytokine mediated JAK/STAT3 pathway following gp30 binding, thus perpetuating the inflammatory state (67). Of note, gp30 is widely expressed both in immune and non-immune cells. IL-6 together with other mediators recruit granulocytes and lymphocytes to the site of infection where these cells secrete

their bio-active molecules, further amplifying the inflammatory response and damaging the lung parenchyma (68). In addition, the high and continual level of IL-6 production is also involved in the induction of pathogenic Th-17 cells and its cytokines IL-17A which can aggravate the lung injuries via the recruitment of neutrophils (69). Taken together, targeting the amplifier IL-6 could present therapeutic potentials to dampen the hyperinflammatory phase.

Increased antibodies

Cumulative studies proposed the titer of antibodies as a complementary marker to classify severe and non-severe cases (70). It was shown that convalescent patients displayed a low level of neutralizing antibodies (NABs) with delayed seroconversion whereas critically ill patients developed high level of IgG antibodies against receptor binding domain (RBD) and spike proteins (71). In particular, there was a shifted induction toward spike specific IgG3 antibodies, a subclass endowed with potent pro-inflammatory and linked to disease severity (72). Interestingly, the seroconversion in hospitalized patients was faster by 4 days in compared to the median time (73). In some particular conditions, depending on the antibody level and spatial proximity of cells, a subclass of antibodies against the receptor binding motif may facilitate cellular fusion with $ACE2^-$ cells, thus enhancing the spread of infection at later stage of the disease (16). These observations could result from the hyperinflammation by the host or massive viral replication which trigger increased antigen presentation and humoral responses.

2. Dendritic cells

2.1 Overview of dendritic cells

Dendritic cells were first discovered by Ralph Steinman in 1973 and acquired the name due to their peculiar shape of long membranous projections which resemble the dendrites of nerve cells (74) (Figure 6). DCs represent a specialized population of antigen presenting cells, serving as sentinels of innate immunity and key initiators of adaptive immune responses. They reside in blood, non-lymphoid and lymphoid tissues with a unique role in the immune system owing to their capacity to direct T cell responses against numerous pathogens and foreign antigens (75). In addition, they are pivotal cellular components that efficiently maintain a delicate balance between protective immunity and self-tolerance (76).

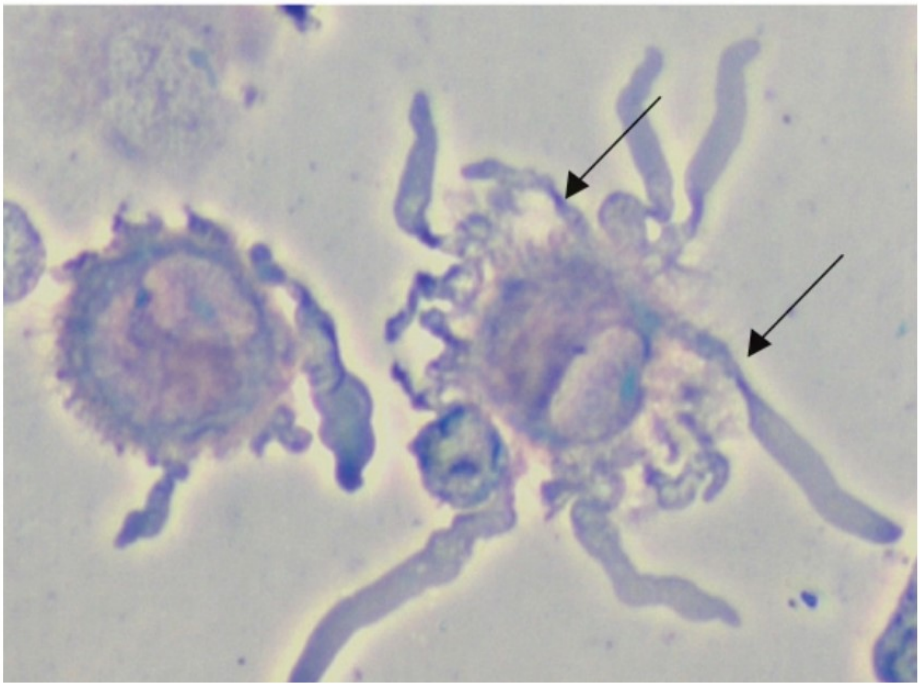

Figure 6. Photomicrograph of DCs stained with May-Grunwald Giemsa. DCs were found displaying typical morphology with long cytoplasmic projections (black arrows) at magnification 400x (74).

Ontogeny of DCs

In general, DCs are a diverse group of cells originated from both myeloid and lymphoid lineage of bone marrow-derived hematopoietic stem cells. Their development and expansion from bone marrow precursors critically depend on a network of transcription factors that facilitate lympho-myeloid differentiation including GATA2, PU.1, GFI1, IKZF1 and IRF8 (77,78) (Figure 7). During early stages of DC development, progenitors express high levels of Irf8 with equal developmental potential towards all DC subsets. A key axis in regulating the balance of pDC and myeloid cDC development is the antagonism between ID2, an inhibitor of DNA binding, and the TF E2-2 (also known as Tcf4). E2-2 is a lineage-determining factor for pDC that is negatively regulated by ID2. Several TFs have been found to impact the relative production of pDCs and cDCs, through interaction with the E2-2 axis. The ETO family protein MTG16 and the TF ZEB2 are reported to repress ID2, thereby increasing pDC development. NFIL3 acts to reduce pDC in favour of cDC1 population (77). Exogenous growth factors GM-CSF (acting through STAT5) and Flt3L (acting through STAT3) respectively inhibit or enhance pDC development by modulating the expression of ID2 and E2-2. In humans, heterozygous mutation or loss of E2-2 causes Pitt-Hopkins syndrome in which mature interferon-α (IFN-α)-secreting

pDC are reduced in number (79). With respect to cDCs, cDC1 development is dependent upon GATA2, PU.1, GFI1, ID2, IRF8 and BATF3. IKZ1 deficiency in humans ablates pDCs but results in an increase of cDC1. IRF8 acts to preserve DC potential at several points in hematopoiesis by direct or indirect competition with a series of TFs that promote other lineages. In particular, IRF8 limits CEBPA-mediated granulocytic differentiation; with PU.1 interacts with KLF4 to modulate the balance to monocyte differentiation; it competes with IRF4 to control cDC1/cDC2 output; a BATF3 "switch" ensures that unopposed IRF8 maintains cDC1 maturation (79,80).

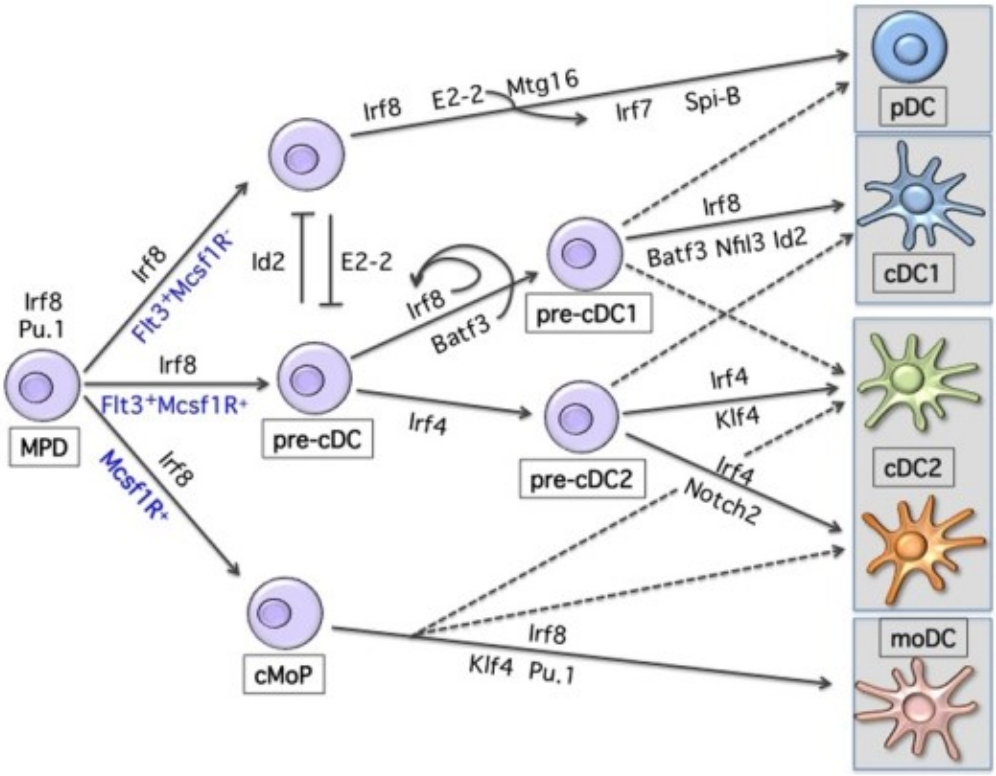

Figure 7. Transcriptional development of DCs (77).

DC subsets

DCs are classified into two major populations including conventional DCs (cDCs) and plasmacytoid DCs (pDCs) (81) (Table1). Based on the ontogeny, cDCs can be subdivided into two groups comprising cDC1 and cDC2. Both subsets display similar capacity to activate $CD4^+$ T cells and being distributed widely in lymphoid, non-lymphoid tissues and blood. However, cDC1 cells constitute only 0.1% of peripheral blood mononuclear cells (79).

cDC1, known as $CD141^+$/$BDCA3^+$ DCs are recognized as a subset with high expression of TLR3, XCR1 and Clec9A denoting their superior cross-presenting capacity, which underlines

their important role in driving anti-viral and anti-tumoral activities (82). In addition, they represent an abundant source of IL-12, CXCL10, IFN-β and IFN-λ in response to the agonist of TLR3 (Poly I:C) (83,84). Depending on the location and stimuli, they exhibit remarkable plasticity in orientating the development of naïve $CD4^+$ T cells towards distinct phenotypes (Th1, Th2 and regulatory T cells or Tregs) (83,85,86).

cDC2 cells expresses the canonical marker CD1c or BDCA1. They are endowed with good T cell stimulating ability but less efficient in cross-presentation compared to cDC1 cells. They respond to a variety of stimuli and secrete a broad panel of proinflammatory cytokines and chemokines such as IL-1β, IL-6, IL-12, TNF-α, CXCL8, CCL3, CCL4, CCL5 and CXCL-10 (83,84). Besides being a potent Th1 stimulator, cDC2 present higher levels of IL-23 mRNA than cDC1 and induce Th-17 polarization upon A. fumigatus challenge (87).

Interestingly, DCs can be generated from monocytes, a class of circulating blood leukocytes, under inflammatory conditions (88). These cells, referred as monocyte-derived DCs (moDCs) or inflammatory DCs, were believed to be a counterpart of cDC2 subset due to their phenotypic and functional similarities (89). To date, the ease of in vitro moDC generation by culturing $CD14^+$ cells with IL-4 and GM-CFS facilitates moDCs as predominant source of DCs for *in vitro* studies.

pDCs are distinguished from cDCs by positive makers of CD123 and BDCA2 and especially their prominent role in the production of type I interferons (IFNs) which is endowed with antiviral properties. Thus pDCs play a critical role in the early phase of viral infection (90). Moreover, they are spherical in shape in the steady state and undergo morphological changes to dendritic form following activation. However, their T cell polarizing capacity is varying and probably context-dependent (79).

Unified classification	Differential TFs	Conventional markers	Extended markers	Notes
Plasmacytoid DC	E2-2	CD123,	FCER1	DC6 [9]
	ZEB2	CD303/CLEC4C/BDCA-2	ILT3, ILT7	
	IRF8	CD304/NRP1/BDCA-4	DR6	
	IRF4			
Myeloid cDC1	ID2	CD141/BDCA-1	CLEC9A	DC1 [9]
	IRF8		CADM1	No antibody for XCR1 in human
	BATF3		XCR1	
			BTLA	
			CD26	
			DNAM-1/CD226	
Myeloid cDC2	ID2	CD1c/BDCA-1	CD2	DC2/DC3 [9]
	ZEB2	CD11c	FCER1	DCIR clone specific [26]
	IRF4	CD11b	SIRPA	
	Notch2/KLF4		ILT1	
			DCIR/CLEC4A	
			CLEC10A	
Langerhans cell	ID2	CD207	EpCAM	
	RUNX3	CD1a	TROP2	
		E-Cadherin		
Pre-DC	ZEB2	CD123, CD303	AXL	DC5 'AS' DC [9]
	IRF4		SIGLEC 6	
	KLF4		CX3CR1	
			CD169 (SIGLEC 1)	
			CD22 (SIGLEC 2)	
			CD33 (SIGLEC 3)	
Mo-DC	MAFB	CD11c	SIRPA	
	KLF4	CD1c/BDCA-1	S100A8/A9	
		CD1a	CD206	
			DC-SIGN/CD209	
Non-classical monocyte		CD16		DC4 [9]
		CX3CR1		SLAN DC?
		+/-SLAN		

cDC, conventional DC; DC, dendritic cell; Mo-DC, monocyte-derived DC; pDC, plasmacytoid DC; TF, transcription factor. IRF4 and IRF8 are highlighted in bold.

Table 1. Human dendritic cell subset characterization (79).

2.2 Pathogen recognition

DCs detect pathogens via distinct sets of pattern recognition receptors (PRRs) such as Toll-like receptors (TLRs), Retinoic acid inducible gene-I like receptors (RLRs), Nod-like receptors (NLRs), and C-type lectin receptors (CLRs) (91). PRRs recognize pathogen-associated molecular patterns (PAMPs) which are derived from invading microorganisms, and damage-associated molecular patterns (DAMPs) released from host cell damage (91). Among PRRs, TLRs are the family receptor being extensively investigated and well-characterized in DCs. As of now, there are ten TLRs in human which are either bound to the cell surface membrane or distributed in the intracellular compartments (e.g., endoplasmic reticulum, endosome, lysosome or endolysosome). TLR1, 2, 4, 5, 6 and 10 are categorized as cell membrane TLRs responsible for the recognition of microbial membrane components such as flagellin, liposaccharide (LPS), etc. TLR3, 7, 8 and 9 are sensors of nucleic acid fragments, termed as intracellular TLRs (92) (Figure 8). TLR3 and TLR7/TLR8 respond to dsRNA and ssRNA, respectively, while TLR9 to single-strand DNA (ssDNA). TLR7 preferentially recognizes guanosine (G) and short uridine (U)-containing ssRNA, such as the UU motif (93), while TLR8 recognizes U and ssRNA (94).

TLRs are type I transmembrane proteins containing an ectodomain with leucine-rich repeats (LRRs), a transmembrane domain, and a cytoplasmic Toll/IL-1 receptor (TIR) domain involving in the initiation of downstream signaling. The engagement of the ectodomains with respective ligands trigger the recruitment of TIR domain-containing adaptor proteins such as MyD88, TRIF, TIRAP/MAL, TRAM and SARM, resulting in the activation of transcriptional factors (TFs) such as NF-kB, IRF3 or IRF7 (Figure 8). While NF-kB is known to regulate the production of pro-inflammatory mediators, IRF3 and IRF7 promote the induction of type I IFNs (Figure 7). All TLRs was shown to utilize MyD88 signaling except TLR3 whereas TRIF pathway is employed by both TLR3 and TLR4. Distinct from other TLRs, TLR4 with its ligand LPS lead to the activation of TIRAP-MyD88 and TRAM-TRIF pathways. SARM negatively regulates TRIF, thus playing a role in controlling TLR3 and 4 signaling (95). Among TLRs, TLR7 and 8 are crucial for the detection as well as the activation of immune responses against ssRNA virus infection such as influenza virus and coronaviruses. MyD88 signaling cascade is essential for these two receptors and associated with the activation of NF-κB and MAPK and production of inflammatory cytokines such as TNF-α, IL-6 and IL-12 at one side, and activation of IRFs (especially IRF5 and IRF7) and type I IFNs at the other (70).

Within DC subsets, cDC1 possess high transcript levels of TLR1, 2, 3, 6, 8, and 10 but lacked expression of TLR4, 5, 7, and 9. cDC2 share similar profile but also express TLR 4, 5 and 7. While TLR repertoire of moDCs resembles that of cDC2 with lesser expression in TLR3, 6 and 10, pDCs predominantly express TLR7 and 9 (92). The preferential expression of TLRs in distinct DC subsets may reflect their differential functions. For example, TLR7 expression by pDCs is crucial to mount a rapid and effective antiviral immune response, as recently demonstrated by severe COVID-19 in patients with loss-of-function TLR7 variants (96). By contrast, TLR8 sustains the production of proinflammatory cytokines. Indeed, recent studies highlighted that TLR7 and TLR8 may activate different downstream pathways in different cell types.

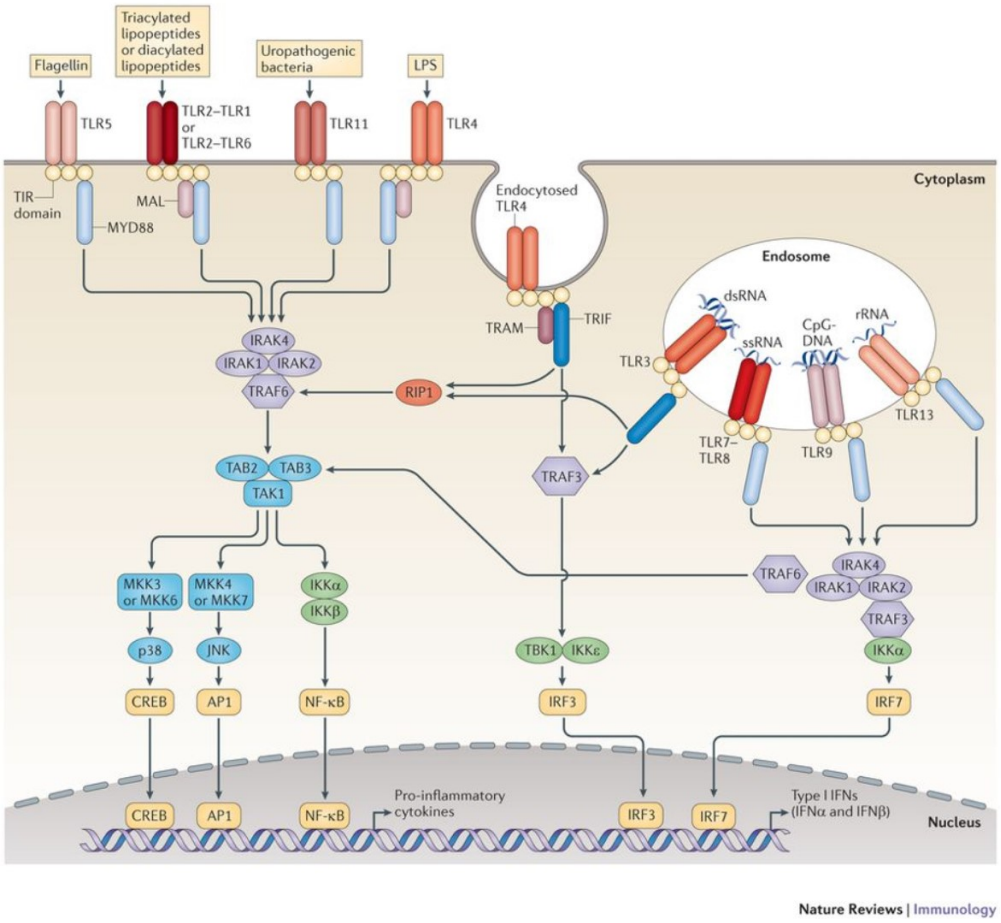

Figure 8. Mammalian TLR localization and signaling pathways (97).

2.3 Dendritic cell activation and functions

Upon receiving activating signals from a variety of inputs (PAMPs, DAMPs, inflammatory cytokines, etc.), DCs undergo a maturation process characterized by major phenotypic and functional alterations, as shown by the upregulation of antigen presentation (MHCI and II) and costimulatory molecules (CD80, CD83 and CD86), the release of pro-inflammatory cytokines/chemokines as well as the loss of endocytic and phagocytic abilities (98). Along with these changes, DCs migrate to secondary lymphoid organs where they present processed antigens to T cells and subsequently induce T cell responses against specific pathogens. Of note, the mobilization of DCs is mediated by the chemokine receptor CCR7 which is highly upregulated during maturation. At the lymph nodes, DCs present short peptides derived from antigens to $CD4^+$ and $CD8^+$ T cells via MHC-II and I molecules, respectively (99) (Figure 9). Of note, MHC-II binds to peptides originated from exogenous antigens whereas MHC-I makes a complex with endogenous peptides. Besides the prominent role in priming T cells, DCs also

amplify the inflammation though the secretion of pro-inflammatory products such as TNF-α, IL-1β, IL-6, IL-8, IL-12, etc.

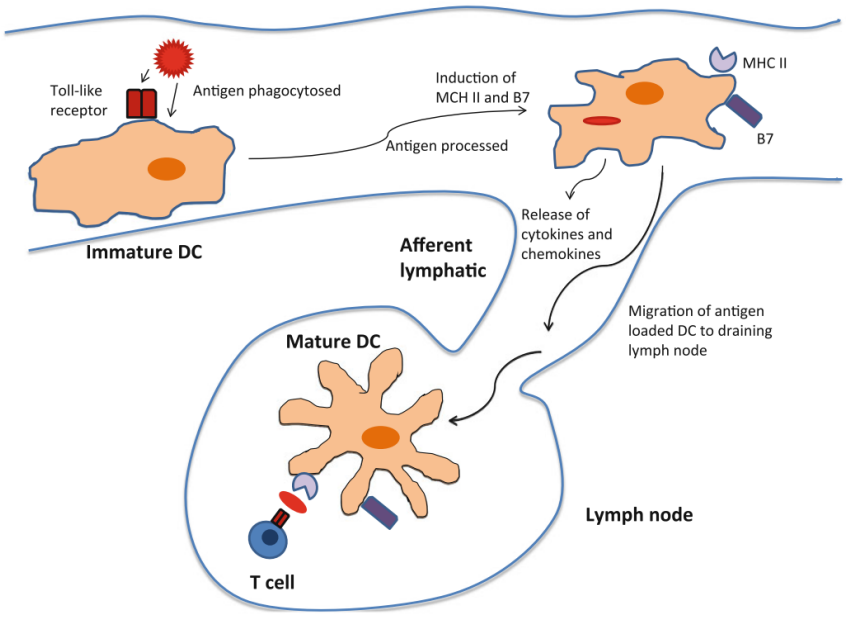

Figure 9. Dendritic cell activation of T cells (99).

Role of DCs in $CD4^+$ T cell activation

The activation of naïve $CD4^+$ T cells is initiated via the engagement of T cell receptor (TCR) with antigen-MHCII complexes presented by DCs, resulting in an immune response specific to particular antigens. In addition to antigen recognition, T cells require second signal from costimulatory molecules CD80/CD6 of DCs to switch on the cascades of signaling essential for T cell proliferation and differentiation. The lack of co-stimulation was shown to induce T cells into a prolonged hyporesponsive state called anergy (100). Thus, this signal is prerequisite to determine the fate of T cells whether being in activation or anergy following antigen encounter. Finally, DCs-derived cytokines represent the third signal responsible for the orientation of T cell development towards distinct effector lineages such as Th1, Th2 and Th17 (101) (Figure 10). IL-12 is well-known for the differentiation of IFN-γ producing T cells or Th1 cells, a subset that confers protection against intracellular pathogens and tumors. T cells activated in the presence of IL-4 develop into Th2 cells which release type 2 cytokines (IL-4, IL-5 and IL-13) to mediate parasite expulsion and tissue repair. IL-1, IL-6 and IL-23 together with TGF-β are essential for Th17 polarization. Th17 cells and their related cytokines (IL-17, IL-21 and IL-22) are known to

combat extracellular agents and also implicated in many autoimmune diseases and chronic inflammation (102).

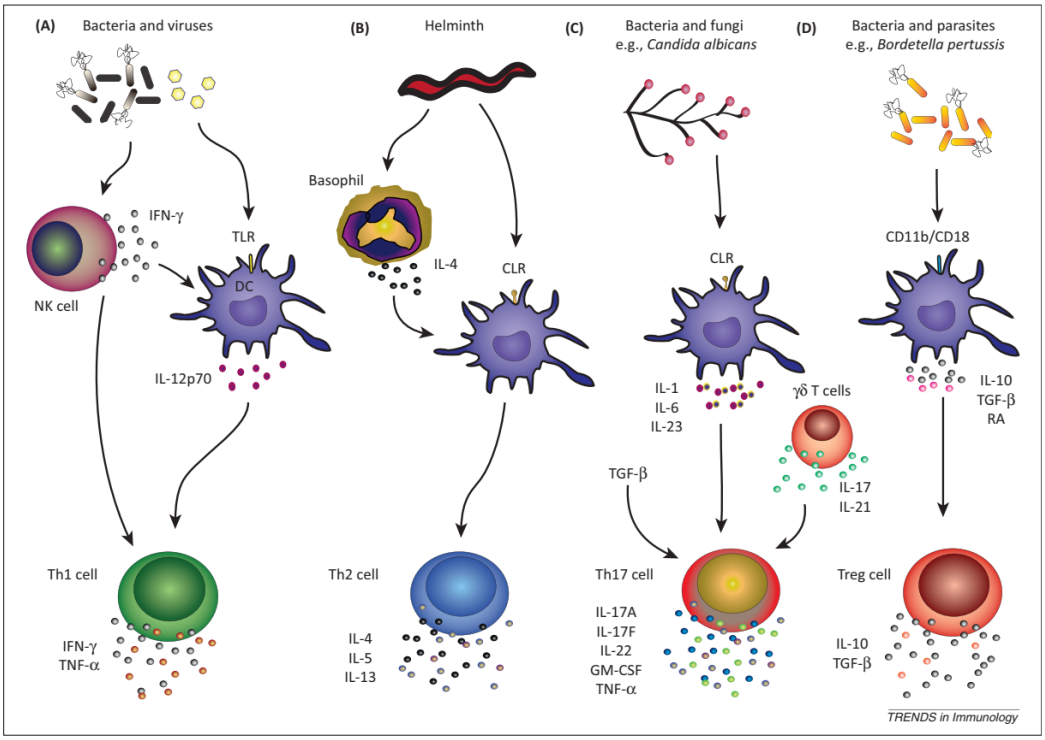

Figure 10. Pathogens direct the induction of Th cell subtypes via distinct effects on innate immune cells (102).

Role of DCs in CD8⁺ T cell activation

CD8⁺ T cells, when activated, differentiate into cytotoxic T cells (CTLs) and acquire potent lytic machinery containing cytotoxic granules (perforin and granzymes) to kill target cells. In addition, CTLs also produce IFN-γ and utilize Fas/FasI pathway as additional mechanisms to control target cells (103). The activation and expansion of CD8⁺ T cells also require two signals including the antigen recognition via MHC class I presentation and the ligation of costimulatory molecules. In addition, IL-12 as the third signal is critical to the acquisition of effector functions both *in vitro* and *in vivo* studies (104,105). Indeed, the absence of IL-12 was shown to render CD8⁺ T cells either tolerogenic or noncytolytic. Interestingly, some DCs such as cDC1 are able to phagocytose dead cells and present processed antigen derived from these cells to naïve CD8⁺ T cells via MHC I (83). This mechanism, known as cross-presentation, is crucial for naïve CD8⁺ T cell activation, particularly in the case of viral infections. It was shown that CD4⁺ T cells may be needed in multiple stages of CD8⁺ T cell response (106) as they can provide essential cytokines such as IL-2, IL-12 and IL-21 which play a role in the generation of CTLs and memory

cells. In addition, DCs activated by $CD4^+$ T cells through CD40-CD40L ligation transfer help signals to $CD8^+$ T cells via CD70-CD27 pathway, thus enhancing $CD8^+$ T cell differentiation and secondary expansion upon re-stimulation (107). However, various *in vivo* studies have revealed that $CD8^+$ T cells require little or no assistance from $CD4^+$ T cells (108,109), especially in the case of potent infectious pathogens which can elicit strongly activated DCs, consequently bypass the need of $CD4^+$ T cells (110). It is likely that $CD4^+$ T cells are important in the induction of memory cells rather than that of effector cells.

2.4 Dendritic cells in immune tolerance

DCs represent a paramount checkpoint of the immune system, being immunogenic to activate adaptive immunity upon pathogen encounter while serving as an active inducer of tolerance in peripheral tissue at steady state (76). DCs promote immune tolerance by mainly targeting T lymphocyte population via clonal deletion of reactive T cells in the thymus (central tolerance) (111), generation of regulatory T cells (Tregs) and induction of T cell anergy or deletion in the periphery (peripheral tolerance) (112), thus maintaining proper homeostasis as well as preventing autoimmune response and transplantation rejection. In the periphery, DCs actively search and capture self-antigen or non-infectious proteins from the environment. Of note, the source of antigens in the absence of inflammation is mostly apoptotic cells as a consequence of physiologic tissue turnover (113). These DCs spontaneously migrate to the lymph nodes where they perform antigen presentation and induce T cell apoptosis and anergy or convert naïve T cells into Treg phenotype (Figure 11).

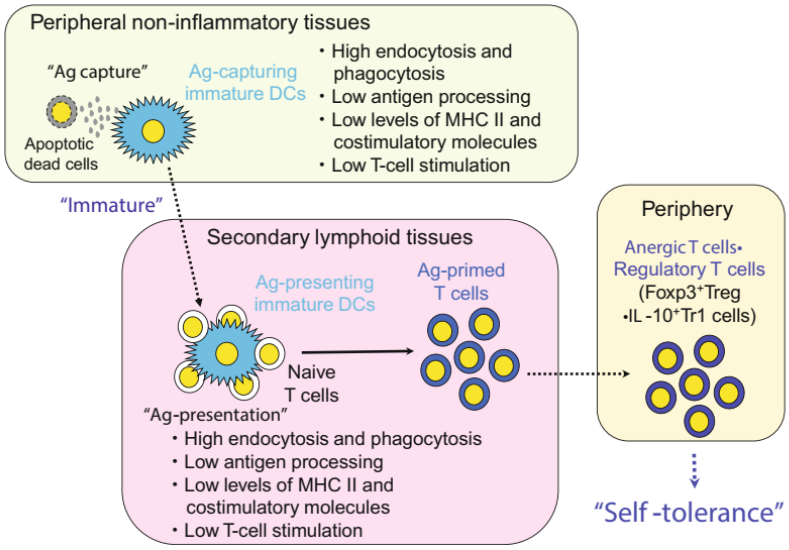

Figure 11. Induction of immune tolerance by DCs under steady-state conditions (114).

Tolerogenic DCs (TolDCs) or Regulatory DCs (DCregs)

TolDCs or DCregs consist of immature DCs (iDCs) and those at different stages of maturation state. Because iDCs themselves are tolerant inducers in the steady state, the suppression of maturation can be considered as a strategy to render DCs tolerogenic (115). However, DCs with phenotypic maturation but lacking the production of pro-inflammatory cytokines, referred as semi-mature DCs, also fail to induce competent T cell immunity (116). Indeed, some subsets of tissue resident DCs display immature phenotype under homeostatic conditions while the others acquire semi-mature state under the influence of environmental cues (114,116,117). For example, the tissue environment in the liver conditions DCs to express high levels of IDO, IL-27, resulting in induction of Tregs or T cell anergy (118). Additionally, $CCR9^{+}$ pDCs as a resident population in resting secondary lymphoid are inherently tolerogenic as they were shown to favor Tregs differentiation and capable of suppressing acute graft-versus-host disease (119). Given the important role of DCs in prevention of autoimmunity, DCs that can induce tolerance have been actively investigated for their use in the treatment of immune dysregulation (114). Indeed, the tolerogenic properties of DCs can be modulated by exposure to immunomodulatory agents such as corticosteroids, calcineurin inhibitors, aspirin and so on, thereby lowering the immunogenic capacity of activated DCs. These agents appear to fully suppress phenotypical and functional DC maturation. Concomitantly, they are capable of promoting a tolerogenic profile characterized by the upregulation of regulatory markers (e.g., PD-L1, ILT3, etc.) and mediators (e.g., IL-10 and TGF-β), the induction of tryptophan metabolism known to suppress T cell activation (IDO) as well as Tregs induced signaling pathway (ERK-RALDH, Wnt-β-catenin, etc.) (120).

2.5 Role of DCs in SARS-CoV-2 infection.

DCs as targets of SARS-CoV-2

DCs are distributed throughout the lung parenchyma as well as in the epithelium of conducting airways where they act as key sentinel cells (121). Given that DCs express a number of PRRs, they can recognize viral components and subsequently mount adequate innate and adaptive immunity to clear the infection. However, the role of DCs in SARS-CoV-2 infection remains to be elucidated. Interstitial lung DCs and moDCs express a relative level of ACE2 (122,123), thus allowing the penetration of SARS-CoV-2 into the cytosol of the cells (Figure 12) . Recent study has uncovered the transmembrane protein CD147 as a novel receptor that facilitate viral entry in DCs (124). Upon SARS-CoV-2 infections, moDCs upregulate the expression of Furin and

DC-SIGN, more than 20 times in comparison to Calu-3 cells (123). Of note, the lectin receptor DC-SIGN is associated with enhancement of SARS-CoV-1 and -2 infection while Furin is a host protease essential for protein fusion. More interestingly, DCs may transmit the viruses to permissive $ACE2^+$ cells via DC-SIGN or L-SIGN receptors (15,16). Yang et al showed that DCs were susceptible to SARS-CoV-2 infection but did not support viral replication and generation, therefore DCs can carry the viruses to the lymph nodes and infect the neighboring cells (123). These proofs indicate that DCs may be not only target cells of SARS-CoV-2 but also play a role in potentiating viral spreading.

The involvement of DCs in SARS-COV-2 infection

As mentioned in previous part, SARS-CoV-2 infection is characterized by pronounced reduction of a broad range of immune cells in peripheral blood. Particularly, all subsets of circulating DCs were shown significantly decreased in numbers, accompanied with functional impairments (125) (Figure 12). However, there was a redistribution of circulating $CD1c^+$ DCs to the lung during disease progression (126). On the contrary, $CD141^+$ DCs and pDCs were constantly low in both compartments regardless of clinical status, even months after disease recovery (127). In addition to this, the ratio between cDCs and pDCs (cDCs/pDCs) was largely increased in severe cases compared to those with mild symptoms (128). Even though type I IFNs can be produced by other cell types, human pDCs are well-known major source of this cytokine family due to their constitutively high level of IRF7. Therefore, the loss of pDCs by SARS-CoV2 may account for the diminution of type I IFN response as well as the defective innate immunity during early phase of the infection. Indeed, the first round of type I IFN production that conferred protection against coronavirus infection in murine was derived from pDCs (129). It was noted that one fifth of COVID-19 patients with life-threatening conditions were deficient in type I IFN production. Increasing pro-apoptotic cascade and decreasing viral sensing (DEAH-Box Helicase (DHX) 36 and TLR7, respectively) were presumably attributed to the suppression of pDC activation (130). On the other hand, Yang et al suggested that SARS-CoV-2 may modulate DCs' immunogenicity by antagonizing the phosphorylation of STAT1. Moreover, these DCs expressed low levels of maturation markers such as CD80, CD86 and HLA-DR thereby impairing antigen presentation, as a consequence, decreasing T cell proliferation rate (123). Additionally, SARS-CoV-2 mediated TRAIL expression may partly contribute to the diminution of T cell subsets (51). It is likely that DC dysfunctions is an important evasion mechanism of SARS-CoV-2 to restrain the transition from innate to adaptive immune response, thus amplifying viral infection and spreading. However, several postmortem studies revealed the infiltration of both $CD4^+$ and

$CD8^+$ T cells in the lung parenchyma with a predominance of $CD4^+$ T cells (39–41). Importantly, excessive Th1/Th17 responses together with continual $CD8^+$ T cell overactivation are characteristics of severity in a subgroup of COVID-19 patients (31,46–49). Given that DCs dictate the outcomes of T cell responses, these findings highlight the active role of DCs in disease progression and intensity. In non-severe case with fast recovery, there was a numeric reduction of $CD16^+$ $CD14^+$ monocytes from day 7 to 9, which may indicate the reflux of these cells to the site of infection (131). Under inflammatory conditions, $CD16^+$ $CD14^+$ monocytes are known to differentiate into inflammatory DC subset, a potent stimulator of T cell response. Hence, these observations reinforce the involvement of DCs against SARS-CoV-2 infection through different stages of the disease as well as their determinant role in disease outcomes.

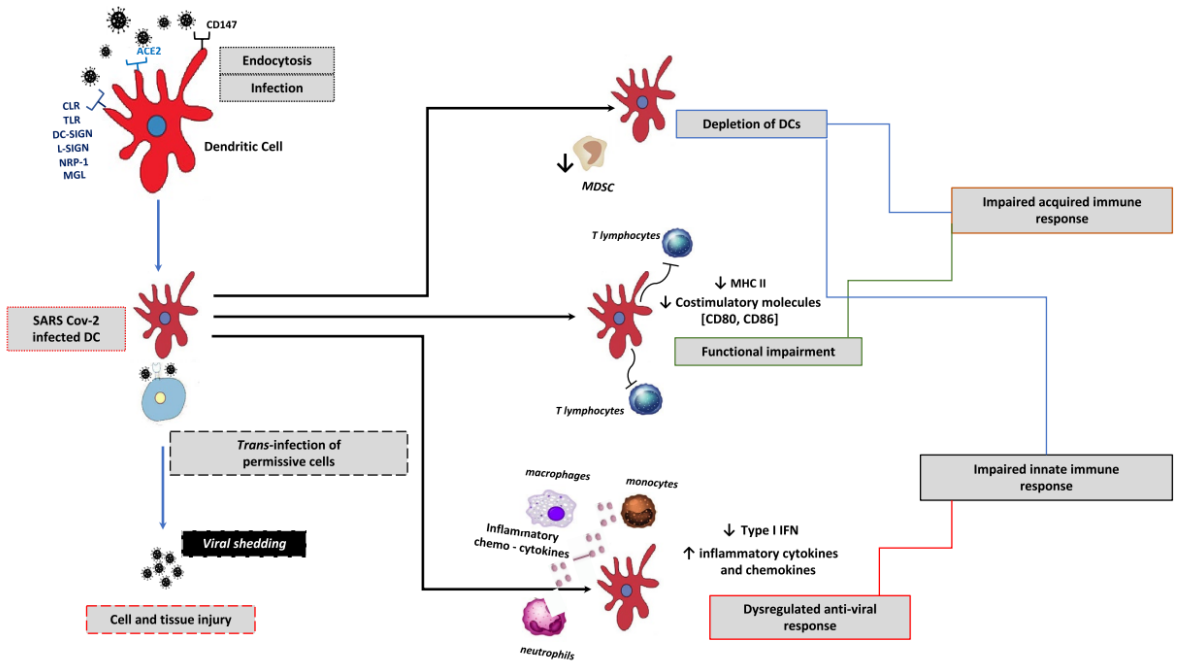

Figure 12. Overview of dendritic cell involvement in SARS-CoV-2 infection (130)

3. Phosphodiesterase (PDE) enzymes and inhibitors

3.1 Overview of PDE family and PDE4 enzymes

cAMP pathway

Cyclic adenosine monophosphate (cAMP) is a ubiquitous second messenger that regulates a plethora of cellular functions such as memory, metabolism, gene transcription, immune responses and others (132). In the immune system, cAMP is a well-known regulator of both

innate and adaptive immunity. The elevation of cAMP level was shown to have potent anti-inflammatory effects as well as to facilitate the resolution of inflammation (132,133). Within the cells, the concentration of cAMP is strictly regulated by two enzymes including adenyl cyclase (AC) and phosphodiesterase (PDE) (Figure 13). While the generation of cAMP is induced by AC, cAMP degradation is promoted by PDEs. Basal level of intracellular cAMP is rather low in microliter range as cAMP is restricted in discrete microdomains containing AC and PDE (134). Particularly, the activation of AC can elicit, at most, a transient increase of cAMP level due to a compensatory degradation of PDE activity. Thus, the combination of cyclase activation and PDE inhibition can produce synergistic effects to sustain a steady level of cAMP inside the cytosol (135).

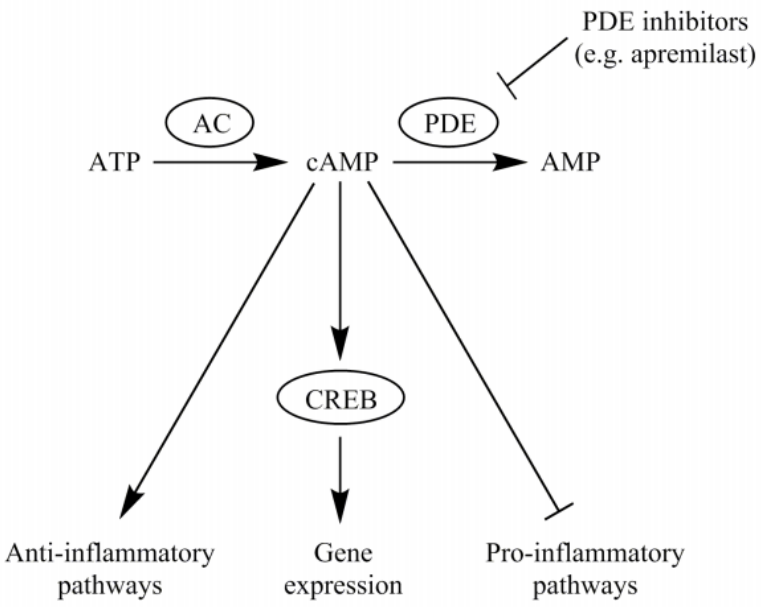

Figure 13. Homeostasis and downstream effects of cAMP signaling in immune cells (132).

PDE family

PDEs are a superfamily comprising 11 different iso-enzymes responsible for the hydrolysis of cyclic nucleotides (cAMP and cGMP) (Table 1), thereby preventing the diffusion of these cyclic nucleotides to other compartments, and consequently compartmentalizing their signals to a defined location (136,137). Indeed, each PDE isoform contains a conserved catalytic domain associated with a regulatory N-terminus that direct single PDE to specific cellular and subcellular localization. Conventionally, PDEs are divided into three groups according to the substrate specificity: the cAMP-specific PDEs (PDE4, PDE7 and PDE8), the cGMP-specific

PDEs (PDE5, PDE6 and PDE9) and dual cAMP/cGMP specific PDEs (PDE1, PDE2, PDE3, PDE10 and PDE11) (138). Interestingly, some dual-specific PDEs are involved in the crosstalk between cAMP and cGMP signaling. It has been shown that the binding of cGMP to PDE2 increases the hydrolysis rate of cAMP by 10 times whereas cGMP restrains cAMP degradation through the competitive interaction with PDE3 (139,140).

Family (no. of genes)	Characteristics	K_m (μmol/L): cAMP; cGMP	Primary tissue distribution	Examples of inhibitors
PDE1 (3)	Ca^{2+}/calmodulin-stimulated	1-30; 3	Heart, brain, lung, smooth muscle	KS-505a Vinpocetine
PDE2 (1)	cGMP-stimulated	50; 50	Adrenal gland, heart, lung, liver, platelets	EHNA (MEP-1)
PDE3 (2)	cGMP-inhibited, cAMP-selective	0.2; 0.3	Heart, lung, liver, platelets, adipose tissue, immunocytes	Cilostamide Enoxamone Milrinone Siguazodan
PDE4 (4)	cAMP-specific, cGMP-insensitive	4; >3000	Sertoli cells, kidney, brain, liver, lung, immunocytes	CDP840 Rolipram SB 207499 Tibenelast
PDE5 (1)	cGMP-specific	150; 1	Lung, platelets, smooth muscle	Dipyridamole MY-5445 Sildenafil Zaprinast
PDE6 (3)	cGMP-specific	2000; 60	Photoreceptors	Dipyridamole Zaprinast
PDE7 (2)	cAMP-specific, high-affinity	0.2; >1000	Skeletal muscle, heart, kidney, brain, pancreas, T lymphocytes	Several in development
PDE8 (2)	cAMP-selective, IBMX insensitive	0.06; N/A	Testes, eye, liver, skeletal muscle, heart, kidney, ovary, brain, T lymphocytes	None selective
PDE9 (1)	cGMP-specific, IBMX insensitive	N/A; 0.17	Kidney, liver, lung, brain	None selective
PDE10 (1)	cGMP-sensitive, cAMP-selective	0.05; 3.0	Testes, brain	None selective
PDE11 (1)	cGMP-sensitive, dual specificity	0.7; 0.5	Skeletal muscle, prostate, kidney, liver, pituitary and salivary glands, testes	None selective

IBMX, 3-isobutyl-1-methylxanthine.

Table 2. Human cyclic nucleotide phosphodiesterase isozymes (135).

Type 4 PDE

Among eleven PDE iso-enzymes, PDE4 family is recognized as predominant cAMP-hydrolyzing enzymes in the inflammatory and immune cells where they promotes the pro-inflammatory activities by inducing cytokine and chemokines production, antibody IgE release and generation of lipid mediators (141). In general, the PDE4 family consists of four subtypes which are encoded by four paralog genes including PDE4A, PDE4B, PDE4C and PDE4D. Surprisingly, PDE4C is the only isoform being absent in inflammatory cells (138). The other three PDE4 isoforms are also detected in various tissues and particularly endowed with specific and nonredundant roles in regulating different pro-inflammatory cellular functions. For instance, studies in PDE4B or PDE4D knockout mice revealed distinct roles of these two isoforms in

inducing cytokine production by LPS-stimulated monocytes and macrophages (142,143). Additionally, in vitro experiments further confirmed the complementary but not redundant effects of PDE4B and D on the recruitment of neutrophils to the site of infection in the lung (144).

With the broad immunomodulatory effects on a wide range of inflammatory cells and the high levels of PDE4 detected in patients suffering from inflammatory diseases, targeting PDE4 by specific inhibitors has been extensively studied and verified as an effective therapy in a number of pathological conditions such as chronic obstructive pulmonary disease (COPD), psoriasis, atopic dermatitis (AD), inflammatory bowel diseases (IBD) and rheumatic arthritis (RA) (145).

3.2 PDE4 inhibition in inflammatory cells

Mode of action

The accumulation of intracellular cAMP following PDE4 inhibition leads to the activation of multiple downstream pathways that are involved in the regulation of inflammatory process (145) (Figure 14). Most prominent, protein kinase A (PKA) activation by cAMP induces the phosphorylation of cAMP-responsive element binding protein (CREB) and activates the activating transcription factor-1 (ATF-1), resulting in the production of anti-inflammatory mediators. Moreover, PKA activation can interfere in the activity of nuclear factor kappa B (NF-κB) by disrupting its interaction with CREB binding protein (CBP) or p300, consequently repressing the expression of numerous pro-inflammatory cytokines. The inflammatory responses were also lessened through the inhibition of B-cell lymphoma 6 protein (Bcl-6). Alternatively, cAMP directly activate Epac1/2 signaling pathway, added to the mechanism of cAMP-elevating effects on the regulation of inflammation and cell proliferation (146).

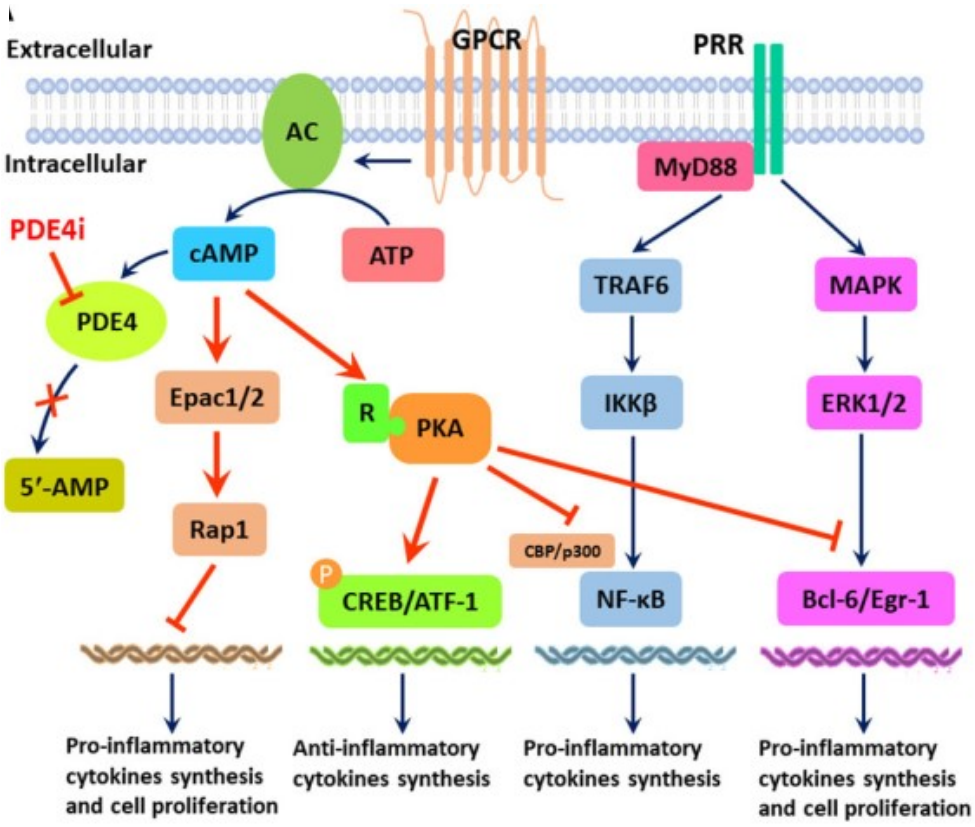

Figure 14. Mode of PDE4 inhibition in the regulation of inflammatory responses (145).

Anti-inflammatory properties

Blocking PDE4 was shown to restrain the release of essential cytokines by most of the inflammatory cells (Figure 15). PDE4 inhibition diminished the secretion of interleukin-8 (IL-8) and neutrophil elastase into the sputum of COPD patients (147). In addition, neutrophil chemotaxis in rat models of LPS-induced lung inflammation was attenuated by the PDE4 inhibitor Roflumilast (148). Resident macrophages, monocytes and human DCs also display defects in TNF-α and chemokine production (149–151). In vivo studies revealed an abrogation of eosinophil infiltration into the lung by PDE4 inhibitor (152). Strikingly, PDE4 inhibition exerted broad inhibitory effects on the three main subsets of $CD4^+$ T cells (Th1, Th2 and Th17) but showed minor impact on B cell function and phenotype (153,154). Silencing PDE4D or PDE4B in $CD4^+$ T cells culminates in IL-2 production, subsequently repressing T cell proliferation (155,156). The lack of PDE4, especially PDE4D, was shown to subdue type 1 cytokine (IFN-γ) and partly type 2 cytokines (IL-4 and IL-5) (156,157) while Th17 cells were dramatically decreased in arthritis mouse models treated with PDE4 inhibitor (158). The anti-inflammatory

properties of PDE4 inhibition are also extended to other cell types in the respiratory tract. For instance, reduction of PDE4 activities was shown to efficiently restrain cytokine secretion by rhinovirus-infected human bronchial epithelial cells (159). PDE4 inhibition also decrease the level of Poly I:C induced IL-8 production by human airway smooth muscle cells, thereby curtailing the recruitment of neutrophils to the lung (160).

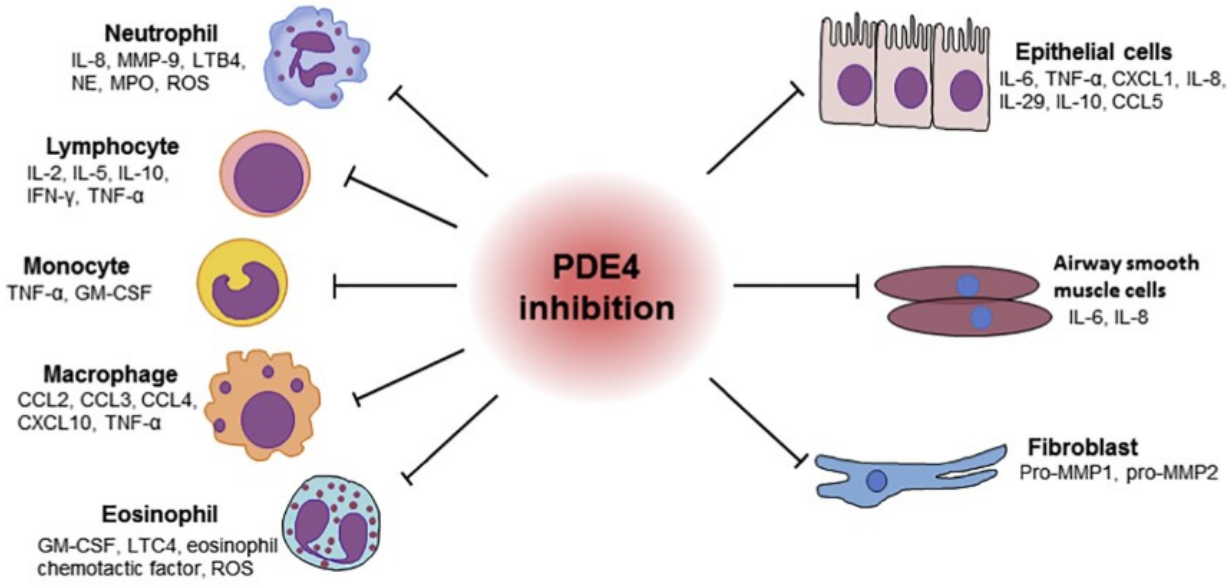

Figure 15. PDE4 inhibition reduces the release of a variety of pro-inflammatory mediators from key inflammatory cells (138).

3.3 PDE4 inhibition as a therapeutic intervention in respiratory diseases.

The prominent immuno-modulatory properties of PDE4 inhibition in various inflammatory cells and structural cells in the airway present therapeutic potentials for inflammatory lung diseases such as chronic obstructive pulmonary disease (COPD), asthma and acute lung injury/acute respiratory distress syndrome (ALI/ARDS).

COPD models

COPD is characterized by chronic lung inflammation, airway obstruction and remodeling with smoking being the most important risk factor of the disease. The administration of PDE4 inhibitors was shown to efficiently reduce the reflux of neutrophils to the murine lung acutely exposed to cigarette smoking (CS) and prevented the progression to emphysema in mice with chronic CS exposure (161,162). Pivotal study with cilomilast was the first report that revealed the decrease of $CD8^+$ T cells and $CD68^+$ macrophages, two critical components associated with

COPD pathogenesis, in the bronchial specimens of COPD patients (163). In a later study, Roflumilast was shown to induce a decrease of soluble mediators in sputum neutrophils and eosinophils, thus partly contribute to the amelioration of lung functions (147). The promising effects of Roflumilast on the treatment of COPD were further confirmed through different clinical trials. Patients treated with Roflumilast displayed better lung functions in comparison with placebos by showing the improved post-bronchodilator Forced expiratory vial 1 (FEV1) (164). Additionally, the continual use of Roflumilast significantly lowered the frequency of mild to severe exacerbations (165). As of now, Roflumilast is the only PDE4 inhibitor approved by FDA for the treatment of COPD.

Asthmatic models

Asthma is a chronic inflammatory condition that causes reversible airway obstruction, resulting in occasional breathing difficulties and wheezing. In ovalbumin-sensitized animal models, PDE4 inhibitors not only counteracted the increase of eosinophils in the blood and bronchoalveolar lavage fluid (BAL) but also relieved the symptoms of airway hypersensitivity (166,167). In addition to this, the production of IL-4, IL-5, TNF-α and NF-κB were appreciably decreased. Recently, Jin et al demonstrated that PDE4B was the main player in driving Th2 development in allergic asthma (168). Knockout of PDE4B reduced the number of Th2 cells and their related cytokines (IL-4, IL-5 and IL-13) in BAL which in turn switch off the airway hyperresponsiveness (AHR) upon allergen challenge. Asthmatic patients on the PDE4 inhibition therapy displayed attenuated allergen-induced airway inflammation, along with lower accumulation of inflammatory cells and cytokines (169). These evidence provide rationales for the utilization of PDE4 inhibitors for the treatment of allergic asthma.

ALI/ARDS models

ALI/ARDS are clinical presentations of an acute systemic inflammation featured by bilateral pulmonary infiltrates and severe hypoxemia. Numerous studies have been conducted to investigate the preventive and therapeutic potentials of PDE4 inhibition for these pathological conditions (Table 3). For example, lung edema and pulmonary functions of rabbits induced to ALI by saline were significantly improved by Roflumilast (170). Interestingly, Roflumilast but not steroids mitigated the lung fibrotic remodeling in bleomycin-induced lung injury models (171). PDE4 inhibition by other PDE4 inhibitors also present similar effects in chemicals and bacteria induced ALI models (172–174). In mice infected with lethal dose of Influenza A H1N1 virus,

rolipram in combination with the antiviral therapy significantly reduced lung injuries and increased the survival rates up to 80 – 100% (175).

Animal model	Findings	References
Saline-induced ALI in rabbits	PDE4i reduced lung edema and improved pulmonary functions	(170)
Bleomycin-induced lung injuries in mice	PDE4i reduced lung inflammation and fibrosis	(171)
Carfilzomib-induced ALI in rats	PDE4i reduced lung inflammation and reversed toxic effects of carfilzomib.	(173)
Murine LPS models	PDE4i reduced lung inflammation, neutrophil accumulation and prevent alveolar collapse	(172)
Neonatal murine LPS models	PDE4i reduced lung inflammation and apoptosis	(174)
Mice infected with influenza H1N1 virus	PDE4i in combination with antiviral drugs reduced lung inflammation and mortality rates.	(175)

Table 3. Pulmonary animal models with PDE4 inhbitors (PDE4i).

3.4 The novel PDE4 inhibitor Tanimilast

Tanimilast (international non-proprietary name of CHF6001) is a novel and potent selective PDE4 inhibitor that has been developed for the management of COPD. This agent inhibits all of four isoforms with equal potency and especially being 10-fold more potent than Roflumilast (176,177). Tanimilast was designed as an extra fine formulation with the mass median aerodynamic diameter ≤ 2 μm for optimal administration through inhalation (178). This allows the drug to be highly retained in the lung along with low systemic exposure, thus reducing systemic adverse events frequently reported with known oral PDE4 inhibitors. The level of Tanimilast in the lung was found 2000-fold higher than those administered through oral route (179).

When tested in *in vitro* and *in vivo* models, Tanimilast presented promising anti-inflammatory effects on the pathogenesis of COPD which is characterized by a continuous inflammation, neutrophils and macrophage infiltration, $CD8^+$ T cell activation and a Th1/Th17 skewed T-cell response (180). In particular, the high levels of TNF-α play critical role in amplifying the innate immune responses in COPD exacerbations (181). In vitro models showed that Tanimilast exhibited potent inhibitory effects on the release of TNF-α by different macrophage cell lines, alveolar macrophage and lung tissue of COPD patients as well as human DCs (150,182). Neutrophil accumulation was efficiently subdued through direct inhibition of oxidative burst and

chemotaxis (177). Moreover, Tanimilast was capable of decreasing human DC-derived cytokines which are essential for the development of Th1/Th17 cells as well as effector $CD8^+$ T cells (150). Interestingly, Tanimilast reduced the neutrophil infiltration in CS models, even in mice resistant to steroids (183).

Tanimilast has completed phase II of development program by showing promising pharmacodynamic results with a safety profile (178). In the study, patients on the treatment with Tanimilast displayed a lower range of pro-inflammatory cytokines in the sputum in comparison to placebos after 32 days. Both high and low doses of Tanimilast diminished all the important mediators in the pathogenesis of COPD such as leukotriene B4 (LTB4), IL-8, macrophage inflammatory protein 1β (MIP1β or CCL4), matrix metalloproteinase 9 (MMP9), monocyte chemotactic protein 1 (MCP-1 or CCL2) and TNFα. In parallel, the number of sputum eosinophils, lymphocytes and macrophages were also decreased by 10% to 30%. More importantly, Tanimilast was highly tolerated with low frequency of gastrointestinal adverse events and weight loss. Furthermore, a post hoc study underlined the promising effects of Tanimilast on reducing exacerbation rate in a subgroup of COPD patients. A phase III clinical trial has started to evaluate this aspect of Tanimilast in COPD patients with chronic bronchitis and a history of exacerbations.

METHODS

1. Identification of potential TLR7/8-triggering ssRNA PAMPs

The reference SARS-CoV-2 genome (NC_045512, positive strand) was scanned for GU-rich ssRNA fragments with the SequenceSearcher tool in the Fuzzy mode (184). We defined "GU-enriched sequences" short strings with a maximal length of 20 bp, that were composed for more than 40% of the length by "GU" and/or "UG" pairs. The identified 491 GU-rich sequences were further selected based on the content of at least one "UGUGU" Interferon Induction Motif (IIM)(21) (see Suppl. Table 1). Within this list, the following were selected and synthesized by Integrated DNA Technologies (IDT) for subsequent studies: SCV2-RNA1 5'-UGCUGUUGUGUGUUU-3' (genome position: 15692-15706); SCV2-RNA2 5'-GUGUGUGUGUUCUGUUAUUG-3' (genome position: 20456-20475). These sequences were checked for uniqueness with BLAST in the database RefSeq Genome Database (refseq_genomes) within the RNA viruses (taxid: 2559587). Two additional sequences were synthesized, in which "U" was substituted with "A", in order to impair TRL7/8 stimulation (SCV2-RNA1A and SCV2-RNA2A).

2. Cell preparation and culture

Buffy coats from blood donations of anonymous healthy donors were obtained and preserved by the Centro Trasfusionale, Spedali Civili of Brescia according to the italian law concerning blood component preparation and analysis. Peripheral blood mononuclear cells (PBMC) were obtained by density gradient centrifugation and monocytes were subsequently purified by immunomagnetic separation using anti CD14-conjugated magnetic microbeads (Miltenyi Biotec) according to the manufacture's protocol and as previously published (185). Briefly, monocytes were cultured for 6 days in tissue culture plates in complete medium (RPMI 1640 supplemented with 10% heat-inactivated, endotoxin free FBS, 2 mM L-Glutamine, penicillin and streptomycin (all from Gibco, Thermo Fisher Scientific) in the presence of 50 ng/ml GM-CSF and 20 ng/ml IL-4 (Miltenyi Biotec). Untouched peripheral blood cDC1 and cDC2 (cDCs) and pDCs were obtained from PBMC after negative immunomagnetic separation with the Myeloid Dendritic Cell Isolation kit (Miltenyi Biotec) and the Plasmacytoid Dendritic Cell Isolation kit II (Miltenyi Biotec), respectively. pDCs were cultured in completed RPMI medium with 20 ng/ml IL-3 (Miltenyi Biotec). RAW264.7 cells were purchased from American Type Culture Collection and cultured in DMEM complemented with 10% FBS.

3. Cell stimulation

Complexation of RNA with DOTAP Liposomal Transfection Reagent (Roche) was performed as previously described (21). Briefly, 5 µg RNA in 50 µl HBS buffer (20 mM HEPES, 150 mM NaCl, pH 7.4) was combined with 100 µl DOTAP solution (30 µl DOTAP plus 70 µl HBS buffer) and incubated for 15 minutes at RT. In some experiments, cells were stimulated with TLR agonists: LPS (100 ng/ml) and R848 (1 µg/ml) (all from Invivogen). Where indicated, cells were pretreated for 1 hour with Chloroquine or CU-CPT9a (from Invivogen); Tanimilast or β-methasone or Budesonide (from Chiesi Pharmaceuticals). In some experiments, the maturation process was conducted in RPMI containing 2% FBS and supplemented with 0.01% DMSO in the presence of Tanimilast to avoid the sequestration of the drug by serum proteins.

4. siRNA silencing

Differentiating monocytes at day 2 of culture were transfected with two different MyD88 Silencer Select Validated siRNA or with a control siRNA (all at 50 nM final concentration; Ambion, Thermo Fisher Scientific) using Opti-MEM I reduced serum medium and Lipofectamine RNAiMAX transfection reagent (Thermo Fisher Scientific) as previously described (186). Transfected cells were incubated for 72 hours and then stimulated for 24 hours with TLR agonists as indicated. The effects of mRNA silencing by siRNA was investigated by real-time PCR using specific QuantiTect primer Assay (Qiagen).

5. Cytokine detection

TNF-α, IL-1β, CXCL10IL-6, IL-12p70, CXCL8, CXCL9, CCL3, CCL17 and mouse TNF-α were measured by ELISA assay (R&D Systems). Human IFN-α was detected using specific Module Set ELISA kit (eBioscience) and human IFN-β by was measured by a bioluminescence kit (InvivoGen). Mouse IFN-α was measured by a bioluminescence kit (InvivoGen). All assays were performed on cell free supernatants according to the manufacturer's protocol.

6. Flow cytometry

Human and mouse DCs were stained with the following antibodies from Miltenyi Biotec or as specified: Vioblue-conjugated anti-human CD86 (clone FM95, Miltenyi Biotec), PE-conjugated anti-human CD83 (clone REA714), FITC-conjugated anti-human BDCA2 (clone AC144), APC-conjugated anti-human CCR7 (clone REA546), VioGreen-conjugated anti-mouse CD45 (clone REA737), VioBlue or FITC-conjugated anti-mouse MHCII (clone REA564), PerCP-Vio 700-conjugated anti-mouse CD11c (clone REA754), PE-conjugated anti-mouse SiglecH (clone

551.3D3), PE-Vio 615-conjugated anti-mouse CD11b (clone REA592), VioBlue-conjugated anti-mouse CD8a (cloneREA601), PE-Vio 770-conjugated anti-mouse B220 (clone RA3-6B2), PE-conjugated anti-mouse CD40 (clone REA965), FITC-conjugated anti-mouse CD40 (clone HM40-3, Biolegend) and APC-CY7-conjugated anti-mouse CD86 (clone GL-1, Biolegend). Samples were read on a MACSQuant Analyzer (Miltenyi Biotec) and analysed with FlowJo (Tree Star Inc.). For intracellular detection of Granzyme B, cells were fixed and permeabilized using the Inside Stain kit (Miltenyi Biotec) and stained with APC-conjugated anti-Granzyme B (clone REA226, Miltenyi Biotec). Cell viability was assessed by LIVE/DEAD staining according to the manufacturer's instruction (Molecular Probes, Thermo Fisher Scientific). Response definition criteria were defined post-hoc.

7. NF-κB luciferase reporter assay

TLR-specific activation assays were performed using human HEK293 cells expressing luciferase under control of the NF-κB promoter and stably transfected with human TLR7 and TLR8 as previously described (187). Briefly, 25000 cells were seeded in complete DMEM without antibiotics in 96-well plates for 24 hours and then stimulated with 10 µg/ml SCV2-RNA for additional 24 hours. After stimulation, cells were lysed using ONE-Glo EX Luciferase Assay System (Promega) according to the manufacturer's recommendations and assayed for luciferase activity using the EnSightMultimode Plate Reader (PerkinElmer). HEK293-transfected cells were maintained in DMEM supplemented with 10% FBS and specific antibiotics were added.

8. SDS-PAGE and Western Blot

Following the indicated stimulations, moDCs were washed twice with PBS and lysed in L1 buffer (50mM Tris-HCl, pH 8.0; 2 mM EDTA; 0.1% NP-40 and 10% glycerol) supplemented with inhibitors (1mM Na_3OV_4, 2 mM DTT, 1 mM NaF, 1 mM PMSF, and protease inhibitor cocktail; all form MilliporeSigma) to separate cytoplasmic proteins. Nuclear pellets were washed twice with L1 buffer with inhibitors and then lysed in NP-40 Lysis buffer (50 mM Tris-HCl, pH 8.0; 250 mM NaCl; 1 mM EDTA; 0.1% NP-40; and 10% glycerol) with inhibitors. For the analysis of TLR expression, moDCs and HEK293-transfected cells were lysed in NP-40/Triton lysis buffer (10 mM Tris-HCl, pH 7.9; 150mM NaCl; 0.6% NP-40; and 0.5% Triton X-100) supplemented with inhibitors. Equal amounts of extracts were analyzed through SDS-PAGE followed by Western blotting with antibodies against NF-kB p65 (rabbit polyclonal, C-20 cat. sc-372, Santa Cruz Biotechnology inc.), Lamin B (goat polyclonal, C-20 cat. 6216, Santa Cruz Biotechnology inc.),

TLR7 (rabbit monoclonal, cat. 5632, Cell Signaling Technologies), TLR8 (rabbit monoclonal, cat. 11886, Cell Signaling Technologies) and b-actin (mouse monoclonal, C4, cat. sc-47778, Santa Cruz Biotechnology inc.). Protein bands were detected with SuperSignal West Pico Chemiluminescent Substrate (Pierce) and quantified by computerized image analysis using Image LabTM software (Bio-Rad). Data were normalized based on b-actin or Lamin B content.

9. Immunofluorescence

moDCs were incubated with Atto-488-tagged SCV2-RNA1 (synthesized by Bio-Fab research) for 15 minutes, fixed with 4% paraformaldehyde (Pierce) for 10 minutes and then seeded on glass slides by cytospin. After permeabilization with 100% cold methanol for 5 minutes, cells were labelled with a rabbit monoclonal anti-human TLR8 (cat. 11886, Cell Signaling Technologies). A conjugate Alexa Fluor 594 anti-rabbit (A-11072, Thermo Fisher Scientific) was used as a secondary antibody. Glass slides were mounted using Prolong antifade with DAPI (Thermo Fisher Scientific). Cells were analyzed under a Zeiss Observer Z1 epifluorescence microscope equipped with a Plan-Apochromat 100x/ 1.4 numerical aperture oil objective and ApoTome2 imaging system for optical sectioning. Z-stack images were elaborated through AxioVision 3D and extended focus modules.

10. T cell proliferation assay

Allogenic naïve $CD4^+$ T cells and $CD8^+$ T cells were isolated from buffycoats using the naïve $CD4^+$ T cell Isolation kit II (Miltenyi Biotec) and $CD8^+$ T cell Isolation kit (Miltenyi Biotec), respectively. Purified T cells were counted by flow cytometry and labeled with CellTrace-CFSE (Molecular Probes, Thermo Fisher Scientific) at a final concentration of 5 μM. Subsequently, T cells ($1x10^5$ cells/well) were cocultured with graded numbers of allogeneic moDCs in 96-well round-bottom culture plates in complete RPMI medium. After 6 days, alloreactive T cell proliferation was assessed by measuring the loss of the dye CellTrace-CFSE upon cell division using flow cytometry. Positive controls of T cell proliferations were routinely performed using IL-2 plus PHA. Response definition criteria were defined post-hoc. Dead cells were excluded by LIVE/DEAD staining according to the manufacturer's instruction. These experiments were performed using general research investigative assays.

11. Analysis of T cell cytokine production

After 6 days of coculture, helper T cells were restimulated with 200 nM PMA (Sigma-Aldrich) plus 1 μg/ml of ionomycin (Sigma) for 5 hours. Brefeldin A (5 μg/ml, Sigma) was added during

the last 2 hours. For intracellular cytokine production, cells were fixed and permeabilized with Inside Stain kit (Miltenyi Biotec) and stained with FITC-conjugated anti-IFN-γ (clone 45-15, Miltenyi Biotec) and PE-conjugated anti-IL-4 (clone 7A3-3, Miltenyi Biotec) following the manufacturer's recommendations. For $CD8^+$ T cells, after 6 days of coculture, IFN-γ production was assessed in the culture supernatants by ELISA (R&D system). Response definition criteria were defined post-hoc. These experiments were performed using general research investigative assays.

12. In vivo experiments

Sex and age matched C57Bl6/J mice were obtained by Charles River Laboratories and housed in the specific pathogen-free animal facility of the Department of Medicine, University of Verona. $MyD88^{-/-}$ mice were kindly provided by S. Akira (Osaka University, Osaka, Japan). Mice were anesthetized with isoflurane and injected i.v. in the retro-orbital vein with 300 µl DOTAP/SCV2-RNA mixture (20 µg/mouse) or with DOTAP alone. After 6 hours, mice were sacrificed and lungs, spleen and blood were harvested. Briefly, lungs were collected upon intracardiac perfusion with cold PBS. Left lung lobes were formalin fixed for 24 hours, dehydrated, and paraffin embedded for histological analysis. Right lungs were immediately frozen at -80°C and used for real-time PCR. Spleens were mechanically and enzymatically treated to obtain a single-cell suspension for cytofluorimetric and real-time PCR analysis. All mouse experiments were carried out in accordance with guidelines prescribed by the Ethics Committee for the use of laboratory animals for research purposes at the University of Verona and by the Italian Ministry of Health. All efforts were made to minimize the number of animals used and their suffering.

13. Lung histological analysis

Histology was performed on three longitudinal serial sections (150 µm apart, 4 µm in thickness) from each left lung, stained with hematoxylin and eosin (H&E), and scanned by VS120 Dot-Slide BX61 virtual slide microscope (Olympus Optical) as previously described (188).

14. Quantitative PCR (qPCR)

RNA was extracted using TRIzol reagent, treated with DNAse according to the manufacturer's instructions and reverse transcription performed using random hexamers and MMLV RT (all from Thermo Fisher Scientific). The SsoAdvanced Universal SYBR Green Supermix (Bio-Rad Laboratories) was used according to the manufacturer's instructions. Reactions were run in

triplicate on a StepOne Plus Real-Time PCR System (Applied Biosystems) and analyzed by the StepOne Plus Software (Version 2.3, Applied Biosystems). Sequences of gene-specific primers are available upon request. Gene expression was normalized based on RPL32 or HPRT mRNA content.

15. Dead cell uptake

Cryopreserved autologous PBMCs were thawed, labeled with CFSE and then heat-killed (90˚C for 30 min) as previously described (189). Dead cells were added to moDCs at a 1:1 ratio for 2 h at 37˚C. For flow cytometric analysis, the moDCs were stained for HLA-DR, and the percentage of dead cell uptake defined as HLA-DR^{+}CFSE^{+} cells was measured.

16. Statistical analysis

Statistical significance among the experimental groups was determined using paired or unpaired Student's t test or one-way ANOVA with Dunnet's post-hoc test (GraphPad Prism 7, GraphPad Software) as indicated in each figure legend. $P< 0.05$ was considered significant.

17. Study approval

Procedures involving animal handling and care conformed to protocols approved by the University of Verona in compliance with national (D.L. N.116, G.U., suppl. 40, 18-2-1992 and N. 26, G.U. March 4, 2014) and international law and policies (EEC Council Directive 2010/63/EU, OJ L 276/33, 22-09-2010; National Institutes of Health Guide for the Care and Use of Laboratory Animals, U.S. National Research Council, 2011). The study was approved by the Italian Ministry of Health (approval number 339/2015-PR).

AIM OF THE THESIS

The ongoing pandemic COVID-19, caused by SARS-CoV-2, presents diverse clinical manifestations ranging from non- to severe life-threatening conditions with the lung being the preferential target of the virus. In a subgroup of patients, immune dysregulation and hyper-inflammation associated with excessive production of pro-inflammatory mediators were shown to contribute to the severity of the disease (61). This condition suggests that an overactive innate immune response may indeed unleash virus-dependent immune pathology (190). Dendritic cells (DCs) are innate immune cells that, by expressing several nucleic acid sensors, play a crucial role in recognizing viral pathogens and mounting protective inflammatory responses (191). Given the central role of DCs in the regulation of the immune response, excessive activation of these cells may induce overt immunity and tissue damage.

Within DC heterogeneity, pDCs play an important role as the major source of type I IFNs in response to viral infection, while cDCs respond to a vast array of pathogens by producing pro-inflammatory cytokines and are the main responsible for T cell activation (27). pDCs sense ssRNA viruses through TLR7 while cDCs express the closely related TLR8 (92). Despite the fact that TLR7 and TLR8 display high structural and functional homology, similar ligand specificity (93) and recruit the same signaling intracellular adaptor molecule, MyD88 (101), the signaling pathways of these two TLRs diverge in the functional significance, with TLR7 more involved in the antiviral immune response and TLR8 mastering the production of pro-inflammatory cytokines. During the progression of SARS-CoV-2 infection, both DCs and $CD4^+$ and $CD8^+$ T cell are recruited to the lung (41,126), with Th1/Th17 effectors reported to play a pivotal role in severe COVID-19 pneumonia (31,47). Thus, DCs represent an interesting pharmacological target to modulate detrimental immune responses, possibly including those observed in severe forms of COVID-19. However, the mechanisms of SARS-CoV-2 recognition and activation by DCs remained to be elucidated.

Several immunomodulatory therapies targeting the inflammation-driven damaging stages were proposed for the treatment of severe COVID-19 (192). Among these, inhibitors of PDEs have been put forward based on the analogy between the clinical features of COVID-19 and other pathologies, associated with inflammation, for which these drugs are already approved (193). Inhibition of PDE4 was shown to increase intracellular cAMP, consequently lead to a shift of the anti-inflammatory/pro-inflammatory balance (141). Such upstream anti-inflammatory mechanism, makes these agents particularly interesting to master critical conditions

characterized by overt release of multiple cytokines, as compared to other single downstream anti-cytokine drugs (194). Tanimilast is an inhaled, selective inhibitor of PDE4 isoforms A-D endowed with anti-inflammatory properties in several in vitro and in vivo models (159,183). In particular, published data by our group highlighted that Tanimilast can reduce the secretion of inflammatory and Th1/Th17 polarizing cytokines by fine tuning the activity of the master inflammatory transcription factor NF-κB, which could be useful to control Th-1 and Th-17 driven pathologies without inducing a global repression of the inflammatory and immune responses (150).

Aims of this thesis were (1) to characterize the SARS-CoV-2-associated molecular patterns (SAMPs) and the potential pathway in the activation of human pDCs and cDCs and (2) to uncover the potential immunomodulatory effects of PDE4 inhibition in inflammatory and immune-mediated conditions, especially in the context of SARS-CoV-2 infection.

RESULTS

A. SARS-COV-2 mRNA ACTIVATE INFLAMMATION AND IMMUNITY VIA TLR7/8

1. Results

1.1 Identification of potential ssRNA SAMPs

Based on previous work identifying RNA40, a ssRNA rich in guanine and uracil (GU-rich) from the U5 region of HIV-1, as the first natural agonist of TLR7 and TLR8 (195) and on known features of TLR7/8 ligands (93,187), we searched for putative immunostimulatory sequences within the SARS-CoV-2 ssRNA genome. Our bioinformatic scan revealed 491 GU-rich sequences, among which more than 250 also bearing at least one “UGUGU” Interferon Induction Motif (IIM) (93,187,195).

We hypothesized that these sequences may represent so far unidentified SAMPs responsible for viral recognition and immune activation via endosomal TLR triggering. The elevated number of sequences detected suggests that, upon endosomal engulfment, the fragmentation of the SARS-CoV-2 genome may generate many TLR7/8-triggering sequences, thus displaying high chances to contact and activate the IFN and inflammatory responses downstream these receptors.

To validate the stimulatory potential on innate immune cells, two representative sequences, SCV2-RNA1 and SCV2-RNA2, were chosen within the previous list, synthesized and tested in in vitro and in vivo models of inflammation.

1.2 ssRNA SAMPs activate human monocyte-derived DCs (moDCs)

moDCs, a model of inflammatory cDCs expressing a wide variety of TLRs (89,92), were treated with increasing concentrations of SCV2-RNA1 and SCV2-RNA2 along with HIV-1-derived RNA40 (195), used as a positive control. U/A alternated control sequences SCV2-RNA1A and SCV2-RNA2A were used as negative controls (see materials and methods). Figure 16A shows that both fragments efficiently activated cytokine secretion by moDCs. In particular, we observed potent induction of pro-inflammatory cytokines (TNF-α, IL-6), of the Th1-polarizing cytokine IL-12 and chemokines recruiting polymorphonuclear neutrophils (CXCL8), myelomonocytic cells (CCL3) and Th1- and cytotoxic effectors cells (CXCL9). Especially at low concentrations, SCV2-RNA1 and SCV2-RNA2 were more efficient than HIV-1-derived RNA40. In all experimental conditions, U/A alternated SCV2-RNA1A and SCV2-RNA2A did not induce

cytokine secretion. SCV2-RNA1 and SCV2-RNA2 also induced moDCs phenotypical maturation in terms of CD83, CD86 and CCR7 expression (Figure 16B). Similar to cytokine secretion, upregulation of maturation markers by RNA40 was less effective. These results demonstrated that both SCV2-RNA1 and SCV2-RNA2 behave as SAMPs endowed with potent DC stimulatory capacity. Because of their similar potency, further experiments were carried out using a mixture of the two SAMPs (indicated as SCV2-RNA), a condition that may also better mimic a physiological stimulation by multiple sequences derived from SARS-CoV-2 genome endosomal fragmentation.

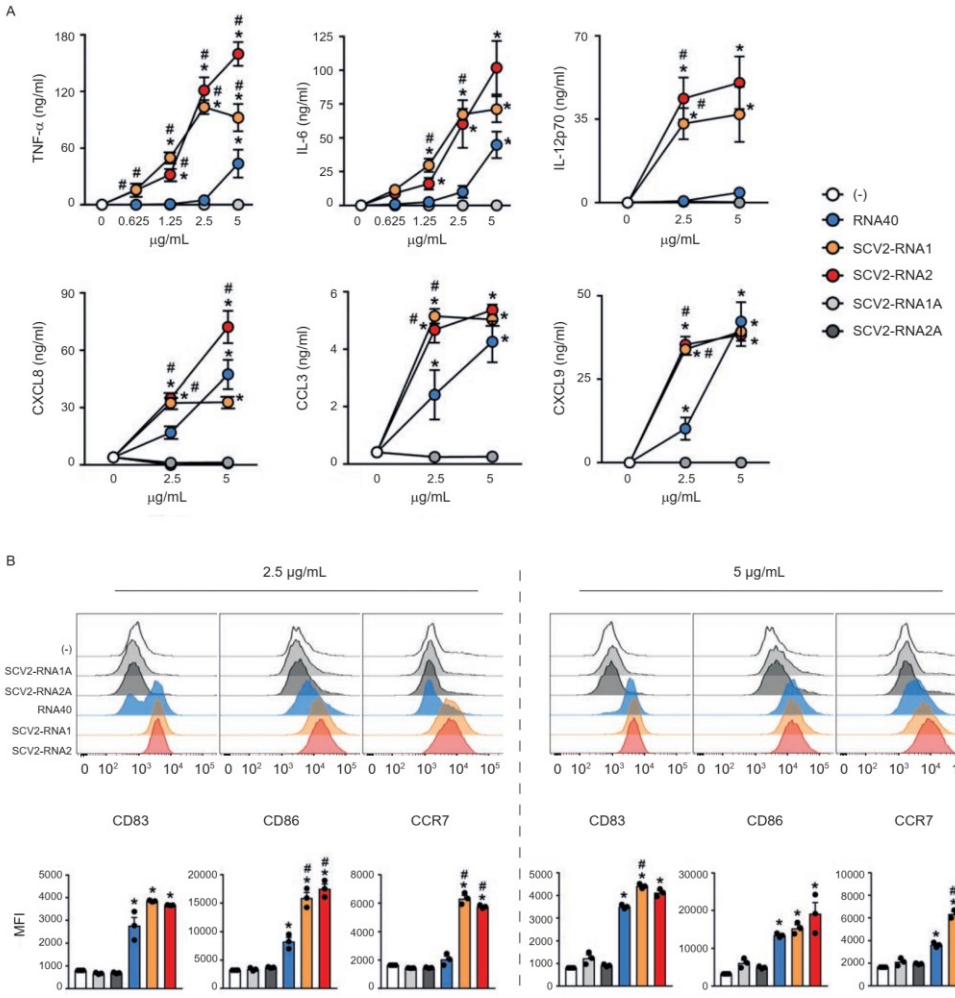

Figure 16. SAMPs activate cytokine secretion and phenotypical maturation of moDCs. (A) moDCs ($2x10^6$/ml) were stimulated with increasing concentrations of the indicated viral RNAs or with vehicle alone (-) for 24 hours. The production of TNF-α, IL-6, IL-12p70, CXCL8, CCL3 and CXCL9 was evaluated by ELISA in cellfree supernatants. Data are expressed as mean ± SEM (n=3). Results of SCV2-RNA1A and SCV2-RNA2A are superimposed in all graphs. (B) moDCs were stimulated as described in (A) and the surface expression of CD83, CD86 and CCR7 evaluated by FACS analysis. Data are expressed as representative cytofluorimetric profiles (upper panels) or as the mean ± SEM (n=3) of the Median of Fluorescence Intensity (MFI) (lower panels). (A-B) *P< 0.05 versus (-) by one-way ANOVA with Dunnett's post-hoc test; #P< 0.05 versus RNA40 by paired Student's t test.

1.3 ssRNA SAMPs activate T cell responses

The impact of SAMPs on the ability of DCs to stimulate T cell functions was investigated in co-culture experiments of SAMP-activated DCs with allogeneic naïve $CD4^+$ and $CD8^+$ T cells. Figure 17A shows that SAMP-activated DCs induced proliferation of both naïve $CD4^+$ (left) and $CD8^+$ (right) T cells. Activated $CD4^+$ T cells produced IFN-g but no IL-4, a typical Th1-effector phenotype (Figure 17B). Functional activation of $CD8^+$ T cells was similarly demonstrated by the detection of secreted IFN-g (Figure 17C, left panel) and the intracellular accumulation of Granzyme B (GrB, right panel), a marker of a cytotoxic phenotype. None of these effects were observed when DCs were activated with U/A alternated SAMPs.

These experiments demonstrated that phenotypical DC maturation induced by SAMPs (Figure 16B) is paralleled by the acquisition of T-cell activating capabilities. Thus, SAMPs have the ability to induce a Th1-oriented immune response.

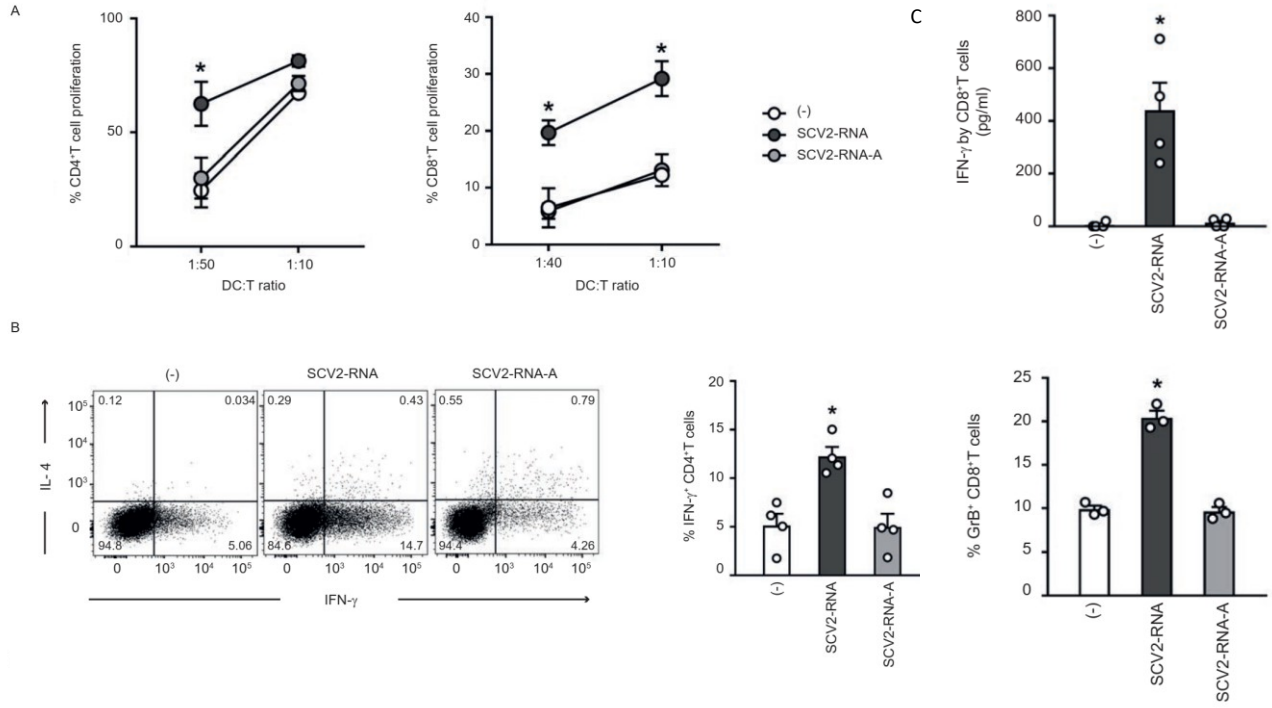

Figure 17. SAMP-activated DCs trigger T cell proliferation and functional activation. (A) moDCs were stimulated with vehicle (-) or with SCV2-RNA or the A-to-U-replaced SCV2-RNA-A (both at 5 µg/ml) for 24 hours. Activated moDCs were co-cultured for 6 days with CFSE-stained allogenic naïve $CD4^+$ T cells or CD8+ T cells at the indicated DC:T cell ratio. Alloreactive T cell proliferation was assessed by measuring CellTraceCFSE dye loss by flow cytometry. Data are expressed as mean ± SEM (n=3) of the percentage of proliferating T cells. (B) moDCs stimulated as in (A) were cocultured for 6 days with allogenic naïve $CD4^+$ T (DC:T cell ratio 1:20). Intracellular IFN-γ and IL-4 were evaluated by FACS analysis. Left, dot plots from one representative experiment out of four is shown. Right, bar graphs from four independent experiments. Data are expressed as mean ± SEM of the percentage of IFN-γ-producing cells. (C) moDCs activated as in (A) were cocultured for 6 days with allogenic CD8+ T (DC:T cell ratio 1:10). IFN-γ production was evaluated by ELISA in cell-free supernatants and intracellular Granzyme B (GrB) by FACS analysis. Data are expressed as mean ± SEM (n=3). (A-C) *P< 0.05 versus (-) by one-way ANOVA with Dunnett's post-hoc test.

1.4 ssRNA SAMPs activate human primary DCs

The ability of SCV2-RNAs to activate DCs was further investigated using primary circulating cDCs (comprising CD141$^+$ cDC1 and CD1c$^+$ cDC2) and BDCA2$^+$ pDCs. SCV2-RNA efficiently induced the secretion of TNF-α and IL-6 (Figure 18A) and the expression of maturation markers, such as CD86 and CCR7 (Figure 18B) in cDCs. Similarly, SAMPs stimulated the release of IFN-α and TNF-α by pDCs (Figure 18C), as well as their maturation in terms of CD86 upregulation and BDCA2 reduction (Figure 18D). Similar to previous results, U/A alternated control sequences did not activate cytokine production or maturation in either pDCs or cDCs (not shown).

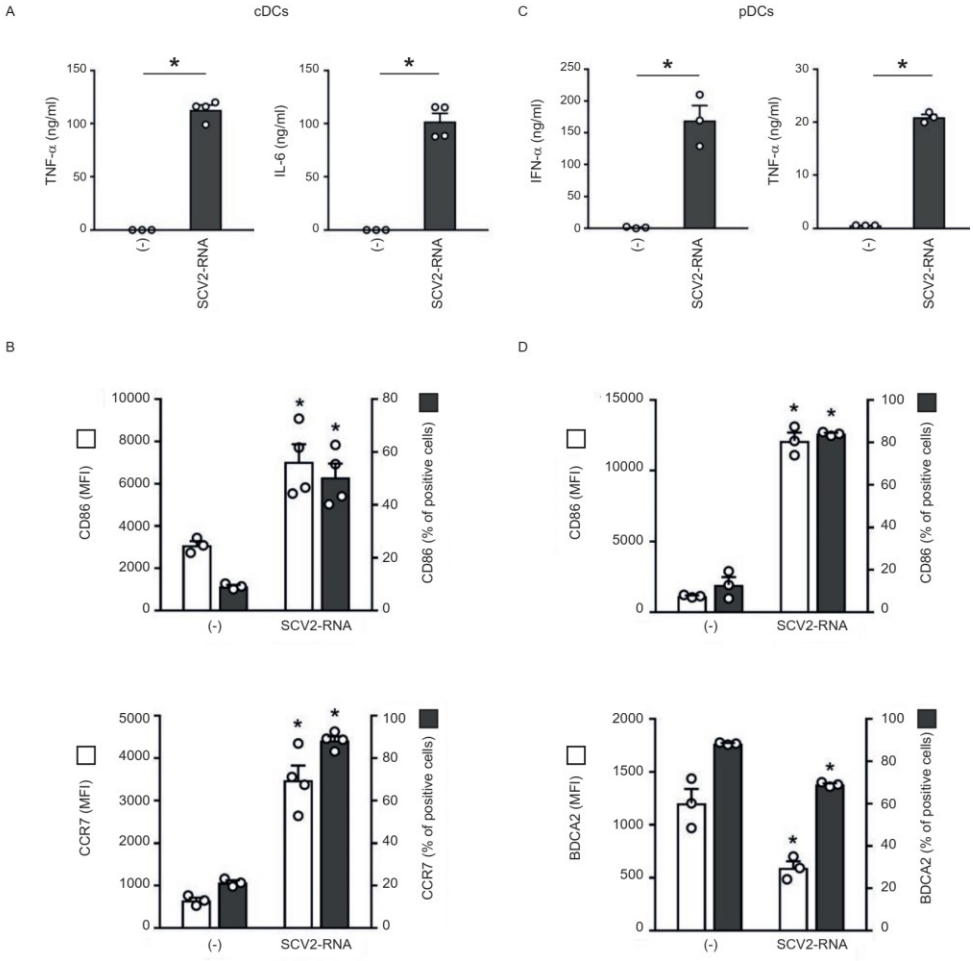

Figure 18. SAMPs activate cytokine secretion and phenotypical maturation in primary circulating DC subsets. cDCs ($2x10^6$/ml) and pDCs ($1x10^6$/ml) were stimulated with 5 µg/ml SCV2-RNA for 24 hours. (A-C) Cytokine secretion was evaluated by ELISA. Data are expressed as mean ± SEM (n=3-4); *P< 0.05 versus (-) by paired Student's t test. (B-D) Surface expression of CD86, CCR7 and BDCA2 was evaluated by FACS analysis. Data are expressed as mean ± SEM of the median fluorescence intensity (MFI) (left y axis), as well as the mean ± SEM of the percentage of positive cells (right y axis) (n=3-4); *P< 0.05 versus (-) by paired Student's t test.

1.5 ssRNA SAMPs activate the TLR8/MyD88/NF-κB axis in moDCs

The cellular sensors responsible for SARS-CoV-2 detection by immune cells remain ill defined. To formally demonstrate the ability of SAMPs to functionally activate TLRs, experiments were performed in HEK293 cells stably transfected with human TLR7 and TLR8 together with a NF-κB reporter gene. Figure 19A depicts the SAMP-dependent activation of NF-κB and luciferase production in both TLR7- and TLR8-expressing cells. NF-κB activation was also detected in SCV2-RNA-stimulated moDCs (Figure 19B). Since both TLR7 and TLR8 signal through the common adaptor MyD88, siRNA interference was performed in moDCs. Figure 19C (left panel) shows that MyD88-specific siRNA could decrease by about 50% the levels of MyD88 mRNA, while the expression of the TLR3-related adaptor TRIF and RLR-related MAVS was not affected. Consistent with this result, IL-6 production by SCV2-RNA was also decreased, supporting a role for MyD88 in moDC activation by SCV2-RNA (Figure 19C, right panel). Because SAMPs, despite designed to activate TLR7/8, may also engage other PRRs expressed by moDCs, we also performed TRIF and MAVS siRNA interference. While siRNAs efficiently and specifically inhibited the expression of target genes (Figure 19C, left panel), they failed to reduce IL-6 production by SCV2-RNA (Figure 19C, right panel). The predominant role of the MyD88/NF-κB pathway as compared with that of TRIF/MAVS/IRF-3 was also supported by the lack of SCV2-RNA-dependent induction of nuclear translocation of IRF-3, a transcription factor downstream TLR3 and RLRs (not shown).

moDCs are known to respond mainly to TLR8 ligands and to express negligible levels of TLR7 mRNA (92). mRNA and protein expression analysis of TLR7 and TLR8 confirmed selective expression of TLR8 in our experimental setting (data not shown). Based on this, we performed TLR8 siRNA in moDCs, showing a reduction in SCV2-RNA-dependent activation correlating to the levels of mRNA reduction (Figure 19D).

Next, moDCs were stimulated in the presence of CU-CPT9a, a specific TLR8 inhibitor (26). CU-CPT9a inhibited both NF-κB nuclear translocation (Figure 19E) and IL-6 production when cells were stimulated with SCV2-RNA or R848 (TLR7/8 ligand) (Figure 19F). On the other hand, the TLR8 inhibitor did not affect the stimulation by LPS, a TLR4 ligand (Figure 19E and F). Finally, we found that SCV2-RNA colocalizes with TLR8 within moDCs (data not shown).

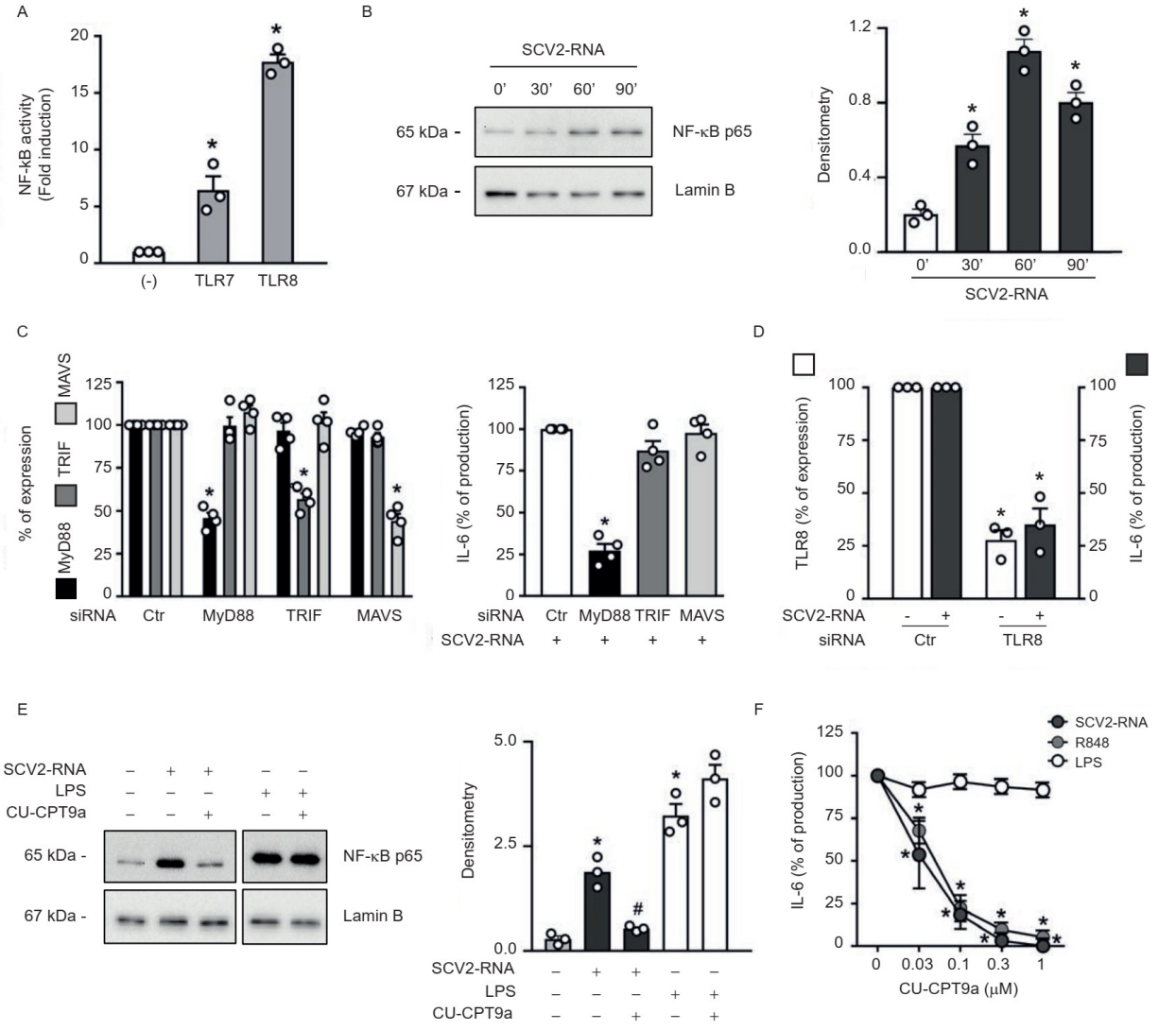

Figure 19. SAMPs activate the TLR8/MyD88/NF-κB axis in moDCs. (A) HEK-293 cells stably transfected with human TLR7, TLR8 or luciferase alone (-) were stimulated with SCV2-RNA for 24 hours. NF-κB activation was evaluated as luciferase activity. Data are expressed ad mean ± SEM (n=3); *P< 0.05 versus (-) by one-way ANOVA with Dunnett's post-hoc test. (B-E) moDCs were stimulated with SCV2-RNA as indicated (B) or pretreated with CU-CPT9a (1 μM) and then stimulated with SCV2-RNA or LPS for 1 hour (E). Nuclear extracts were blotted against NF-κB p65 and Lamin B. One representative donor and densitometry of three donors are shown. *P< 0.05 versus untreated by one-way ANOVA with Dunnett's post-hoc test; #P< 0.05 versus "SCV2-RNA" by paired Student's t test. (C, left panel) moDCs were transfected with indicated siRNAs and target gene expression evaluated by qPCR. Results depict percentage of target gene expression (mean ± SEM n=4). (C, right panel) moDCs transfected with indicated siRNAs were stimulated with SCV2-RNA for 24 hours and IL-6 production evaluated by ELISA. Data are expressed as percentage of production (n=4); *P< 0.05 versus "ctr siRNA" by one-way ANOVA with Dunnett's post-hoc test. (D) moDCs were transfected with indicated siRNAs and the expression of TLR8 was evaluated by qPCR (left y axis, white bars). IL-6 production upon SCV2-RNA stimulation was evaluated by ELISA (right y axis, grey bars). Data (percentage of expression/production) represent the mean + SEM (n=3); *P< 0.05 versus respective "ctr" by paired Student's t test. (F) moDCs were pre-treated with CU-CPT9a, then stimulated as indicated for 24 hours and IL-6 production evaluated by ELISA. Data are expressed as percentage of production for each individual stimulation (n=3); *P< 0.05 versus respective "0" by one-way ANOVA with Dunnett's post-hoc test.

1.6 ssRNA SAMPs act as TLR7/8 ligands in primary DCs

TLR7 and TLR8 display a mutual exclusive expression in primary DCs. Indeed, cDCs express TLR8 as their unique endosomal ssRNA receptor, while pDCs express TLR7 (92). Consistent with this, CU-CPT9a blocked the production of pro-inflammatory cytokines in cDCs (Figure 20A), but not in TLR7-expressing pDCs (Figure 20B). Our effort to block TLR7 signaling using commercially available receptor antagonists was unsuccessful since none of these inhibitors blocked TLR7 activation in pDCs stimulated with R848 or Imiquimod (data not shown). As an alternative strategy to demonstrate the involvement of TLR7 in SCV2-RNA sensing we performed TLR desensitization (187). pDCs were stimulated withSCV2-RNA or R848 or left untreated, washed, and then re-stimulated with R848. Figure 20C shows that, upon re-stimulation, only untreated cells could respond to R848 in terms of IFN-α and TNF-α production as a result of TLR7 desensitization by its ligand R848 as well as by SCV2-RNA. The limited yield following blood DC purification hampered the use of siRNAs. However, the involvement of endosomal TLRs as SCV2-RNA receptors was further supported by the blocking of cytokine release in both cDCs (Figure 20D) and pDCs (Figure 20E) by chloroquine (CQ), a drug known to block endosomal TLR triggering by interfering with endosomal acidification (196).

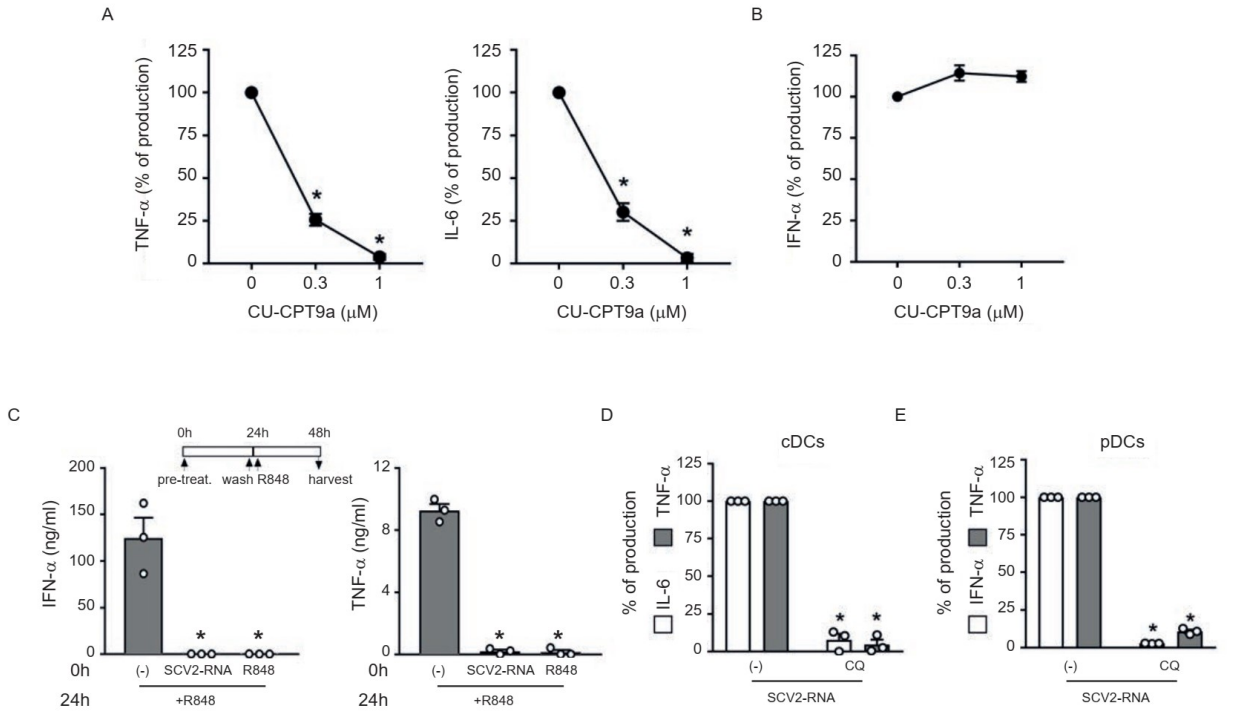

Figure 20. TLR7 and TLR8 are responsible for primary DC activation by SAMPs. cDCs (A) and pDCs (B) were pre-treated with increasing concentration of CU-CPT9a and then stimulated with SCV2-RNA (5 μg/ml) for 24 hours. Secreted TNF-α, IL-6 and IFN-α were quantified by ELISA. Data are expressed as percentage of production (n=3); *P< 0.05 versus "0" by one-way ANOVA with Dunnett's post-hoc test. (C) pDCs were pretreated (0h) with SCV2-RNA (5 μg/ml) or R848 (1 μg/ml) or left untreated for 24 hours, washed and restimulated with R848 for additional 24 hours. Secreted IFN-α and TNF-α were quantified by ELISA. Data are expressed as mean ± SEM (n=3); *P< 0.05 versus "(-)" by one-way ANOVA with Dunnett's post-hoc test. (D) cDCs were pre-treated for 1 hour with Chloroquine (CQ, 10 μM) and then stimulated with SCV2-RNA (5 μg/ml) for 24 hours. Secreted IL-6 (white bars) and TNF-α (grey bars) were evaluated by ELISA. Data are expressed as percentage of production (n=3); *P< 0.05 versus respective "(-) SCV2-RNA" by paired Student's t test. (E) pDCs were pre-treated for 1 hour with CQ (10 μM) and then stimulated with SCV2-RNA (5 μg/ml) for 24 hours. Secreted IFN-α (white bars) and TNF-α (grey bars) were quantified by ELISA. Data are expressed as percentage of production (n=3); *P< 0.05 versus respective "(-) SCV2-RNA" by paired Student's t test.

1.7 ssRNA SAMPs induce DC activation and lung inflammation in vivo

To address the capacity of SAMPs to induce inflammation and immune activation in vivo, we first investigated if SAMPs can also trigger murine TLR7, the only GU-rich ssRNA-sensing TLR in mouse (195). Murine TLR7 activation by SAMPs could be hypothesized based on previous works demonstrating that activation of human TLR7/8 and murine TLR7 by common GU-rich ssRNA ligands (195,197). In support of this, we show that TLR7-expressing RAW264.7 cells (Figure 21A) responded to SAMP stimulation by producing TNF-α, an effect that was reduced by CQ pretreatment (Figure 21B) confirming that SCV2-RNA activate murine cells, presumably via TLR7. In addition, splenocytes from MyD88$^{-/-}$ mice did not respond to SCV2-RNA stimulation either in terms of pro-inflammatory cytokine production (Figure 21D) and of TLR modulation

(data not shown) despite expressing similar levels of TLRs as compared to WT mice (Figure 21C).

Based on these results, C57Bl6/J WT and MyD88$^{-/-}$ mice were injected i.v. with SAMPs or vehicle and sacrificed 6 hours later. A significant increase of type I IFN was detected in the sera of WT SAMP-treated mice indicating systemic immune activation (Figure 21E). Consistent with this, SAMPs induced the upregulation of CD40 and CD86 on splenic pDCs (CD11cintMHC-II^{+}B220^{+}SiglecH^{+}) (Figure 21F). Activation of splenic cDC1s (CD11c^{+}MHC-II^{+}CD8a^{+}CD11b^{-}) and cDC2s (CD11c^{+}MHC-II^{+}CD8a^{-}CD11b^{+}) was also detected (Figure 6G and H). Figure 22A shows that SAMP treatment induced the expression of pro-inflammatory cytokines TNF-α, IL-1β, IL-6 and of IFN-α and IFN-γ in the lung. In addition, a marked increase in the expression of chemokines active on myeloid and Th1 effector cells (i.e. CCL3, CCL4 and CXCL10) was also detected. Conversely, CCL20 and CCL22, two chemokines active in Th17 and Th2 T cell recruitment, were not increased (Figure 22B). We could also detect the accumulation of molecules involved in cytotoxic tissue damage such as GrB and TRAIL (Figure 22C) that, given the short kinetics of stimulation, may reflect the recruitment of NK cells to the lungs. The increase of CD45 and MHC-II levels (data not shown) further suggested immune cell infiltration, which was confirmed by histological analysis. Lung histology revealed a marked infiltration of inflammatory cells into peri-bronchial and peri-vascular connective tissue and alveolar septal thickening in SAMP-treated mice (Figure 22D). On the contrary, SAMP administration to MyD88-/- mice did not induce any inflammatory response, including the increase of circulating levels of type I IFN, DC maturation and the generation of a lung infiltrate (Fig. 21 D-H and Figure 22). These data extend to the in vivo condition the observation that SAMPs use a TLR/MyD88-dependent pathway to trigger a type I IFN/pro-inflammatory activation program and highlight lung as a primary target organ.

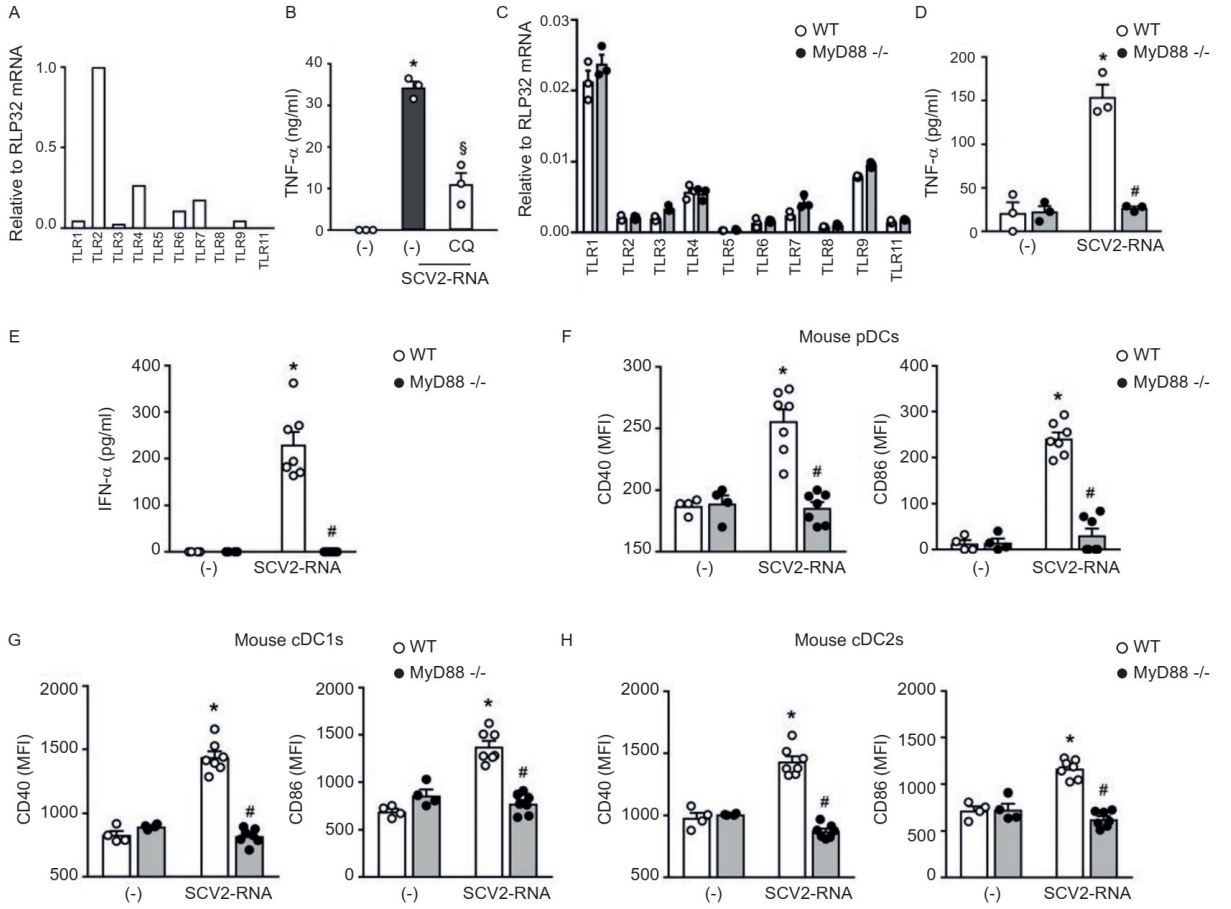

Figure 21. SAMPs activate murine cells in vitro and in vivo. (A) Expression of TLR mRNAs in RAW264.7 cells. Data are expressed as 2-ΔCt relative to RPL32 of one representative experiment out of three. (B) RAW264.7 ($1x10^6$/ml) were pre-treated for 1 hour with CQ (12.5 μM), then stimulated with 5 μg/ml SCV2-RNA or vehicle (-) for 24 hours. Secreted TNF-α was evaluated by ELISA. Data are expressed as mean ± SEM (n=3); *P< 0.05 versus (-); #P<0.05 versus "(-) SCV2-RNA" by paired Student's t test. (C) Expression of TLR mRNAs in splenocytes from WT (white circle) or MyD88$^{-/-}$ mice (black circle). Data are expressed as mean ± SEM (n=3) of $2^{-\Delta Ct}$ relative to RPL32 of one representative experiment out of three. (D) Splenocytes ($3x10^6$/ml) from WT (white circle) or MyD88$^{-/-}$ mice (black circle) were stimulated with 5 μg/ml SCV2-RNA or vehicle (-) for 24 hours. Secreted TNF-α was evaluated by ELISA. Data are expressed as mean ± SEM (n=3); *P< 0.05 versus (-) or #P < 0.05 versus "SCV2-RNA MyD88$^{-/-}$" by paired Student's t test. (E) Circulating IFN-α in WT (white circle) or MyD88$^{-/-}$ mice (black circle) treated with SCV2-RNA or vehicle (-) for 6 hours. Data are expressed as mean ± SEM ((-) n=4, SCV2-RNA n=7); *P< 0.05 versus (-) or #P < 0.05 versus "SCV2-RNA MyD88$^{-/-}$" by unpaired Student's t test of one representative experiment out of three. (F-H) Activation of splenic pDCs (CD11cintMHCII$^+$B220$^+$SiglecH$^+$) (F), cDC1s (CD11c$^+$MHC-II$^+$CD8α$^+$CD11b$^-$) (G) or cDC2s (CD11c$^+$MHC-II$^+$CD8α$^-$CD11b$^+$) (H) from WT (white circle) or MyD88$^{-/-}$ mice (black circle), treated with SCV2-RNA or vehicle (-) for 6 hours evaluated in terms of CD40 and CD86 expression. Data are expressed as mean ± SEM of the median fluorescence intensity (MFI) ((-) n=4, SCV2-RNA n=7); *P< 0.05 versus (-) or #P < 0.05 versus "SCV2-RNA MyD88$^{-/-}$" by unpaired Student's t test.

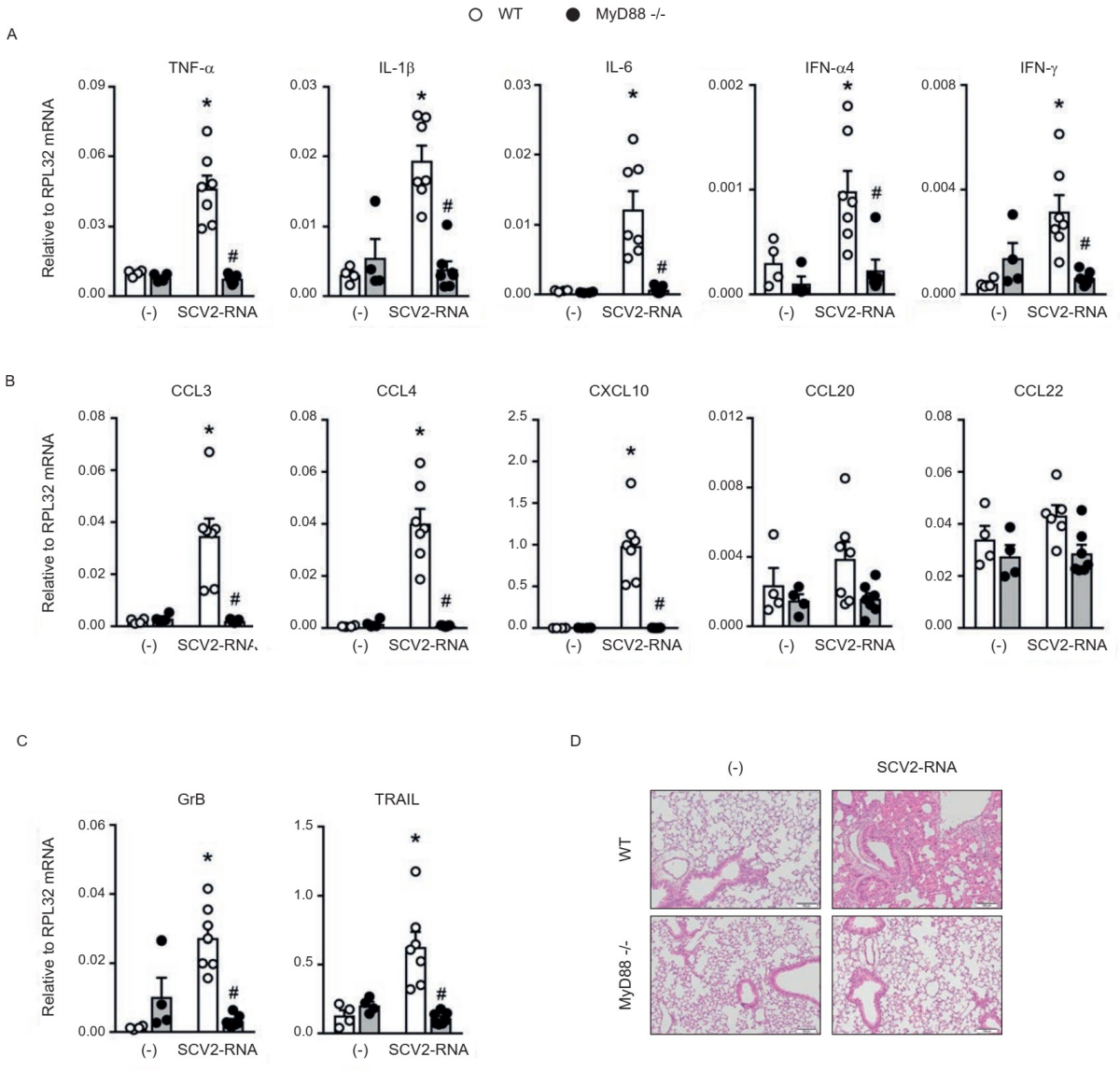

Figure 22. SAMPs induce inflammation in vivo. (A-C) Real-time PCR for cytokines, chemokines and effector proteins in lungs of WT (white circle) or MyD88$^{-/-}$ (black circle) treated or not with SCV2-RNA for 6 hours. Data are expressed as mean ± SEM ((-) n=4, SCV2-RNA n=7) of $2^{-\Delta Ct}$ relative to housekeeping mRNA (RPL32); *P< 0.05 versus (-) or $^{\#}$P < 0.05 versus "SCV2-RNA MyD88$^{-/-}$" by unpaired Student's t test of one representative experiment out of three. (D) Histological evaluation of lungs from WT or MyD88$^{-/-}$ mice treated or not with SCV2-RNA for 6 hours. Image shows one section out of the three longitudinal serial sections performed of one representative left lung out of 7. Scale bars = 100 µm.

2. Discussion

Here, we report that two short sequences within the ssRNA genome of SARS-CoV-2 activate the production of type I IFNs and the T cell-activating ability of human DCs by triggering endosomal TLR7 and TLR8. Of note, these sequences represent prototypical examples of the

several hundreds of potential TLR ligands identified by SARS-CoV-2 genome scan. This finding is in line with previous work demonstrating a twenty-fold higher density of GU-rich fragments in the closely related SARS-CoV as compared to HIV-1 (198) and with a recent bioinformatic study showing that SARS-CoV-2 encodes a number of such fragments even larger than SARS-CoV (199). Thus, endosomal processing of SARS-CoV-2 nucleic acids may give rise to multiple fragments endowed with the property to trigger innate immune activation.

TLR7/8 are sensors of ssRNA viruses including coronaviruses. In the past, TLR7-dependent recognition of MERS-CoV and human and murine pDC activation was demonstrated (200). In addition, murine coronavirus activated protective type-I IFN production by TLR7-expressing murine pDC (201) and ssRNA SARS-CoV genome was shown to induce TLR7/8 dependent cytokine secretion by human PBMCs and RAW264.7 murine cells (198). By contrast, the involvement of TLR7/8 in the immune response against SARS-CoV-2, as well as their role in COVID-19 pathogenesis and therapeutic potential has been only hypothesized (202). Notably, very rare loss-of-function variants of TLR7 in two independent families were associated with severe COVID-19 in males (203). Thus, our report on the ability of SAMPs to activate the TLR7/8 and MyD88 pathways provides the missing link between clinical evidence and molecular knowledge on the cellular sensors for SARS-CoV-2 detection. Viral recognition by endosomal TLRs takes place before and independently of infection, as a consequence of pathogen endocytosis (92). Indeed, pDCs were reported to be resistant to infection, although they were activated by SARS-CoV-2 (204). This is an important process that gives innate immune cells the opportunity to activate early antiviral response. One limitation of our experimental approach is that it does not shed light on the actual triggering of endosomal TLRs during active SARS-CoV-2 infection. However, this is a likely event based on the reported SARS-CoV-2-dependent pDC activation, which use TLR7 as the main ssRNA receptor (92,204). In addition, endosomal TLRs expressed by innate immune cells were shown to be activated by viral RNAs packaged within extracellular vesicles by infected tissue cells (205), a mechanisms that is mimicked by SCV2-RNA-delivery by liposomal particles. Indeed, in another experimental setting, liposome-delivered ssRNA40 from HIV-1 activated human macrophages via TLR8 in a way that recapitulated intact HIV-1 administration (206). It remains to be elucidated if SARS-CoV-2 uptake for endosomal processing is a direct process or mediated by receptors, such as ACE2 or CD147 (124).

DCs are heterogeneous cells that master activation of inflammation and antiviral responses, adaptive immune responses and tolerance as well (76). These functions are largely shared among different phenotypical and functional DC subsets (79). Indeed, pDCs are the major

producers of type I IFNs in response to viral infections (27), while cDCs, and cDC2s in particular, sustain inflammation via cytokine secretion and activate naïve T cells (79). Notably, this specialization mirrors the respective expression and function of TLR7 and TLR8 (92). The protective role of TLR7 and type I IFNs in life-threatening COVID-19 has been documented based on the clinical outcome of patients with inborn errors in type I IFN immunity, producing blocking auto-Abs against different types of type I IFNs (28,29) or expressing loss-of-function variants of TLR7 (203). Therefore, SAMPs may represent one of the essential signals in the activation of an IFN response and Th1-oriented adaptive immunity (207,208). In this regards it is of note that SARS-CoV-2 infection affected the number of pDCs in vivo (125) and primary virus isolates induced the activation of pDCs, in vitro (204). By contrast, an aggravated inflammatory response causes damage to the host and frequently advances to ARDS in severe COVID-19 patients. Here, we show that the activation program induced by SAMPs is not restricted to type I IFNs but encompassed the production of pro-inflammatory cytokines and the generation of Th1-oriented responses, which may contribute to the exuberant pro-inflammatory response observed in life-threatening COVID-19 (209). Whether TLR8 or cDC overactivation or genetic variants are involved in this process is difficult to speculate, and more studies on selected patient cohorts are needed. However, TLR7 and TLR8 selective agonists or antagonists, inducing antiviral interferon response and/or controlling inflammation, deserve consideration and have entered Phase II clinical trial as interesting therapeutic options to control the different manifestations of COVID-19 (https://clinicaltrials.gov/ct2/show/NCT04448756). ssRNA-sensing TLRs are expressed also by cells other than DCs such as macrophages, as well as by peripheral tissues such as lung, bronchus, rectum, and cerebral cortex (124). Thus, other cells may contribute to the complex balance of protective versus detrimental immune activation (210). Finally, since the magnitude of TLR activation differs in individuals, such as elderly people, differences in TLR activation may help explain differences in the quality of the antiviral immune response independently of SAMP potency (79).

By all means, other SAMPs and DAMPs as well as the simultaneous engagement of different PRRs are likely to contribute to COVID-19-associated protective response and cytokine storm, including cytosolic sensors, such as retinoid-inducible gene-I (RIG-I)-like receptors (188), Interferon Induced proteins with tetratricopeptide repeats, or members of a large group of RNA-binding molecules with poorly defined ligand specificity (188). A search for specific candidate ligands of cytosolic RNA-sensors was hampered because the scarce definition of their ligand consensus sequences. However, the finding that SARS-CoV-2 can evade innate immune

restriction provided by intracellular RNA-sensors via methylation the 5′-end of its cellular mRNAs (211) further reinforces the role for TLRs as crucial sentinels and regulators of immune response to SARS-CoV-2 infection. SARS-CoV-2 is known to induce inflammasome assembly despite the exact mechanism still need to be characterized (212). Since intracellular nucleic acid sensors are known to activate inflammasomes (213), and TLR activation is intimately connected with inflammasome functions (214), it is possible that SCV2-RNAs used in this study may also contribute to activate this pathway.

In conclusion, this work describes that SARS-CoV-2 is as a potential powerful source of immunostimulatory nucleic acid fragments and identifies the first SARS-CoV-2-specific PAMPs endowed with the ability to promote inflammation and immunity triggering TLR7 and TLR8. Based on previous works demonstrating a) the crucial protective role of type I IFNs against COVID-19 (207,208); b) the crucial protective role of TLR7 against life-threatening SARS-CoV-2 infection (203) and c) pDC activation in vitro by SARS-CoV-2 (204), we believe that our findings fill a gap in the understanding of SARS-CoV-2 host-pathogen interaction.

B. TANIMILAST SKEWS DENDRITIC CELL ACTIVATION BY SARS-COV2 ssRNA TOWARDS AN IMMUNOMODULATORY PHENOTYPE

1. Results

1.1 Tanimilast selectively reduces the secretion of cytokines and chemokines by moDCs stimulated with SCV2-RNA (SCV2-moDCs)

The effects of Tanimilast on the pro-inflammatory properties of SCV2-moDCs were assessed in terms of cytokine and chemokine regulation. moDCs were pre-treated with Tanimilast (10^{-11}, 10^{-9},10^{-7} M) for 1 hour and then stimulated with an optimal concentration of SCV2-RNA (215). β-methasone (10^{-7} M), a glucocorticoid anti-inflammatory drug commonly used to treat overactive inflammation (216), was used as a comparison. Figure 23A shows that Tanimilast dose-dependently decreased the production of the pro-inflammatory cytokines TNF-α and IL-6 and of the Th1-polarizing cytokines IL-12 and IFN-β, although with different efficacy. Similarly, also the myelomonocyte-attracting chemokine CCL3 and the Th1-attracting chemokines CXCL9 and CXCL10 were dose-dependently reduced, while the secretion of the neutrophil-attracting chemokine CXCL8 was not affected (Figure 23B). In most cases, β-methasone showed a similar inhibition pattern, but was more effective on IL-6 secretion (60% versus 30% reduction) and reduced CXCL8 by half. β-methasone, however, unlike Tanimilast, could not counteract the induction of CXCL9 and CXCL10.

These results indicate that both Tanimilast and β-methasone reduce the overall pro-inflammatory potential of SCV2-moDCs. However, the modulatory pattern of target cytokines differs between the two drugs.

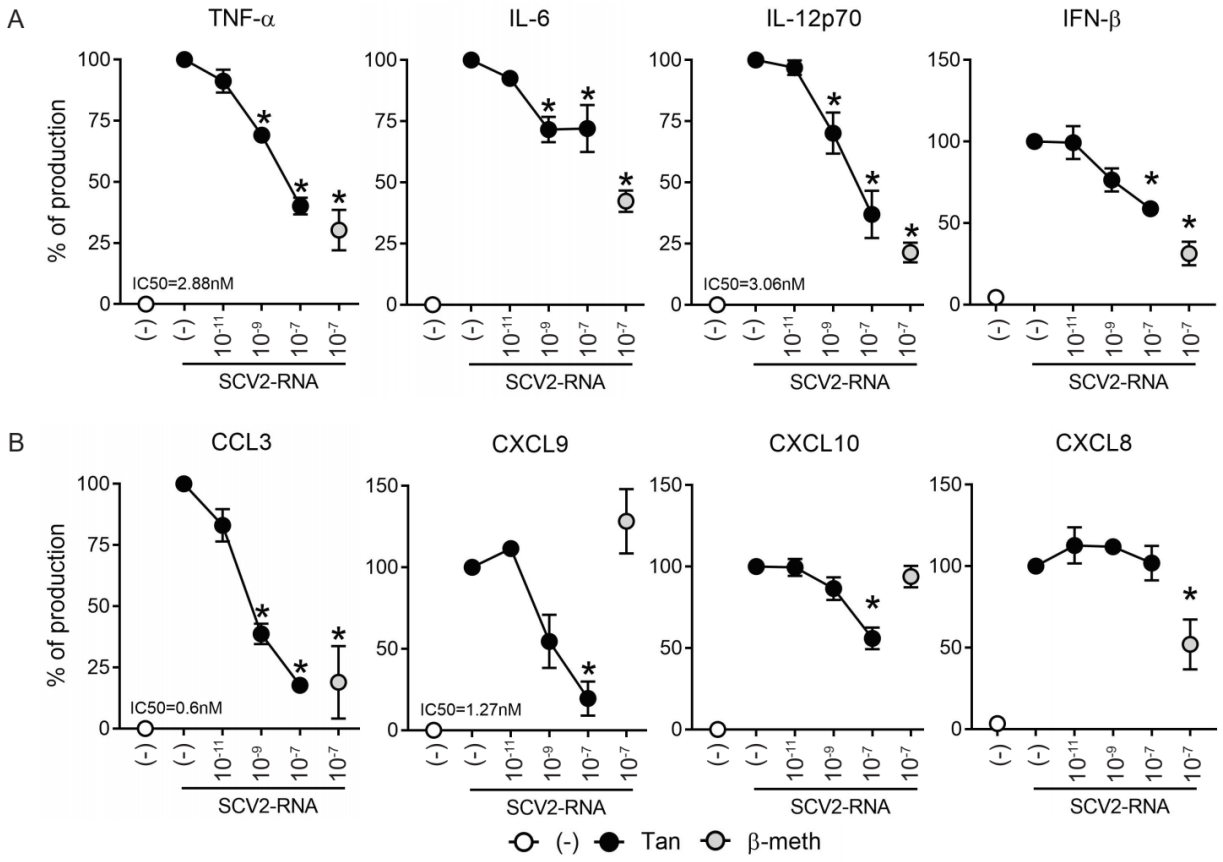

Figure 23. Effect of Tanimilast on cytokine and chemokine secretion by moDCs challenged with SCV2-RNA. (A-B) moDCs (2x10^6/ml) were pre-treated or not (-) with the indicated doses of Tanimilast (Tan) or β-methasone (β-meth) for 1 hour and then stimulated with SCV2-RNA (5 µg/ml) for 24 hours. Cytokine (A) and chemokine (B) production was evaluated by ELISA in cell-free supernatants. Cytokine/chemokine expression was normalized to SCV2-RNA condition (represented as 100%) to control donor-dependent variation. Absolute levels of SCV2-RNA induced cytokines (ng/ml) were: TNF-α=154.79 ± 26.37; IL-6=131.66 ± 16.8; IL-12=62.53 ± 21.5; IFN-β=0.38 ± 0.2; CCL3=42.21 ± 9.79; CXCL9=76.1 ± 22.7; CXCL10=33 ± 5.8 and CXCL8=94.1 ± 10.6. Data are expressed as mean ± SEM (n=3); *P< 0.05 versus SCV2-RNA by one-way ANOVA with Dunnett's post-hoc test.

1.2 Tanimilast does not impair the acquisition of maturation markers by SCV2-moDCs

Consistent with our previous findings in LPS-treated moDCs (150), Tanimilast pre-treatment (10^{-7} M) did not restrain the upregulation of the costimulatory molecules CD83 and CD86 and of the lymph-node-homing receptor CCR7 induced by SCV2-RNA (Figure 24A, left panels). Indeed, the expression of these markers showed the tendency to be even higher on a per-cell-basis in the presence of Tanimilast as demonstrated by higher MFI, although no statistical significance was reached (Figure 24A, right panels). Similarly, Tanimilast pretreatment did not block the upregulation of HLA-DR, while consistently reverting that of HLA-ABC (Figure 24B). By contrast, β-methasone counteracted the SCV2-RNA-dependent upregulation of all these markers. Both drugs did not modify the phenotype of unstimulated moDCs (Figure 24A-B, white bars).

Thus, unlike β-methasone, Tanimilast does not grossly impair the phenotypical maturation of moDCs. However, it selectively targets the upregulation of HLA class I, which may result in the modulation of antigen presentation to $CD8^+$ T cells.

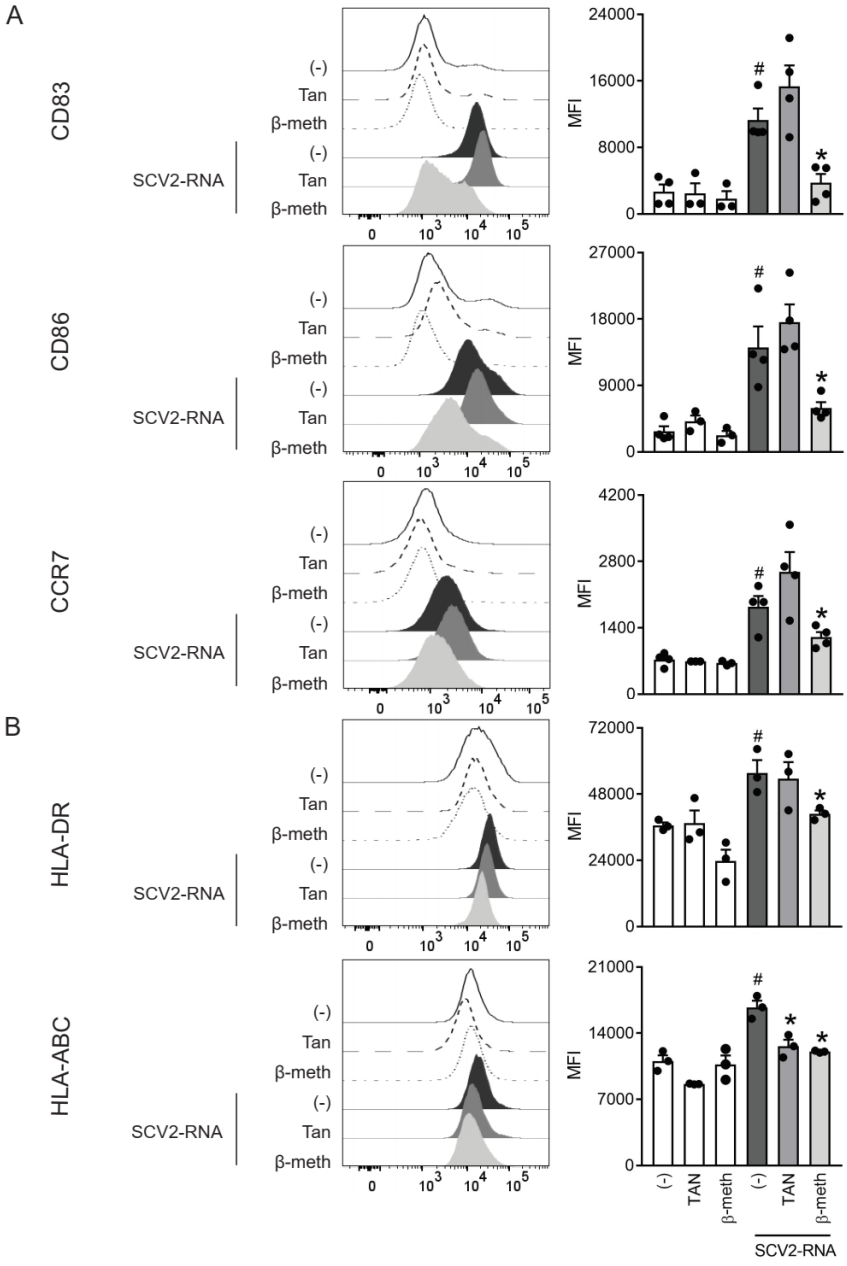

Figure 24. Effect of Tanimilast on moDC phenotypic maturation induced by SCV2-RNA. (A-B) moDCs were pre-treated or not (-) with either Tanimilast or β-methasone (both at 10^{-7}M) for 1 hour and subsequently stimulated or not with SCV2-RNA for 24 hours. The surface expression of activating markers CD83, CD86, CCR7 (A) and of antigen presenting molecules HLA-ABC, HLA-DR (B) were evaluated by FACS analysis. Data are expressed as representative cytofluorimetric profiles (left panels) and as the mean ± SEM (n=3-4) of the Median Fluorescence Intensity (MFI) (right panels). #P< 0.05 versus (-) and *P< 0.05 versus SCV2-RNA by one-way ANOVA with Dunnett's post-hoc test.

1.3 Tanimilast restrains CD8⁺ T cell activation by SCV2-moDCs

Based on findings described above, we set up allogeneic co-colture experiments to characterize the CD8⁺ T-cell activating properties of SCV2-moDCs in the presence of Tanimilast. Figure 25 shows that, consistent with the observed HLA-ABC reduction, both Tanimilast and β-methasone impaired CD8⁺ T cell proliferation induced by stimulation with SCV2-moDCs, as assessed by CFSE staining. In addition, both drugs also reduced the percentage of cells producing IFN-γ and Granzyme B, two key effector molecules of activated CD8⁺ T cells (Figure 25B).

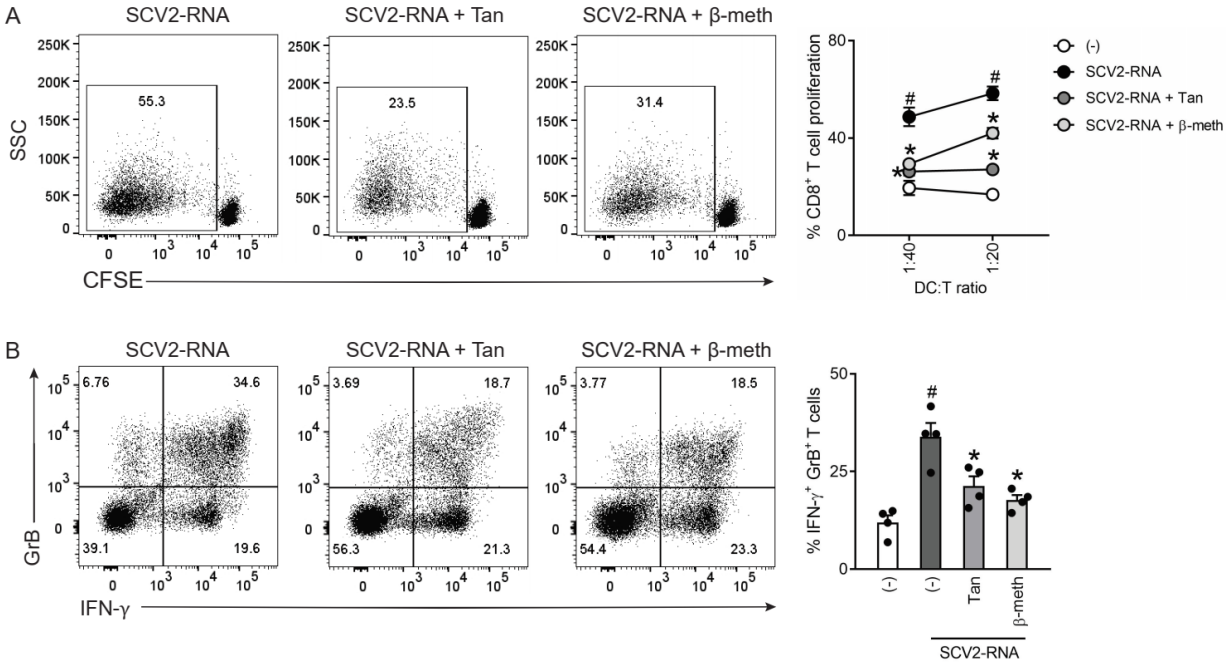

Figure 25. Effect of Tanimilast on CD8⁺ T cell activation by SCV2-moDCs. (A) moDCs were treated or not (-) with either Tanimilast or β-methasone (both at 10^{-7}M) for 1 hour and then stimulated with SCV2-RNA. After 24 hours, moDCs were collected and co-cultured with graded numbers of CFSE-stained allogenic CD8⁺ T cells for 6 days. Alloreactive T cell proliferation was assessed by measuring CellTrace-CFSE dye loss by flow cytometry. Left, dot plot from one representative experiment (1:40 ratio). Right, line graphs from three independent experiments with different DC:T cell ratio. Data are expressed as mean ± SEM (n=3) of the percentage of proliferating CD8⁺ T cells. (B) moDCs treated as described in (A) were co-cultured with graded numbers of CD8⁺ T cells for 6 days. Intracellular IFN-γ and Granzyme B (GrB) were evaluated by FACS analysis. Left, dot plot from one representative experiment. Right, bar graphs from four independent experiments. Data are expressed as mean ± SEM (n=4) of the percentage of double positive T cells. (A-B) #P versus (-) and *P< 0.05 versus SCV2-RNA by one-way ANOVA with Dunnett's post-hoc test.

1.4 SCV2-moDCs induce a Th2-skewed CD4+ T cell response in the presence of Tanimilast

The same experiments were performed using naïve $CD4^+$ T cells as responders. As expected, based on the lack of HLA class II and costimulatory molecule modulation, Tanimilast did not affect the proliferative response of $CD4^+$ T cells induced by SCV2-moDCs (Figure 26A). By contrast, β-methasone reverted T cell proliferation almost to basal levels, in accordance with HLA-DR downregulation. Next, the effects of Tanimilast on the polarizing properties of SCV2-moDC were assessed by measuring the levels of intracellular cytokines in activated $CD4^+$ T cells. We have previously shown that SCV2-RNA induces a prominent Th-1 response (215), which was consistently blocked by both Tanimilast and β-methasone (Figure 26B). However, pre-treatment with Tanimilast, but not with β-methasone, enhanced the development of T cells producing IL-4 and IL-13, which characterize Th2-skewed $CD4^+$ effectors (Figure 26B). Of note, Tanimilast alone did not induce either IL-4^+ or IL-13^+ T cells (data not shown). We also stained for IL-17 production, but this was undetectable in our experimental conditions (data not shown).

Taken together, these results indicate that DCs matured in the presence of Tanimilast fully retain the stimulatory capacity to induce $CD4^+$ T cell proliferation while skewing the T helper response toward a Th2 profile. By contrast, the effect of β-methasone results in a general inhibition of $CD4^+$ T cell activation, resembling the inhibition observed on $CD8^+$ T cells.

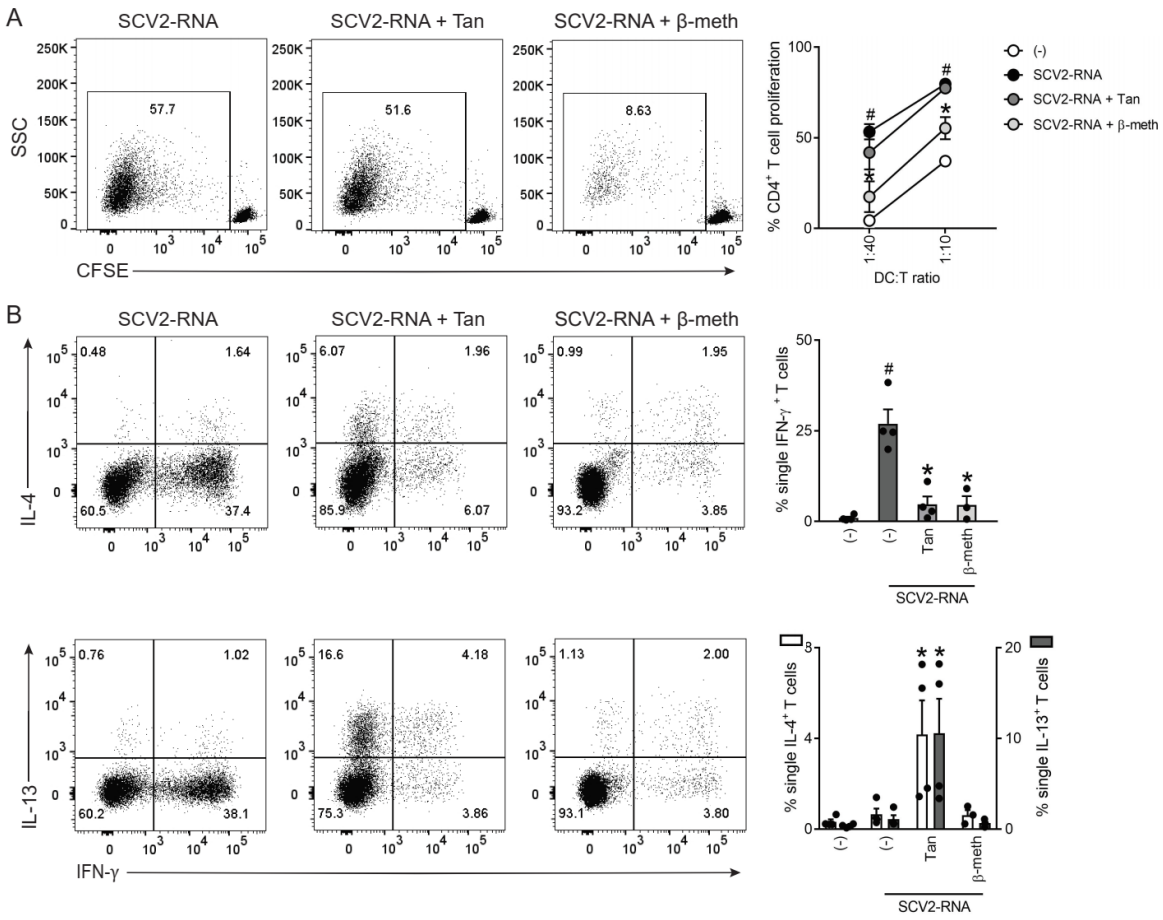

Figure 26. Effect of Tanimilast on CD4⁺ T cell activation by moDCs. (A) moDCs were treated or not (-) with Tanimilast or β-methasone (both at 10^{-7}M) for 1 hour before stimulation with SCV2-RNA. After 24 hours, moDCs were collected and co-cultured with graded numbers of CFSE-stained allogenic CD4⁺ T cells for 6 days. Alloreactive T cell proliferation was assessed by measuring CellTrace-CFSE dye loss by flow cytometry. Left, dot plot from one representative experiment (1:40 ratio). Right, line graphs from four independent experiments with different DC:T cell ratio. Data are expressed as mean ± SEM (n=4) of the percentage of proliferating CD4⁺ T cells. (B) Activated moDCs were incubated with graded numbers of T cells for 6 days. Intracellular IFN-γ, IL-4 and IL-13 were evaluated by FACS analysis. Left, dot plot from one representative experiment. Right, bar graphs from four independent experiments. Data are expressed as mean ± SEM (n=3-4) of single IFN- γ- (upper right panel) or single IL-4- (right Y axis) and IL-13- (left Y axis) (lower right panel) producing T cells. (A-B) #P< 0.05 versus (-) and *P< 0.05 versus SCV2-RNA by one-way ANOVA with Dunnett's post-hoc test.

1.5 Primary DC subsets recapitulate the effects of Tanimilast pre-treatment of moDCs

To confirm the results obtained in moDCs also in primary DCs, we immunomagnetically sorted the two main subsets of circulating DCs, namely cDCs and pDCs. Because of the rarity of these cells, only a fixed concentration of Tanimilast was used (10^{-7}M). In cDCs, a substantial lack of CD86 and CCR7 modulation by Tanimilast was confirmed, both in terms of percentage of positive cells and of mean fluorescence intensity of the population (Figure 27A). By contrast, the production of TNF-α was significantly decreased (Figure 27B). Regarding pDCs, though Tanimilast did not interfere with the acquisition of a mature phenotype characterized by the

upregulation of CD86 and downregulation of BDCA2 (Figure 27C), it decreased IFN-α secretion to 40% (Figure 27D).

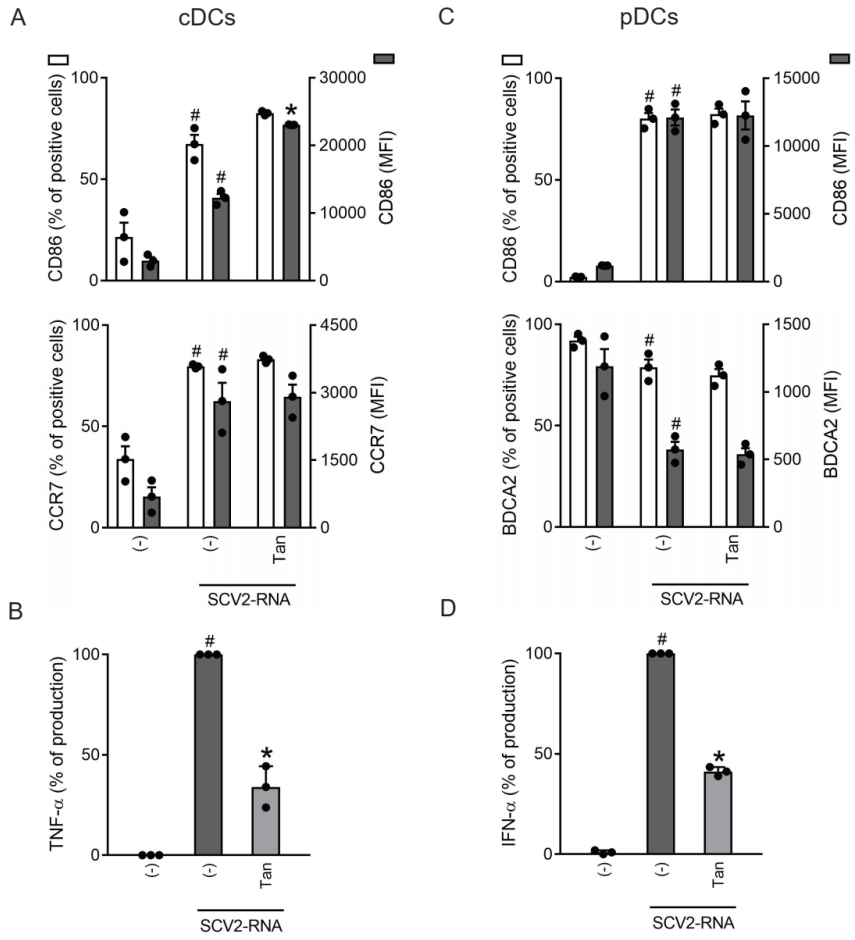

Figure 27. Effect of Tanimilast on primary DC activation by SCV2-RNA. cDCs ($2x10^6$/ml) and pDCs ($1x10^6$/ml) were pre-treated with Tanimilast (10^{-7}M) and then stimulated with SCV2-RNA for 24 hours. (A, C) The surface expression of CD86, CCR7 and BDCA2 was evaluated by FACS analysis. Data are expressed as the mean ± SEM (n=3) of the percentage of positive cells (left y axis) and of the Median Fluorescence Intensity (MFI) (right y axis). (B, D) The production of TNF-α and IFN-α was evaluated by ELISA in cell-free supernatants. Cytokine expression is normalized to SCV2-RNA condition (represented as 100%). Absolute levels of SCV2-RNA induced cytokines (ng/ml) were: TNF-α= 20.92 ± 0.55; IFN-α= 169.36 ± 23.39. Data are expressed as mean ± SEM (n=3). (A-D) #P< 0.05 versus (-) and *P< 0.05 versus SCV2-RNA by one-way ANOVA with Dunnett's post-hoc test.

2. Discussion

Tanimilast is currently undergoing phase III clinical development as a novel inhaled anti-inflammatory agent for COPD by showing promising pharmacodynamic results associated with a good tolerability and safety profile (178). Tanimilast was previously shown to act as a potent anti-inflammatory agent in several cell-based models (177), including leukocytes derived from

asthma (217) and COPD patients (218) and rhinovirus-infected human bronchial epithelial cells (159), as well as in experimental rodent models of pulmonary inflammation (183). In this study, Tanimilast is investigated as an agent capable of modulating the strong inflammatory activation induced by SCV2-RNA in human DCs. Consistent with previous work of our group (150), Tanimilast reduced the secretion of selected, but not all cytokines without affecting the acquisition of a mature phenotype. This is a condition previously defined as “semi-mature DCs”, suited to prevent excessive responses in peripheral tissues (116). Our analysis was conducted in parallel with β-methasone, since corticosteroids are established drugs in the treatment of overactive immune conditions, also undergoing clinical trials for the treatment of COVID-19 (192). Unlike Tanimilast, β-methasone induced a widespread and clear-cut shift from competent to suppressive moDCs.

Tanimilast decreased the expression of TNF-α, IL-6 and CXCL10, which are cytokines highly correlated with severity and mortality rate of Covid-19 (63,64). Additionally, Tanimilast induced a marked reduction in the release of chemokines that amplify the inflammatory and immune response via the recruitment of innate cells (e.g. CCL3) or Th1 effector cells (e.g. CXCL9/10). To date, the many ongoing trials to test the efficacy of anti-TNF-α or anti-IL-6 drugs in severe COVID-19 have provided conflicting results (219,220). It is tempting to speculate that Tanimilast may prove beneficial because of its broad modulatory effect on several cytokines, as compared to drugs selectively targeting one particular cytokine.

We observed that Tanimilast, unlike β-methasone, did not inhibit the SCV2-RNA-dependent release of the neutrophil attracting CXCL8, another prognostic marker in COVID-19 (221). However, CXCL8 is produced by many cell types in addition to DCs and was shown to be efficiently blocked by Tanimilast in other experimental settings (150,222). Thus, our experimental model, by focusing on DCs, may not fully recapitulate the modulation of CXCL8 occurring in vivo upon administration of Tanimilast. By contrast, DCs are by far the principal producers of type I IFN, which was decreased by Tanimilast. Because both type I IFNs and pDCs play crucial protective roles in the early phases of SARS-CoV-2 infection (204), the administration of Tanimilast may need to be timely targeted during SARS-CoV-2 infections, especially when tissue damage mostly depends on overwhelming immune activation rather than to viral replication per se. This holds true and has been clearly assessed also for corticosteroids, where early addition impairs viral eradication, while late-stage usage reduces symptoms and immune-dysregulation (223).

In the in vitro experimental setting utilized in this study, the combined reduction of selected cytokines elicited by Tanimilast, together with the conserved expression of co-stimulatory molecules and HLA class II, skewed the predominantly Th1 polarization of $CD4^+$ naïve T cells induced by SCV2-activated DCs (215) towards a Th2-oriented activation, without affecting T cell proliferation. This apparent Th-2 skewing effect of Tanimilast appears to be related to the presence of the SCV2 stimulus. Indeed, we observed that Tanimilast alone induced neither IL-4- nor IL-13-producing T cells. Additionally, Tanimilast is very effective in inhibiting allergen-induced eosinophilia in rats which is Th-2 driven (183). A further evidence of the modulatory effects of tanimilast on Th-2 driven pulmonary inflammation comes from its ability in reducing the allergen challenge response in asthmatic patients (178). In this regard, the effect of β-methasone was a clear-cut inhibition of phenotypical maturation, $CD4^+$T cell proliferation and Th1 blockade, with no observed skewing towards Th2 polarization. We could not evaluate the effects of Tanimilast on Th17 polarization because it was not induced in our experimental setting. However, we demonstrate a reduction in the secretion of crucial Th17-polarizing cytokines such as IL-6 and TNF-α. This is of particular importance, since Th1/Th17 responses have been associated to COVID-19 immunopathogenesis and exacerbation (31,47). SARS-CoV-2-specific $CD4^+$ effector cells generally do not express Th2 traits (56), which could play a protective role as shown by the lower susceptibility and less severe outcomes of COVID-19 in asthmatic and atopic patients (224,225). Accordingly, IL-13 was shown to reduce viral burden, possibly by downregulating the expression of angiotensin-converting enzyme 2 (ACE2) in airway epithelial cells (226). In addition, M2 macrophage polarization induced by IL-4 and IL-13 fostered tissue repair and resolution of inflammation in ARDS (227). Finally, Th2 cytokines rescue the anti-thrombotic properties of endothelial cells by inhibiting the expression of pyrogen-induced tissue factor (228), which is highly expressed in the lungs of severe COVID-19 patients (229). A number of reports, however, described Th2 signature and eosinophilia in the inflamed areas of lungs in subgroups of severe COVID-19 patients (52). This complex picture reinforces the hypothesis that Tanimilast administration may prove beneficial in blunting the excessive inflammatory response that can occur in severe COVID-19, provided careful patient evaluation and stratification is performed.

Tanimilast reduced the expression of HLA class I molecules. This effect may depend on increased levels of cAMP, reproducing the activation of the cAMP/PKA/ICER pathway previously described to repress HLA class I transcription (230). In addition, PDE4 inhibition by Rolipram was shown to reduce antigen production (and therefore HLA class I expression) by

decreasing the activity of the ubiquitin proteasome system in rodent skeletal muscle cells (231). Further research is granted to elucidate if these mechanisms are involved in the block of MHC-I upregulation in Tanimilast-treated moDCs. HLA class I reduction, together with IL-12 blockade, are likely responsible for the observed curtailing of $CD8^+$ T cell proliferation and activation, characterized by a decrease of both IFN-γ and Granzyme-B levels. This effect is shared by both Tanimilast and β-methasone. Activated $CD8^+$ effector cells play a dual role in SARS-CoV-2 infection, being critical for virus eradication as well as detrimental, when excessive cytotoxic activation results in lung damage, even more lethal than viral replication itself (58). Both hyperactive and exhausted cytotoxic T cells were described in COVID-19 patients, possibly correlating with the course of the illness (232,233). Indeed, an early immune profile characterized by high expression of interferon stimulated gene and viral load with limited lung damage was shown to precede a later stage with low interferon stimulated gene levels, low viral load and abundant infiltration of activated cytotoxic cells (57). In addition, continual proliferation and overactivation of $CD8^+$ T cells observed in severe, late stage COVID-19 were correlated to disease aggravation (49). Thus, the inhibition of $CD8^+$ T cells proliferation and activation observed upon Tanimilast treatment may be beneficial to alleviate cytotoxic hyperactivation but might be not relevant, if not contraindicated, in COVID-19 cases displaying an exhausted $CD8^+$ T cell phenotype.

In addition to immunomodulation, Tanimilast may interfere with SARS-CoV-2 infection via other mechanisms. For example, Rolipram and Roflumilast were both shown to inhibit viral replication (234,235). In addition, compounds with properties of PDE4 inhibition were suggested to bind to N-terminal RNA-binding domain of SARS-CoV-2 N-protein, a critical component of the viral replication and genome packaging machinery that may affect viral replication (236,237). By analogy with other PDE4 inhibitors, it is tempting to speculate that Tanimilast may be helpful in COVID-19 pneumonia not only by regulating the inflammatory balance but also by directly reducing viral replication and load. However, this aspect could not be investigated using our system of moDCs stimulation by SCV2-RNA.

Overall, the data presented in this study suggest that the PDE4 inhibitor Tanimilast could be a promising immunomodulator in the scenario of COVID-19. Nevertheless, further studies are needed to evaluate the benefits of this agent in clinical settings. In particular, it will be important to determine the optimal disease stage at which starting such treatment, with a particular focus on the identification of subgroups of patients (clinical phenotypes) with increased chances of therapeutic success.

C. TANIMILAST INDUCES AN IMMUNOMODULATORY PHENOTYPE ASSOCIATED WITH CD141 UPREGULATION IN HUMAN DENDRITIC CELLS

1. Results

1.1 Tanimilast impairs the Th1-promoting capacity of moDCs activated by LPS (LPS-moDCs)

We previously demonstrated that Tanimilast diminishes the Th1/Th17 polarizing potential of LPS-moDCs by decreasing the secretion of cytokines such as IL-12, IL-23 and IL-1β, while increasing the Th2-recruiting chemokine CCL22 (150). Here, we set up allogeneic co-culture experiments to investigate the functional outcome of these modulations in terms of T cell stimulatory and polarizing capacity. Budesonide, an inhaled corticosteroid commonly prescribed in asthma and COPD, was used as a comparison (238). moDCs matured by LPS exposure in the presence of Tanimilast (Tan-LPS-moDCs) or Budesonide (Bude-LPS-moDCs) were co-cultured with naïve $CD4^+$ T cells for 6 days. The proliferative capacity of naïve $CD4^+$ T cells was not affected by Tanimilast, whereas Budesonide significantly reduced the percentage of proliferating cells (Figure 28A). By contrast, both drugs blunted the prominent Th-1 response elicited by LPS-moDCs, as evaluated in terms of decreased percentage of IFN-γ producing T cells by intracellular staining (Figure 28B, left panel). However, Tan-LPS-moDCs, but not Bude-LPS-moDCs, enhanced the development of T cells producing IL-13, which characterizes a Th2 response (Figure 28B, right panel). In the present experimental conditions, both $CD25^+Fox3p^+$ T cells and $IL\text{-}17^+$ cells were barely detectable and not modulated by the drugs (data not shown). Control experiments demonstrated that Tanimilast did not induce $IL\text{-}13^+$ T cells when administered to immature moDCs (data not shown).

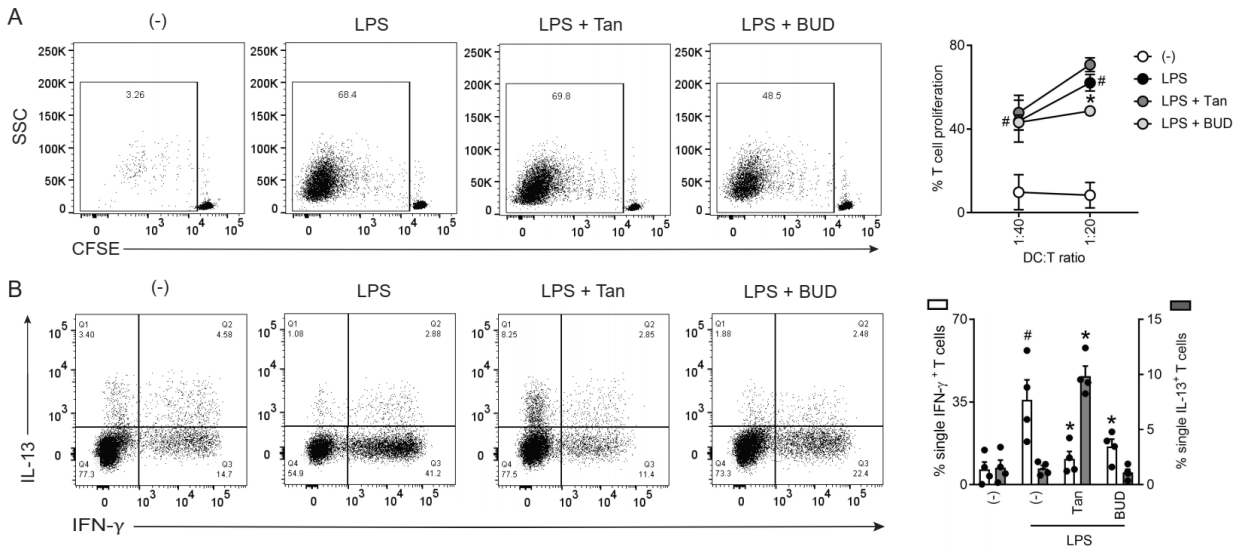

Figure 28. Effect of Tanimilast on CD4⁺ T cell activation by LPS-moDCs. (A) moDCs were treated or not (-) with Tanimilast (Tan) or Budesonide (BUD) (both at 10^{-7}M) for 1 hour before stimulation with LPS. After 24 hours, moDCs were collected and co-cultured with graded numbers of CFSE-stained allogenic CD4⁺ T cells for 6 days. Alloreactive T cell proliferation was assessed by measuring CellTrace-CFSE dye loss by flow cytometry. Left, dot plot from one representative experiment (1:20 ratio). Right, line graphs from four independent experiments with different DC:T cell ratio. Data are expressed as mean ± SEM (n=3) of the percentage of proliferating CD4⁺ T cells. (B) Activated moDCs were incubated with graded numbers of T cells for 6 days. Intracellular IFN-γ and IL-13 were evaluated by FACS analysis. Left, dot plot from one representative experiment. Right, bar graphs from four independent experiments. Data are expressed as mean ± SEM (n=4) of single IFN-γ-(right Y axis) and IL-13- (left Y axis) producing T cells. (A-B) #P< 0.05 versus (-) and *P< 0.05 versus LPS by one-way ANOVA with Dunnett's post-hoc test.

1.2 Tanimilast suppresses activation of CD8⁺ T cells by LPS-moDCs

Co-culture experiments were also performed using CD8⁺ T cells as responders. At difference with CD4⁺ T effectors, both Tanimilast and Budesonide similarly attenuated the proliferation of CD8⁺ T cells induced by LPS-moDCs (Figure 29A). Also, both drugs substantially decreased the percentage of cells producing IFN-γ and Granzyme B, two key effector molecules of activated CD8⁺ T cells (Fig 29B).

Taken together, these results indicate that both Tanimilast and Budesonide modulate the T activating potential of LPS-moDCs resulting in impaired Th1 induction and reduced cytotoxic potential of CD8⁺ T cells. Unlike Budesonide, Tanimilast did not affect the capacity of LPS-moDCs to stimulate CD4⁺ T cell proloferation and favored the developments of a Th2-oriented immune profile.

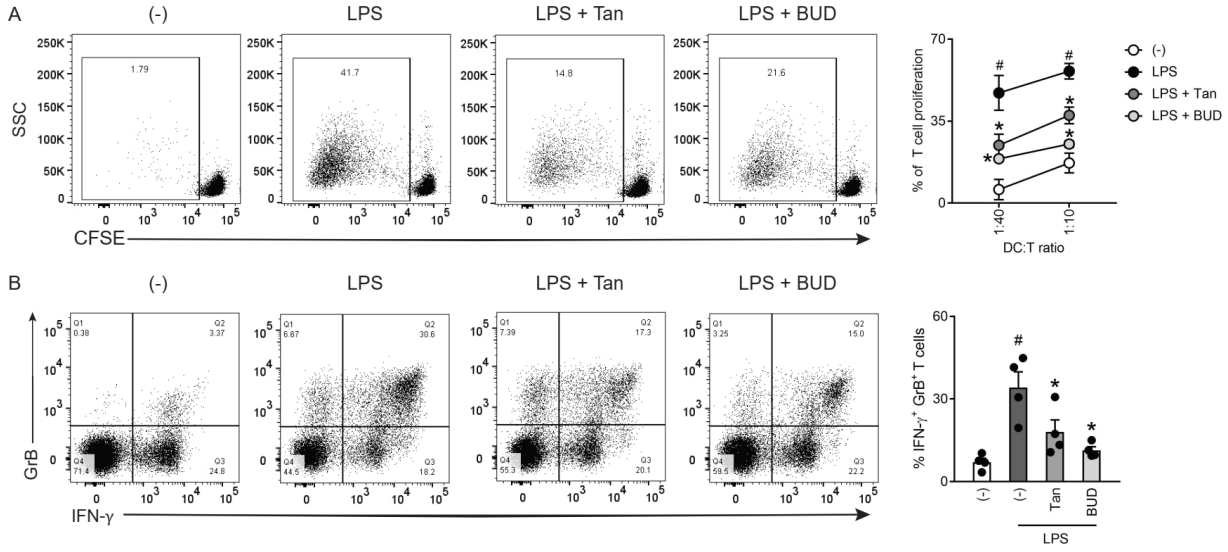

Figure 29. Effect of Tanimilast on CD8⁺ T cell activation by LPS-moDCs. (A) moDCs were treated or not (-) with either Tanimilast or Budesonide (both at 10^{-7}M) for 1 hour and then stimulated with LPS. After 24 hours, moDCs were collected and co-cultured with graded numbers of CFSE-stained allogenic CD8⁺ T cells for 6 days. Alloreactive T cell proliferation was assessed by measuring CellTrace-CFSE dye loss by flow cytometry. Left, dot plot from one representative experiment (1:40 ratio). Right, line graphs from three independent experiments with different DC:T cell ratio. Data are expressed as mean ± SEM (n=3) of the percentage of proliferating CD8⁺ T cells. (B) moDCs treated as described in (A) were co-cultured with graded numbers of CD8⁺ T cells for 6 days. Intracellular IFN-γ and Granzyme B (GrB) were evaluated by FACS analysis. Left, dot plot from one representative experiment. Right, bar graphs from four independent experiments. Data are expressed as mean ± SEM (n=4) of the percentage of double positive T cells. (A-B) #P versus (-) and *P< 0.05 versus LPS by one-way ANOVA with Dunnett's post-hoc test.

1.3 Tanimilast regulates a broad panel of genes involved in T cell immunosuppression

Based on the findings above, we set out to better characterize the immunomodulatory potential of Tan-LPS-moDCs. To this extent, immature and mature moDCs in the presence or absence of the two drugs were analysed for the levels of steady-state mRNAs encoding for proteins associated with tolerance induction (Figure 30). In line with the marked reduction of the protein levels described in our previous work (150), IL-12 mRNA was considerably downregulated in response to both drugs. Both Tanimilast and Budesonide also remarkably inhibited the expression of IRF-8, a transcription factor involved in IL-12 production (239,240). In accordance with this functional relationship, the regulation of IRF-8 shows a faster kinetic as compared to its target IL-12. By contrast, Tanimilast upregulated the levels of IDO and TSP-1, two potent negative regulators of T cell activation (241,242) and of VEGF-A and Amphiregulin (AREG), two immunosuppressive molecules linked to angiogenesis (243,244). Bude-LPS-moDCs displayed a delayed IDO upregulation and low or no induction of the other mRNAs. This difference may be partially explained by the sensitivity to cAMP elevating agents (such as Tanimilast), previously

described to play a role in the upregulation of these genes in the context of inflammation (245,246).

These data show that multiple immunosuppressive molecules are upregulated in Tan-LPS-moDCs but not in Bude-LPS-moDCs, consistent with the view of Budesonide as a direct and rapid-acting suppressor of pro-inflammatory signals.

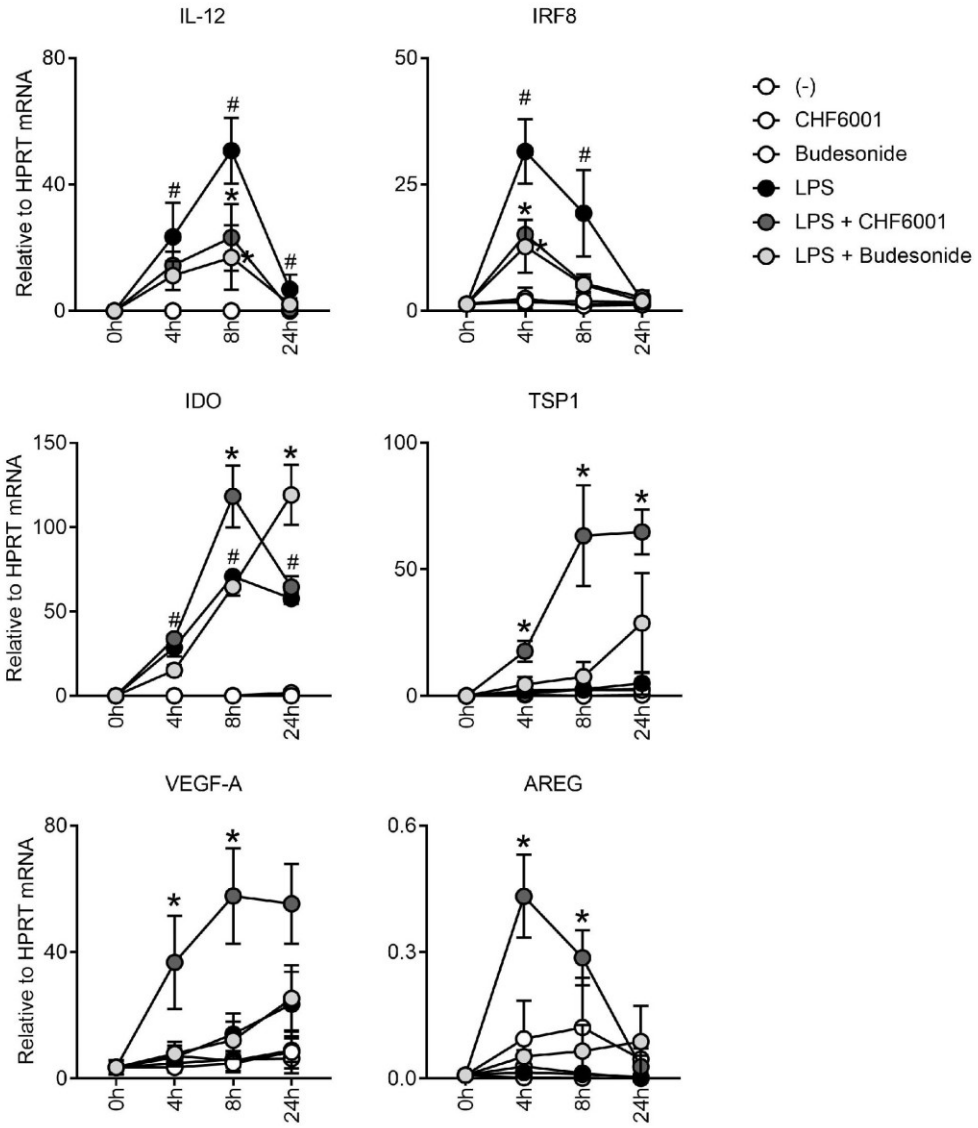

Figure 30. Effect of Tanimilast on genes involved in regulation of inflammation. moDCs pre-treated or not with Tanimilast or Budesonide and subsequently stimulated with LPS for various periods of time (0h, 4h, 8h and 24h). SYBR Green real-time PCR was used to measure mRNA level of 6 genes IL-12, IRF8, IDO, TSP-1, VDGF-A, AREG. Data are expressed as mean ± SEM (n = 3) of $2^{-}\Delta Ct$ relative to housekeeping mRNA (HPRT); $^{\#}P < 0.05$ versus (-) or $^{*}P < 0.05$ versus LPS by one-way ANOVA with Dunnett's post-hoc test.

1.4 Tanimilast modulates the phenotype of LPS-moDCs

Next, we investigated if Tan-LPS-moDCs differ from LPS-moDCs in terms of phenotypic markers, with a particular focus on surface molecules that play a role in T cell activation and immunoregulation. Figure 4A shows the analysis of the regulatory molecules PD-L1, which restrains the functions of activated T cells (247) and ILT3/CD85k (Figure 31A. right panel), a molecule that negatively regulates the activation of DCs in an autologous manner (248). We also investigated the expression of Ox40L, a positive signal for Th2 differentiation (249), but this was undetectable in our system in all conditions (data not shown). PD-L1 (Figure 31A, left panel) was constitutively expressed at low levels in resting moDCs and potently increased by LPS stimulation. Both Tanimilast and Budesonide decreased its mean fluorescence intensity (MFI) without modifying the maximal percentage of PD-L1$^+$ cells. A very similar scenario is observed for ILT3/CD85k (Figure 31A, right panel). Because the observed upregulation by LPS is often interpreted as a feedback loop to prevent excessive T cell responses, Tanimilast may counteract this effect via the suppression of TNF-α and IL-10 (150,250,251). However, ILT3/CD85k is also negatively regulated by the increase of COX2 that characterize moDCs in the presence of cAMP-elevating agents (data not shown and (185)).

When checking the regulation of classical maturation markers, we found that Tan-LPS-moDCs showed reduced expression of HLA-ABC and CD80 as compared to LPS-moDCs, at striking difference with CD86 (Figure 31B and C) and HLA-DR (150) that were not affected. Of note, HLA-ABC and CD80 expression are both known to be regulated by intracellular cAMP levels (230,252). The reduction of HLA-ABC well correlates with decreased proliferation of CD8$^+$ T cells (Figure 29), while untouched HLA-DR is consistent with unaffected CD4 T cell proliferation when Tan-LPS-moDCs were used as activators (Figure 28). Budesonide behaved similarly to Tanimilast, with the notable exception of a significant decrease of CD86 (Figure 33B and C). The counter regulation of CD80 and CD86 determined a higher CD86/CD80 ratio in Tan-LPS-moDCs as compared to Bude-LPS-moDCs, which correlated with the higher induction of IL-13$^+$ T cells (Figure 31D). This is in line with the previously reported association between high CD86 levels and increased Type 2 immune responses (253–255).

We also investigated the expression of CCR2 and CCR6, two chemokine receptors responsible for DC accumulation into the lung (256), which remained unaltered and undetectable, respectively, in all our experimental conditions (data not shown). When administered to immature moDCs, both Tanimilast and Budesonide did not modify the basal levels of any of the analyzed markers (data not shown).

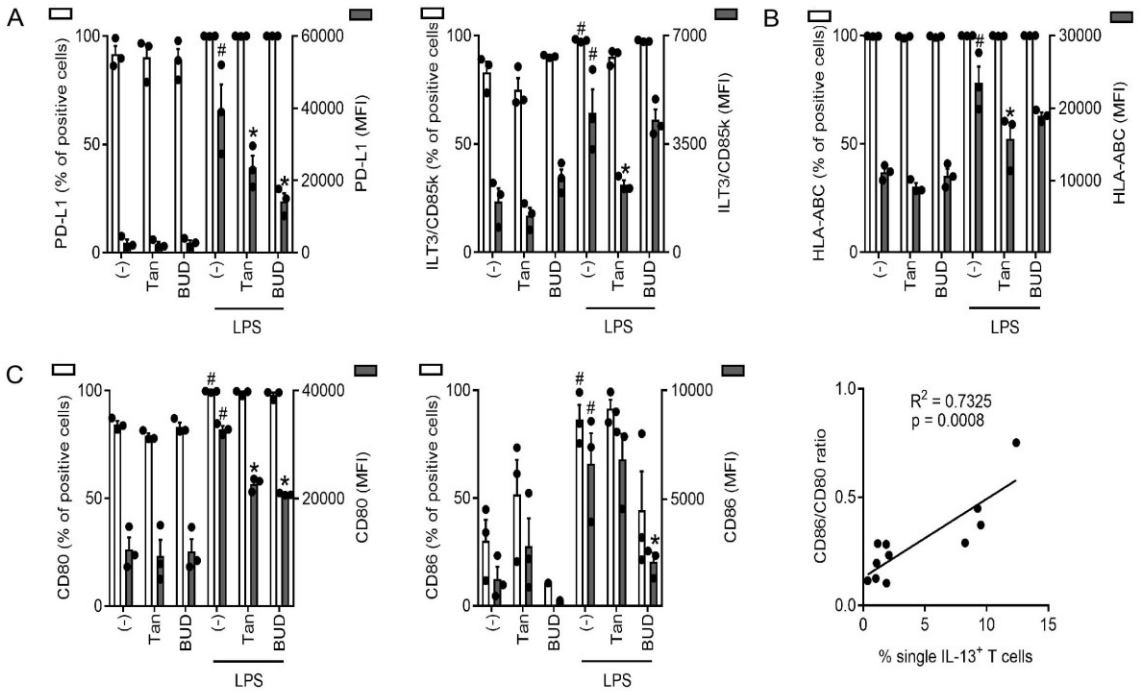

Figure 31. Effect of Tanimilast on LPS-moDCs' phenotype. moDCs were pre-treated or not (-) with either Tanimilast or Budesonide (both at 10^{-7}M) for 1 hour and subsequently stimulated or not with LPS for 24 hours. The surface expression of regulatory markers PD-L1, ILT3/CD85k (A) and of maturation markers HLA-ABC (B), CD80, CD86 (C) were evaluated by FACS analysis. Data are expressed as the mean ± SEM (n=3) of the percentage of positive cells (left y axis) and of the Median Fluorescence Intensity (MFI) (right y axis). (A-C) #P< 0.05 versus (-) and *P< 0.05 versus LPS by one-way ANOVA with Dunnett's post-hoc test. (C) Correlation between CD86/CD80 ratios and % of single IL-13$^+$ T cells induced by moDCs stimulated with LPS in the absence or presence of Tanimilast or Budesonide (3 donors) (y = 0.03615*x + 0.1299, R^2 = 0.7325; Spearman r = 0.8559, *P = 0.0008).

1.5 CD141 expression marks DCs matured in the presence of Tanimilast

In the search for markers of Tan-LPS-moDCs, we serendipitously observed that these cells expressed high levels of CD141, also known as Thrombomodulin or BDCA-3. CD141, together with Clec9A and XCR1, is the distinctive marker of conventional DCs type 1 (cDC1s) (79), a subpopulation of primary DCs specialized in antigen cross-presentation following dead cell uptake (83) and also known to induce T cells that preferentially produce type 2 cytokines (85). Thus, we asked if moDCs in the presence of Tanimilast may acquire features of cDC1s. Immature moDCs expressed very low CD141 and no Clec9A nor XCR1. Tan-LPS-moDCs upregulated the surface levels of CD141 both in terms of percentage of positive cells and MFI, while Bude-LPS-moDCs did not (Figure 32A). In both cell types, Clec9A and XCR1 remained undetectable (data not shown). Additionally, Tanimilast (but not Budesonide) potentiated the capacity of LPS-moDCs to uptake dead cells and this effect positively correlated with the percentage of CD141$^+$ cells in the different populations (Figure 32B). The upregulation of CD141 was not restricted to Tan-LPS-moDCs, since it could be reproduced by Tanimilast

pretreatment of moDCs matured in the presence of several proinflammatory agonists such as E. coli, R848, SCV2-RNA and β-glucan. (Figure 32C). Finally, we investigated the ability of Tanimilast to upregulate the expression of CD141 in primary DCs. Circulating conventional DC subsets comprise cDC1s (CD141$^+$ DCs) and cDC2s (CD1c$^+$ DCs). Because of the already maximal expression of CD141, this could not be further increased by Tanimilast in activated cDC1s (data not shown) but was upregulated in LPS-cDC2s (Figure 32D). Thus, CD141 expression clearly differentiate DCs matured in the presence of Tanimilast and Budesonide and may represent a marker of immunomodulatory DCs induced by Tanimilast.

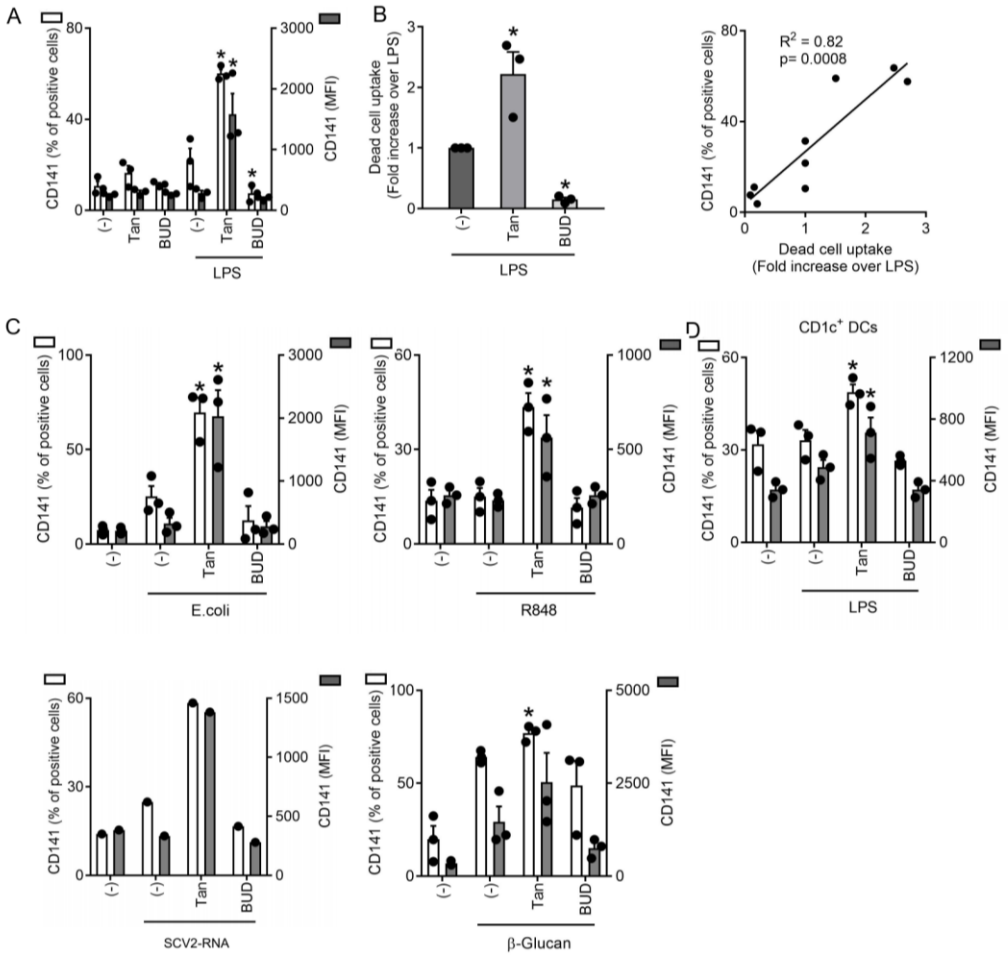

Figure 32. Tanimilast induce the upregulation of CD141 (Thrombomodulin/BDCA3) in DCs. (A, C) moDCs or CD1c$^+$ DCs (D) were pre-treated or not (-) with either Tanimilast or Budesonide (both at 10^{-7}M) for 1 hour and subsequently stimulated or not with LPS (A, D) or with E.coli, R848, SCV2-RNA, β-glucan (C) for 24 hours. The surface expression of CD141 were evaluated by FACS analysis. Data are expressed as the mean ± SEM (n=1/3) of the percentage of positive cells (left y axis) and of the Median Fluorescence Intensity (MFI) (right y axis). (B) moDCs treated as described in (A) were labeled with HLA-DR and then co-cultured with heat-killed autologous CFSE$^+$ PBMC at ratio 1:1 for 2 hours. The dead cells uptake was defined as the percentage of HLA-DR$^+$CFSE$^+$ cells. Data are expressed as the mean ± SEM (n=3) of the fold increase in percentage of dead cell uptake over LPS condition (left panel) and correlation between the percentage of CD141$^+$ cells with the fold increase [(3 donors), (right panel)] ($y = 23.03*x + 3.696$, $R^2 = 0.82$; Spearman r = 0.9055, *P = 0.0008). (A, C, D) $^{\#}$P< 0.05 versus (-) and *P< 0.05 versus LPS by one-way ANOVA with Dunnett's post-hoc test.

2. Discussion

Tanimilast displays prominent anti-inflammatory properties in several cell-based models (177,217) as well as in experimental rodent models of pulmonary inflammation (183). However, we have previously demonstrated that it also finely tunes, rather than suppressing, the cytokine network resulting from DC maturation, thus potentially modulating T cell polarization and adaptive effector functions (150). Here, we characterized Tan-LPS-moDCs as compared to Bude-LPS-moDCs as activators of $CD4^+$ and $CD8^+$ T cells. Both Tanimilast and Budesonide reduced the secretion of IFN-γ by activated T cells and inhibited $CD8^+$ T cell proliferation and acquisition of the cytotoxic protease Granzyme B. However, only Tan-LPS-moDCs also induced the differentiation of IL-13^+ $CD4^+$ T cells, which indicate a type 2 oriented skewing of the immune response (Figure 33).

Type 2 immunity was initially linked to host defence against helminths and, when occurring in response to environmental proteins, to allergy and anaphylaxis. According to a more current view, however, type 2 responses may play a broader role in immune surveillance at tissue barrier sites, repair responses, and finally in the restoration of tissue homeostasis (257). Thus, our finding may uncover one so far overlooked property of Tanimilast that further support its application to pathological conditions characterized by inflammation- and immune-mediated tissue damage such as COPD. Although the link between cAMP-elevating agents (such as Tanimilast) and type 2 responses is well established (258–261), our work details a number of mechanisms underlying the Th2-promoting properties of Tanimilast. Of paramount importance is possibly the reduction of IL-12 (150), the master Th1-promoting and Th-2 suppressing cytokine. This reduction may partly depend on the decrease of IRF8, a transcription factor known to positively regulate the mRNA levels of IL12 p40 (239,240). Of note, IRF8 also support other functions such as antigen presentation and pro-inflammatory cytokine production; indeed, it can foster chronic inflammatory diseases characterized by excessive Th1/Th17 response (262,263). In this view, its reduction may impact on the immunomodulatory properties of DCs well beyond IL-12 inhibition. Tanimilast also upregulated the expression of IDO, a marker of regulatory DCs involved in the suppression of Th1/Th17 mediated pathologic conditions (241,264), as well as that of TSP1, VEGF-A and AREG that play roles both in inhibiting the activity of T cells (242–244) and in resolving inflammation (265–267). IDO and VEGF-A were also shown to act as direct Th2-orienting mediators in some conditions (268,269) and VEGF protects against progression and severity of COPD, where its deficiency induced by cigarette smoke impairs the alveolar structure (270). Of note, human DCs are a well-known source of these factors,

especially in inflammatory context characterized by elevated intracellular levels of cAMP, such as in the presence of PDE4 inhibitors (185,245,246,271,272). Finally, we also postulate a role for the differentially regulated co-stimulatory molecules CD80 and CD86. Indeed, Th1 polarization may be hampered by lowering CD80 expression without affecting the upregulation of the Th2-associated molecule CD86 (253–255), leading to a higher CD86/CD80 ratio which strongly correlated with the number of IL-13$^+$ cells (262,263).

CD141 (Thrombomodulin/BDCA-3) is a transmembrane protein that is abundantly expressed by endothelial cells, where it is regulated by the levels of intracellular cAMPs (273,274). In this cell type, CD141 exerts various and well-characterized anti-coagulant and anti-inflammatory activities such as LPS and HMGB1 sequestration and degradation and inhibition of complement deposition (275,276). CD141 is also a marker of cDC1 cells, a subpopulation of human DCs known for their superior antigen cross-presenting capacity (83). However, the function of CD141 in DCs remains unknown. Recently, the lectin domain of this molecule was suggested to play a role in DC-mediated immune-stimulation in the lung (277). Consistent with this view, CD141$^+$ DCs within peripheral tissues were shown to display a tolerant phenotype (278), to preferentially induce type 2 immunomodulatory responses (85) and even potent regulatory T cells (86). In addition, CD141$^+$ DCs reduced the severity of asthma in murine models via the lectin domain (277) and CD141$^+$ monocytes and DCs were associated with low-risk features in myelodysplastic syndromes and were proposed to dampen excessive immune activation (279,280). In the present study, CD141 expression correlated with increased uptake of dead cells, a function that is pivotal in the resolution phase of inflammation and maintenance of tissue homeostasis, especially in autoimmunity or acute injury (281). Finally, CD141$^+$ DCs antagonized the pro-inflammatory effects of HMGB1 and enhanced fibrinolysis (282,283), an activity reminiscent of the functional role of CD141 on endothelial cells. It is thus tempting to hypothesize that CD141 expression on Tan-LPS-moDCs may help dampen the inflammatory milieu enriched in HMGB1 and Thrombin associated with lung tissue damage and acute exacerbation in COPD (284,285).

Taken together, our data depicts Tan-LPS-moDCs as immunomodulatory cells with a distinct phenotype, characterized by the upregulation of CD141. In particular, we propose these cells as pro-resolving mediators that, by skewing strong Th1/Th17 immune activation towards a type 2 response, may help restore homeostasis at the site of injury (286). In this scenario, Tanimilast may display a therapeutic potential also in the treatment of acute diseases associated with

devastating tissue damage due to hyperinflammation such as severe COVID-19 and its sequelae.

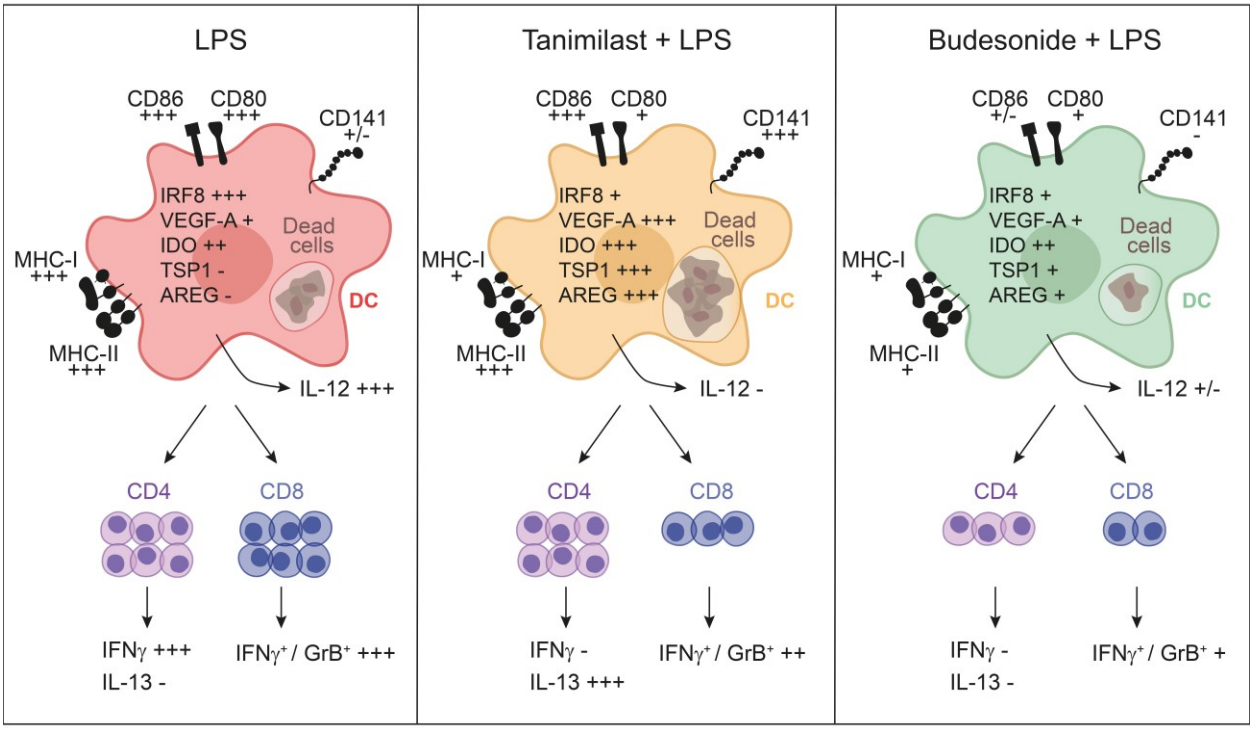

Figure 33. Effects of Tanimilast and Budesonide on LPS-moDCs' phenotype and function

CONCLUDING REMARKS

PDE4 inhibitors have been actively investigated for their therapeutic potential in inflammatory or immune-mediated conditions because of prominent anti-inflammatory properties. This thesis adds further elements supporting not only anti-inflammatory but also more complex immunomodulatory properties of PDE4 inhibitors, with a particular focus on DC modulation by the novel selective PDE4 inhibitor Tanimilast. When DCs were activated with both a SARS-CoV-2-derived PAMP, that we define as a novel TLR7 ligand, or with the classical pro-inflammatory PAMP LPS, Tanimilast skewed immunogenic DCs toward regulatory DCs associated with distinguishable upregulation of CD141 molecules. Importantly, Tanimilast-conditioned DCs displayed defective Th1 and cytotoxic T cell-promoting capacity, and more interestingly skewed $CD4^+$ T cells toward a Th2-oriented profile. Thus, Tanimilast is not only capable of blunting the inflammatory properties of innate cells but also shape the outcoming adaptive immune response.

Altogether, our findings provide rationale for considering PDE4 inhibition in pathological conditions associated with excessive T cell-mediated immune responses.

BIBLIOGRAPHY

1. Haque SM, Ashwaq O, Sarief A, Azad John Mohamed AK. A comprehensive review about SARS-CoV-2. Future Virol. 2020 Sep 1;15(9):625–48.

2. Harrison AG, Lin T, Wang P. Mechanisms of SARS-CoV-2 Transmission and Pathogenesis. Trends Immunol. 2020 Dec;41(12):1100–15.

3. Koff AG, Laurent-Rolle M, Hsu JC-C, Malinis M. Prolonged incubation of severe acute respiratory syndrome coronavirus 2 (SARS-CoV-2) in a patient on rituximab therapy. Infect Control Hosp Epidemiol. :1–2.

4. Johansson MA, Quandelacy TM, Kada S, Prasad PV, Steele M, Brooks JT, et al. SARS-CoV-2 Transmission From People Without COVID-19 Symptoms. JAMA Netw Open. 2021 Jan 7;4(1):e2035057.

5. Oran DP, Topol EJ. Prevalence of Asymptomatic SARS-CoV-2 Infection. Ann Intern Med. 2020 Sep 1;173(5):362–7.

6. Huang C, Wang Y, Li X, Ren L, Zhao J, Hu Y, et al. Clinical features of patients infected with 2019 novel coronavirus in Wuhan, China. Lancet Lond Engl. 2020;395(10223):497–506.

7. Wang L, He W, Yu X, Hu D, Bao M, Liu H, et al. Coronavirus disease 2019 in elderly patients: Characteristics and prognostic factors based on 4-week follow-up. J Infect. 2020 Jun;80(6):639–45.

8. Alunno A, Najm A, Mariette X, Marco GD, Emmel J, Mason L, et al. Immunomodulatory therapies for SARS-CoV-2 infection: a systematic literature review to inform EULAR points to consider. Ann Rheum Dis [Internet]. 2021 Feb 13 [cited 2021 May 4]; Available from: https://ard.bmj.com/content/early/2021/02/14/annrheumdis-2020-219725

9. Zhou L, Ayeh SK, Chidambaram V, Karakousis PC. Modes of transmission of SARS-CoV-2 and evidence for preventive behavioral interventions. BMC Infect Dis. 2021 May 28;21(1):496.

10. Enriquez M. Vaccine Hesitancy and COVID-19: Nursing's Role. Hisp Health Care Int. 2021 Jun 1;19(2):74–74.

11. Hoffmann M, Kleine-Weber H, Schroeder S, Krüger N, Herrler T, Erichsen S, et al. SARS-CoV-2 Cell Entry Depends on ACE2 and TMPRSS2 and Is Blocked by a Clinically Proven Protease Inhibitor. Cell. 2020 Apr 16;181(2):271-280.e8.

12. Zhu N, Wang W, Liu Z, Liang C, Wang W, Ye F, et al. Morphogenesis and cytopathic effect of SARS-CoV-2 infection in human airway epithelial cells. Nat Commun. 2020 Aug 6;11:3910.

13. Li M-Y, Li L, Zhang Y, Wang X-S. Expression of the SARS-CoV-2 cell receptor gene ACE2 in a wide variety of human tissues. Infect Dis Poverty. 2020 Apr 28;9(1):45.

14. Cantuti-Castelvetri L, Ojha R, Pedro LD, Djannatian M, Franz J, Kuivanen S, et al. Neuropilin-1 facilitates SARS-CoV-2 cell entry and infectivity. Science. 2020 Nov 13;370(6518):856–60.

15. Thépaut M, Luczkowiak J, Vivès C, Labiod N, Bally I, Lasala F, et al. DC/L-SIGN recognition of spike glycoprotein promotes SARS-CoV-2 trans-infection and can be inhibited by a glycomimetic antagonist. PLOS Pathog. 2021 May 20;17(5):e1009576.

16. Lempp FA, Soriaga LB, Montiel-Ruiz M, Benigni F, Noack J, Park Y-J, et al. Lectins enhance SARS-CoV-2 infection and influence neutralizing antibodies. Nature. 2021 Oct;598(7880):342–7.

17. Triggle CR, Bansal D, Ding H, Islam MM, Farag EABA, Hadi HA, et al. A Comprehensive Review of Viral Characteristics, Transmission, Pathophysiology, Immune Response, and Management of SARS-CoV-2 and COVID-19 as a Basis for Controlling the Pandemic. Front Immunol. 2021;12:338.

18. Schifanella L, Anderson JL, Galli M, Corbellino M, Lai A, Wieking G, et al. Massive viral replication and cytopathic effects in early COVID-19 pneumonia. ArXiv200500004 Q-Bio [Internet]. 2020 Apr 30 [cited 2021 Dec 11]; Available from: http://arxiv.org/abs/2005.00004

19. de Maat S, de Mast Q, Danser AHJ, van de Veerdonk FL, Maas C. Impaired Breakdown of Bradykinin and Its Metabolites as a Possible Cause for Pulmonary Edema in COVID-19 Infection. Semin Thromb Hemost. 2020 Oct;46(7):835–7.

20. Siddiqi HK, Mehra MR. COVID-19 illness in native and immunosuppressed states: A clinical–therapeutic staging proposal. J Heart Lung Transplant. 2020 May;39(5):405–7.

21. Ortega MA, Fraile-Martínez O, García-Montero C, García-Gallego S, Sánchez-Trujillo L, Torres-Carranza D, et al. An integrative look at SARS-CoV-2 (Review). Int J Mol Med. 2021 Feb 1;47(2):415–34.

22. Mason RJ. Pathogenesis of COVID-19 from a cell biology perspective. Eur Respir J [Internet]. 2020 Apr 1 [cited 2021 Nov 26];55(4). Available from: https://erj.ersjournals.com/content/55/4/2000607

23. Tan L, Wang Q, Zhang D, Ding J, Huang Q, Tang Y-Q, et al. Lymphopenia predicts disease severity of COVID-19: a descriptive and predictive study. Signal Transduct Target Ther. 2020 Mar 27;5(1):1–3.

24. Calabrese F, Pezzuto F, Fortarezza F, Hofman P, Kern I, Panizo A, et al. Pulmonary pathology and COVID-19: lessons from autopsy. The experience of European Pulmonary Pathologists. Virchows Arch. 2020;477(3):359–72.

25. Tian S, Xiong Y, Liu H, Niu L, Guo J, Liao M, et al. Pathological study of the 2019 novel coronavirus disease (COVID-19) through postmortem core biopsies. Mod Pathol. 2020 Apr 14;1–8.

26. Yang L, Liu S, Liu J, Zhang Z, Wan X, Huang B, et al. COVID-19: immunopathogenesis and Immunotherapeutics. Signal Transduct Target Ther. 2020 Jul 25;5(1):1–8.

27. Lee AJ, Ashkar AA. The Dual Nature of Type I and Type II Interferons. Front Immunol. 2018;9:2061.

28. Zhang Q, Bastard P, Liu Z, Le Pen J, Moncada-Velez M, Chen J, et al. Inborn errors of type I IFN immunity in patients with life-threatening COVID-19. Science. 2020 Oct 23;370(6515):eabd4570.

29. Bastard P, Rosen LB, Zhang Q, Michailidis E, Hoffmann H-H, Zhang Y, et al. Autoantibodies against type I IFNs in patients with life-threatening COVID-19. Science [Internet]. 2020 Oct 23 [cited 2021 Jul 2];370(6515). Available from: https://science.sciencemag.org/content/370/6515/eabd4585

30. Ramasamy S, Subbian S. Critical Determinants of Cytokine Storm and Type I Interferon Response in COVID-19 Pathogenesis. Clin Microbiol Rev. 34(3):e00299-20.

31. Tincati C, Cannizzo ES, Giacomelli M, Badolato R, d'Arminio Monforte A, Marchetti G. Heightened Circulating Interferon-Inducible Chemokines, and Activated Pro-Cytolytic Th1-Cell Phenotype Features Covid-19 Aggravation in the Second Week of Illness. Front Immunol [Internet]. 2020 [cited 2021 Apr 22];11. Available from: https://www.frontiersin.org/articles/10.3389/fimmu.2020.580987/full

32. Lee JS, Park S, Jeong HW, Ahn JY, Choi SJ, Lee H, et al. Immunophenotyping of COVID-19 and influenza highlights the role of type I interferons in development of severe COVID-19. Sci Immunol. 2020 Jul 10;5(49):eabd1554.

33. Blanco-Melo D, Nilsson-Payant BE, Liu W-C, Uhl S, Hoagland D, Møller R, et al. Imbalanced Host Response to SARS-CoV-2 Drives Development of COVID-19. Cell. 2020 May 28;181(5):1036-1045.e9.

34. Salman AA, Waheed MH, Ali-Abdulsahib AA, Atwan ZW. Low type I interferon response in COVID-19 patients: Interferon response may be a potential treatment for COVID-19. Biomed Rep. 2021 May;14(5):43.

35. Ribero MS, Jouvenet N, Dreux M, Nisole S. Interplay between SARS-CoV-2 and the type I interferon response. PLOS Pathog. 2020 Jul 29;16(7):e1008737.

36. Xiong Y, Liu Y, Cao L, Wang D, Guo M, Jiang A, et al. Transcriptomic characteristics of bronchoalveolar lavage fluid and peripheral blood mononuclear cells in COVID-19 patients. Emerg Microbes Infect. 2020 Jan 1;9(1):761–70.

37. da Costa LS, Outlioua A, Anginot A, Akarid K, Arnoult D. RNA viruses promote activation of the NLRP3 inflammasome through cytopathogenic effect-induced potassium efflux. Cell Death Dis. 2019 Apr 25;10(5):1–15.

38. He Z, Zhao C, Dong Q, Zhuang H, Song S, Peng G, et al. Effects of severe acute respiratory syndrome (SARS) coronavirus infection on peripheral blood lymphocytes and their subsets. Int J Infect Dis IJID Off Publ Int Soc Infect Dis. 2005 Nov;9(6):323–30.

39. Ackermann M, Verleden SE, Kuehnel M, Haverich A, Welte T, Laenger F, et al. Pulmonary Vascular Endothelialitis, Thrombosis, and Angiogenesis in Covid-19. N Engl J Med [Internet]. 2020 May 21 [cited 2021 May 4]; Available from: https://www.nejm.org/doi/10.1056/NEJMoa2015432

40. Bryce C, Grimes Z, Pujadas E, Ahuja S, Beasley MB, Albrecht R, et al. Pathophysiology of SARS-CoV-2: targeting of endothelial cells renders a complex disease with thrombotic microangiopathy and aberrant immune response. The Mount Sinai COVID-19 autopsy experience. medRxiv. 2020 May 22;2020.05.18.20099960.

41. Fox SE, Akmatbekov A, Harbert JL, Li G, Quincy Brown J, Vander Heide RS. Pulmonary and cardiac pathology in African American patients with COVID-19: an autopsy series from New Orleans. Lancet Respir Med. 2020 Jul 1;8(7):681–6.

42. Kuri-Cervantes L, Pampena MB, Meng W, Rosenfeld AM, Ittner CAG, Weisman AR, et al. Comprehensive mapping of immune perturbations associated with severe COVID-19. Sci Immunol [Internet]. 2020 Jul 15 [cited 2021 Apr 25];5(49). Available from: https://www.ncbi.nlm.nih.gov/pmc/articles/PMC7402634/

43. De Biasi S, Meschiari M, Gibellini L, Bellinazzi C, Borella R, Fidanza L, et al. Marked T cell activation, senescence, exhaustion and skewing towards TH17 in patients with COVID-19 pneumonia. Nat Commun. 2020 Jul 6;11(1):3434.

44. Kusnadi A, Ramírez-Suástegui C, Fajardo V, Chee SJ, Meckiff BJ, Simon H, et al. Severely ill COVID-19 patients display impaired exhaustion features in SARS-CoV-2-reactive CD8+ T cells. Sci Immunol [Internet]. 2021 Jan 21 [cited 2021 May 7];6(55). Available from: https://immunology.sciencemag.org/content/6/55/eabe4782

45. Li M, Guo W, Dong Y, Wang X, Dai D, Liu X, et al. Elevated Exhaustion Levels of NK and CD8+ T Cells as Indicators for Progression and Prognosis of COVID-19 Disease. Front Immunol [Internet]. 2020 [cited 2021 May 7];11. Available from: https://www.frontiersin.org/articles/10.3389/fimmu.2020.580237/full

46. Weiskopf D, Schmitz KS, Raadsen MP, Grifoni A, Okba NMA, Endeman H, et al. Phenotype and kinetics of SARS-CoV-2–specific T cells in COVID-19 patients with acute respiratory distress syndrome. Sci Immunol [Internet]. 2020 Jun 26 [cited 2021 Apr 4];5(48). Available from: https://immunology.sciencemag.org/content/5/48/eabd2071

47. De Biasi S, Meschiari M, Gibellini L, Bellinazzi C, Borella R, Fidanza L, et al. Marked T cell activation, senescence, exhaustion and skewing towards TH17 in patients with COVID-19 pneumonia. Nat Commun. 2020 Jul 6;11(1):3434.

48. Xu Z, Shi L, Wang Y, Zhang J, Huang L, Zhang C, et al. Pathological findings of COVID-19 associated with acute respiratory distress syndrome. Lancet Respir Med. 2020 Apr 1;8(4):420–2.

49. Kang CK, Han G-C, Kim M, Kim G, Shin HM, Song K-H, et al. Aberrant hyperactivation of cytotoxic T-cell as a potential determinant of COVID-19 severity. Int J Infect Dis. 2020 Aug;97:313–21.

50. Parackova Z, Bloomfield M, Klocperk A, Sediva A. Neutrophils mediate Th17 promotion in COVID-19 patients. J Leukoc Biol. 2021;109(1):73–6.

51. Lucas C, Wong P, Klein J, Castro TBR, Silva J, Sundaram M, et al. Longitudinal analyses reveal immunological misfiring in severe COVID-19. Nature. 2020 Aug;584(7821):463–9.

52. Vaz de Paula CB, de Azevedo MLV, Nagashima S, Martins APC, Malaquias MAS, Miggiolaro AFR dos S, et al. IL-4/IL-13 remodeling pathway of COVID-19 lung injury. Sci Rep [Internet]. 2020 Oct 29 [cited 2021 Apr 25];10. Available from: https://www.ncbi.nlm.nih.gov/pmc/articles/PMC7596721/

53. Gil-Etayo FJ, Suàrez-Fernández P, Cabrera-Marante O, Arroyo D, Garcinuño S, Naranjo L, et al. T-Helper Cell Subset Response Is a Determining Factor in COVID-19 Progression. Front Cell Infect Microbiol [Internet]. 2021 [cited 2021 May 4];11. Available from: https://www.frontiersin.org/articles/10.3389/fcimb.2021.624483/full

54. Grifoni A, Weiskopf D, Ramirez SI, Mateus J, Dan JM, Moderbacher CR, et al. Targets of T Cell Responses to SARS-CoV-2 Coronavirus in Humans with COVID-19 Disease and Unexposed Individuals. Cell. 2020 Jun 25;181(7):1489-1501.e15.

55. Rydyznski Moderbacher C, Ramirez SI, Dan JM, Grifoni A, Hastie KM, Weiskopf D, et al. Antigen-Specific Adaptive Immunity to SARS-CoV-2 in Acute COVID-19 and Associations with Age and Disease Severity. Cell. 2020 Nov 12;183(4):996-1012.e19.

56. Sekine T, Perez-Potti A, Rivera-Ballesteros O, Strålin K, Gorin J-B, Olsson A, et al. Robust T Cell Immunity in Convalescent Individuals with Asymptomatic or Mild COVID-19. Cell. 2020 Oct 1;183(1):158-168.e14.

57. Nienhold R, Ciani Y, Koelzer VH, Tzankov A, Haslbauer JD, Menter T, et al. Two distinct immunopathological profiles in autopsy lungs of COVID-19. Nat Commun. 2020 Oct 8;11(1):5086.

58. Puzyrenko A, Felix JC, Sun Y, Rui H, Sheinin Y. Acute SARS-CoV-2 pneumonitis with cytotoxic CD8 positive T-lymphocytes: Case report and review of the literature. Pathol - Res Pract. 2021 Apr 1;220:153380.

59. Schurink B, Roos E, Radonic T, Barbe E, Bouman CSC, Boer HH de, et al. Viral presence and immunopathology in patients with lethal COVID-19: a prospective autopsy cohort study. Lancet Microbe. 2020 Nov 1;1(7):e290–9.

60. Song J-W, Zhang C, Fan X, Meng F-P, Xu Z, Xia P, et al. Immunological and inflammatory profiles in mild and severe cases of COVID-19. Nat Commun. 2020 Jul 8;11(1):3410.

61. Manson JJ, Crooks C, Naja M, Ledlie A, Goulden B, Liddle T, et al. COVID-19-associated hyperinflammation and escalation of patient care: a retrospective longitudinal cohort study. Lancet Rheumatol. 2020 Oct 1;2(10):e594–602.

62. Bhaskar S, Sinha A, Banach M, Mittoo S, Weissert R, Kass JS, et al. Cytokine Storm in COVID-19—Immunopathological Mechanisms, Clinical Considerations, and Therapeutic Approaches: The REPROGRAM Consortium Position Paper. Front Immunol. 2020;11:1648.

63. Blot M, Jacquier M, Aho Glele L-S, Beltramo G, Nguyen M, Bonniaud P, et al. CXCL10 could drive longer duration of mechanical ventilation during COVID-19 ARDS. Crit Care. 2020 Nov 2;24(1):632.

64. Del Valle DM, Kim-Schulze S, Huang H-H, Beckmann ND, Nirenberg S, Wang B, et al. An inflammatory cytokine signature predicts COVID-19 severity and survival. Nat Med. 2020 Oct;26(10):1636–43.

65. Zhu J, Pang J, Ji P, Zhong Z, Li H, Li B, et al. Elevated interleukin-6 is associated with severity of COVID-19: A meta-analysis. J Med Virol. 2021;93(1):35–7.

66. Gubernatorova EO, Gorshkova EA, Polinova AI, Drutskaya MS. IL-6: Relevance for immunopathology of SARS-CoV-2. Cytokine Growth Factor Rev. 2020 Jun;53:13–24.

67. Magro G. SARS-CoV-2 and COVID-19: Is interleukin-6 (IL-6) the 'culprit lesion' of ARDS onset? What is there besides Tocilizumab? SGP130Fc. Cytokine X. 2020 Jun 1;2(2):100029.

68. Gabay C. Interleukin-6 and chronic inflammation. Arthritis Res Ther. 2006;8(Suppl 2):S3.

69. Shibabaw T. Inflammatory Cytokine: IL-17A Signaling Pathway in Patients Present with COVID-19 and Current Treatment Strategy . J Inflamm Res. 2020 Oct 6;13:673–80.

70. Zhao J, Yuan Q, Wang H, Liu W, Liao X, Su Y, et al. Antibody Responses to SARS-CoV-2 in Patients With Novel Coronavirus Disease 2019. Clin Infect Dis. 2020 Nov 19;71(16):2027–34.

71. Shrivastava S, Palkar S, Shah J, Rane P, Lalwani S, Mishra AC, et al. Early and High SARS-CoV-2 Neutralizing Antibodies Are Associated with Severity in COVID-19 Patients from India. Am J Trop Med Hyg. 2021 Aug 11;105(2):401–6.

72. Yates JL, Ehrbar DJ, Hunt DT, Girardin RC, Dupuis AP, Payne AF, et al. Serological analysis reveals an imbalanced IgG subclass composition associated with COVID-19 disease severity. Cell Rep Med. 2021 Jul 20;2(7):100329.

73. Long Q-X, Liu B-Z, Deng H-J, Wu G-C, Deng K, Chen Y-K, et al. Antibody responses to SARS-CoV-2 in patients with COVID-19. Nat Med. 2020 Jun;26(6):845–8.

74. Tan Y-F, Leong C-F, Cheong S-K. Observation of dendritic cell morphology under light, phase-contrast or confocal laser scanning microscopy. Malays J Pathol. 2010 Dec;32(2):97–102.

75. Boltjes A, Van Wijk F. Human Dendritic Cell Functional Specialization in Steady-State and Inflammation. Front Immunol [Internet]. 2014 [cited 2019 Aug 29];5. Available from: https://www.frontiersin.org/articles/10.3389/fimmu.2014.00131/full

76. Banchereau J, Steinman RM. Dendritic cells and the control of immunity. Nature. 1998 Mar;392(6673):245–52.

77. Tussiwand R, Gautier EL. Transcriptional Regulation of Mononuclear Phagocyte Development. Front Immunol. 2015;6:533.

78. Murphy TL, Grajales-Reyes GE, Wu X, Tussiwand R, Briseño CG, Iwata A, et al. Transcriptional Control of Dendritic Cell Development. Annu Rev Immunol. 2016 May 20;34:93–119.

79. Collin M, Bigley V. Human dendritic cell subsets: an update. Immunology. 2018 May;154(1):3–20.

80. Tamura T, Kurotaki D, Koizumi S. Regulation of myelopoiesis by the transcription factor IRF8. Int J Hematol. 2015 Apr;101(4):342–51.

81. Sichien D, Lambrecht BN, Guilliams M, Scott CL. Development of conventional dendritic cells: from common bone marrow progenitors to multiple subsets in peripheral tissues. Mucosal Immunol. 2017 Jul;10(4):831–44.

82. Noubade R, Majri-Morrison S, Tarbell KV. Beyond cDC1: Emerging Roles of DC Crosstalk in Cancer Immunity. Front Immunol. 2019 May 9;10:1014.

83. Jongbloed SL, Kassianos AJ, McDonald KJ, Clark GJ, Ju X, Angel CE, et al. Human CD141+ (BDCA-3)+ dendritic cells (DCs) represent a unique myeloid DC subset that cross-presents necrotic cell antigens. J Exp Med. 2010 Jun 7;207(6):1247–60.

84. Lauterbach H, Bathke B, Gilles S, Traidl-Hoffmann C, Luber CA, Fejer G, et al. Mouse CD8alpha+ DCs and human BDCA3+ DCs are major producers of IFN-lambda in response to poly IC. J Exp Med. 2010 Nov 22;207(12):2703–17.

85. Yu C, Becker C, Metang P, Marches F, Wang Y, Toshiyuki H, et al. Human CD141(+) Dendritic Cells Induce CD4(+) T Cells To Produce Type 2 Cytokines. J Immunol Baltim Md 1950. 2014 Sep 22;193.

86. Chu C-C, Ali N, Karagiannis P, Meglio PD, Skowera A, Napolitano L, et al. Resident CD141 (BDCA3)+ dendritic cells in human skin produce IL-10 and induce regulatory T cells that suppress skin inflammation. J Exp Med. 2012 May 7;209(5):935–45.

87. Schlitzer A, McGovern N, Teo P, Zelante T, Atarashi K, Low D, et al. IRF4 Transcription Factor-Dependent CD11b+ Dendritic Cells in Human and Mouse Control Mucosal IL-17 Cytokine Responses. Immunity. 2013 May 23;38(5):970–83.

88. Qu C, Brinck-Jensen N-S, Zang M, Chen K. Monocyte-derived dendritic cells: targets as potent antigen-presenting cells for the design of vaccines against infectious diseases. Int J Infect Dis. 2014 Feb 1;19:1–5.

89. Cabeza-Cabrerizo M, Cardoso A, Minutti CM, Pereira da Costa M, Reis e Sousa C. Dendritic Cells Revisited. Annu Rev Immunol. 2021;39(1):131–66.

90. Fitzgerald-Bocarsly P, Dai J, Singh S. Plasmacytoid dendritic cells and type I IFN: 50 years of convergent history. Cytokine Growth Factor Rev. 2008 Feb;19(1):3–19.

91. Li D, Wu M. Pattern recognition receptors in health and diseases. Signal Transduct Target Ther. 2021 Aug 4;6(1):1–24.

92. Schreibelt G, Tel J, Sliepen KHEWJ, Benitez-Ribas D, Figdor CG, Adema GJ, et al. Toll-like receptor expression and function in human dendritic cell subsets: implications for dendritic cell-based anti-cancer immunotherapy. Cancer Immunol Immunother. 2010 Oct 1;59(10):1573–82.

93. Shimizu T. Structural insights into ligand recognition and regulation of nucleic acid-sensing Toll-like receptors. Curr Opin Struct Biol. 2017 Dec;47:52–9.

94. Tanji H, Ohto U, Shibata T, Taoka M, Yamauchi Y, Isobe T, et al. Toll-like receptor 8 senses degradation products of single-stranded RNA. Nat Struct Mol Biol. 2015 Feb;22(2):109–15.

95. El-Zayat SR, Sibaii H, Mannaa FA. Toll-like receptors activation, signaling, and targeting: an overview. Bull Natl Res Cent. 2019 Dec 12;43(1):187.

96. van der Made CI, Simons A, Schuurs-Hoeijmakers J, van den Heuvel G, Mantere T, Kersten S, et al. Presence of Genetic Variants Among Young Men With Severe COVID-19. JAMA. 2020 Aug 18;324(7):663–73.

97. O'Neill LAJ, Golenbock D, Bowie AG. The history of Toll-like receptors — redefining innate immunity. Nat Rev Immunol. 2013 Jun;13(6):453–60.

98. Al-Ashmawy GMZ. Dendritic Cell Subsets, Maturation and Function. Dendritic Cells [Internet]. 2018 Nov 7 [cited 2020 Jan 14]; Available from: https://www.intechopen.com/books/dendritic-cells/dendritic-cell-subsets-maturation-and-function

99. Mantia-Smaldone GM, Chu CS. A Review of Dendritic Cell Therapy for Cancer: Progress and Challenges. BioDrugs. 2013 Oct 1;27(5):453–68.

100. Sharpe AH. Mechanisms of Costimulation. Immunol Rev. 2009 May;229(1):5–11.

101. Neves BM, Lopes MC, Cruz MT. Pathogen Strategies to Evade Innate Immune Response: A Signaling Point of View [Internet]. Protein Kinases. IntechOpen; 2012 [cited 2021 Dec 11]. Available from: https://www.intechopen.com/chapters/37360

102. Walsh KP, Mills KHG. Dendritic cells and other innate determinants of T helper cell polarisation. Trends Immunol. 2013 Nov;34(11):521–30.

103. Shresta S, Pham CT, Thomas DA, Graubert TA, Ley TJ. How do cytotoxic lymphocytes kill their targets? Curr Opin Immunol. 1998 Oct;10(5):581–7.

104. Curtsinger JM, Lins DC, Mescher MF. Signal 3 determines tolerance versus full activation of naive CD8 T cells: dissociating proliferation and development of effector function. J Exp Med. 2003 May 5;197(9):1141–51.

105. Curtsinger JM, Lins DC, Johnson CM, Mescher MF. Signal 3 Tolerant CD8 T Cells Degranulate in Response to Antigen but Lack Granzyme B to Mediate Cytolysis. J Immunol. 2005 Oct 1;175(7):4392–9.

106. Novy P, Quigley M, Huang X, Yang Y. CD4 T Cells Are Required for CD8 T Cell Survival during Both Primary and Memory Recall Responses. J Immunol. 2007 Dec 15;179(12):8243–51.

107. Feau S, Garcia Z, Arens R, Yagita H, Borst J, Schoenberger SP. The CD4+ T-cell help signal is transmitted from APC to CD8+ T-cells via CD27–CD70 interactions. Nat Commun. 2012 Jul 10;3(1):948.

108. Buller RML, Holmes KL, Hügin A, Frederickson TN, Morse HC. Induction of cytotoxic T-cell responses in vivo in the absence of CD4 helper cells. Nature. 1987 Jul;328(6125):77–9.

109. Stevenson PG, Belz GT, Altman JD, Doherty PC. Virus-specific CD8+ T cell numbers are maintained during γ-herpesvirus reactivation in CD4-deficient mice. Proc Natl Acad Sci. 1998 Dec 22;95(26):15565–70.

110. Bevan MJ. Helping the CD8+ T-cell response. Nat Rev Immunol. 2004 Aug;4(8):595–602.

111. Brocker T, Riedinger M, Karjalainen K. Targeted expression of major histocompatibility complex (MHC) class II molecules demonstrates that dendritic cells can induce negative but not positive selection of thymocytes in vivo. J Exp Med. 1997 Feb 3;185(3):541–50.

112. Ohnmacht C, Pullner A, King SBS, Drexler I, Meier S, Brocker T, et al. Constitutive ablation of dendritic cells breaks self-tolerance of CD4 T cells and results in spontaneous fatal autoimmunity. J Exp Med. 2009 Mar 16;206(3):549–59.

113. Tan JKH, O'Neill HC. Maturation requirements for dendritic cells in T cell stimulation leading to tolerance versus immunity. J Leukoc Biol. 2005;78(2):319–24.

114. Sato K, Uto T, Fukaya T, Takagi H. Regulatory Dendritic Cells. Emerg Concepts Target Immune Checkp Cancer Autoimmun. 2017;47–71.

115. Raker VK, Domogalla MP, Steinbrink K. Tolerogenic Dendritic Cells for Regulatory T Cell Induction in Man. Front Immunol. 2015;6:569.

116. Lutz MB, Schuler G. Immature, semi-mature and fully mature dendritic cells: which signals induce tolerance or immunity? Trends Immunol. 2002 Sep 1;23(9):445–9.

117. Joffre O, Nolte MA, Spörri R, Reis e Sousa C. Inflammatory signals in dendritic cell activation and the induction of adaptive immunity. Immunol Rev. 2009 Jan;227(1):234–47.

118. Xia S, Guo Z, Xu X, Yi H, Wang Q, Cao X. Hepatic microenvironment programs hematopoietic progenitor differentiation into regulatory dendritic cells, maintaining liver tolerance. Blood. 2008 Oct 15;112(8):3175–85.

119. Hadeiba H, Sato T, Habtezion A, Oderup C, Pan J, Butcher EC. CCR9 expression defines tolerogenic plasmacytoid dendritic cells capable of suppressing acute graft-versus-host disease. Nat Immunol. 2008 Nov;9(11):1253–60.

120. Manicassamy S, Pulendran B. Dendritic cell control of tolerogenic responses. Immunol Rev. 2011 May;241(1):206–27.

121. Holt P g., Stumbles P a. Characterization of Dendritic Cell Populations in the Respiratory Tract. J Aerosol Med. 2000 Jan 1;13(4):361–7.

122. Bertram S, Heurich A, Lavender H, Gierer S, Danisch S, Perin P, et al. Influenza and SARS-Coronavirus Activating Proteases TMPRSS2 and HAT Are Expressed at Multiple Sites in Human Respiratory and Gastrointestinal Tracts. PLOS ONE. 2012 Apr 30;7(4):e35876.

123. Yang D, Chu H, Hou Y, Chai Y, Shuai H, Lee AC-Y, et al. Attenuated Interferon and Proinflammatory Response in SARS-CoV-2–Infected Human Dendritic Cells Is Associated With Viral Antagonism of STAT1 Phosphorylation. J Infect Dis. 2020 Aug 4;222(5):734–45.

124. Wang K, Chen W, Zhang Z, Deng Y, Lian J-Q, Du P, et al. CD147-spike protein is a novel route for SARS-CoV-2 infection to host cells. Signal Transduct Target Ther. 2020 Dec 4;5:283.

125. Winheim E, Rinke L, Lutz K, Reischer A, Leutbecher A, Wolfram L, et al. Impaired function and delayed regeneration of dendritic cells in COVID-19. PLOS Pathog. 2021 Oct 6;17(10):e1009742.

126. Sánchez-Cerrillo I, Landete P, Aldave B, Sánchez-Alonso S, Sánchez-Azofra A, Marcos-Jiménez A, et al. COVID-19 severity associates with pulmonary redistribution of CD1c+ DCs and inflammatory transitional and nonclassical monocytes. J Clin Invest. 2020 Dec 1;130(12):6290–300.

127. Pérez-Gómez A, Vitallé J, Gasca-Capote C, Gutierrez-Valencia A, Trujillo-Rodriguez M, Serna-Gallego A, et al. Dendritic cell deficiencies persist seven months after SARS-CoV-2 infection. Cell Mol Immunol. 2021 Sep;18(9):2128–39.

128. Zhou R, To KK-W, Wong Y-C, Liu L, Zhou B, Li X, et al. Acute SARS-CoV-2 Infection Impairs Dendritic Cell and T Cell Responses. Immunity. 2020 Oct 13;53(4):864-877.e5.

129. Cervantes-Barragan L, Züst R, Weber F, Spiegel M, Lang KS, Akira S, et al. Control of coronavirus infection through plasmacytoid dendritic-cell–derived type I interferon. Blood. 2006 Sep 19;109(3):1131–7.

130. Galati D, Zanotta S, Capitelli L, Bocchino M. A bird's eye view on the role of dendritic cells in SARS-CoV-2 infection: Perspectives for immune-based vaccines. Allergy [Internet]. [cited 2021 Nov 23];n/a(n/a). Available from: https://onlinelibrary.wiley.com/doi/abs/10.1111/all.15004

131. Thevarajan I, Nguyen THO, Koutsakos M, Druce J, Caly L, van de Sandt CE, et al. Breadth of concomitant immune responses prior to patient recovery: a case report of non-severe COVID-19. Nat Med. 2020 Apr;26(4):453–5.

132. Cyclic Adenosine Monophosphate Signaling in Inflammatory Skin Disease | Abstract [Internet]. [cited 2021 Dec 11]. Available from: https://www.longdom.org/abstract/cyclic-adenosine-monophosphate-signaling-in-inflammatory-skin-disease-13275.html

133. Tavares LP, Negreiros-Lima GL, Lima KM, E Silva PMR, Pinho V, Teixeira MM, et al. Blame the signaling: Role of cAMP for the resolution of inflammation. Pharmacol Res. 2020 Sep 1;159:105030.

134. Zaccolo M, Di Benedetto G, Lissandron V, Mancuso L, Terrin A, Zamparo I. Restricted diffusion of a freely diffusible second messenger: mechanisms underlying compartmentalized cAMP signalling. Biochem Soc Trans. 2006 Aug;34(Pt 4):495–7.

135. Essayan DM. Cyclic nucleotide phosphodiesterases. J Allergy Clin Immunol. 2001 Nov 1;108(5):671–80.

136. Maurice DH, Ke H, Ahmad F, Wang Y, Chung J, Manganiello VC. Advances in targeting cyclic nucleotide phosphodiesterases. Nat Rev Drug Discov. 2014 Apr;13(4):290–314.

137. Zaccolo M, Pozzan T. Discrete microdomains with high concentration of cAMP in stimulated rat neonatal cardiac myocytes. Science. 2002 Mar 1;295(5560):1711–5.

138. Zuo H, Cattani-Cavalieri I, Musheshe N, Nikolaev VO, Schmidt M. Phosphodiesterases as therapeutic targets for respiratory diseases. Pharmacol Ther. 2019 May 1;197:225–42.

139. Shakur Y, Holst LS, Landstrom TR, Movsesian M, Degerman E, Manganiello V. Regulation and function of the cyclic nucleotide phosphodiesterase (PDE3) gene family. In: Progress in Nucleic Acid Research and Molecular Biology [Internet]. Academic Press; 2000 [cited 2021 Dec 11]. p. 241–77. Available from: https://www.sciencedirect.com/science/article/pii/S0079660300660312

140. Pavlaki N, Nikolaev VO. Imaging of PDE2- and PDE3-Mediated cGMP-to-cAMP Cross-Talk in Cardiomyocytes. J Cardiovasc Dev Dis. 2018 Mar;5(1):4.

141. Serezani CH, Ballinger MN, Aronoff DM, Peters-Golden M. Cyclic AMP: master regulator of innate immune cell function. Am J Respir Cell Mol Biol. 2008 Aug;39(2):127–32.

142. Jin S-LC, Conti M. Induction of the cyclic nucleotide phosphodiesterase PDE4B is essential for LPS-activated TNF-alpha responses. Proc Natl Acad Sci U S A. 2002 May 28;99(11):7628–33.

143. Jin S-LC, Lan L, Zoudilova M, Conti M. Specific role of phosphodiesterase 4B in lipopolysaccharide-induced signaling in mouse macrophages. J Immunol Baltim Md 1950. 2005 Aug 1;175(3):1523–31.

144. Ariga M, Neitzert B, Nakae S, Mottin G, Bertrand C, Pruniaux MP, et al. Nonredundant function of phosphodiesterases 4D and 4B in neutrophil recruitment to the site of inflammation. J Immunol Baltim Md 1950. 2004 Dec 15;173(12):7531–8.

145. Li H, Zuo J, Tang W. Phosphodiesterase-4 Inhibitors for the Treatment of Inflammatory Diseases. Front Pharmacol [Internet]. 2018 Oct 17 [cited 2019 Nov 11];9. Available from: https://www.ncbi.nlm.nih.gov/pmc/articles/PMC6199465/

146. Schmidt M, Dekker FJ, Maarsingh H. Exchange Protein Directly Activated by cAMP (epac): A Multidomain cAMP Mediator in the Regulation of Diverse Biological Functions. Michel MC, editor. Pharmacol Rev. 2013 Apr 1;65(2):670–709.

147. Grootendorst DC, Gauw SA, Verhoosel RM, Sterk PJ, Hospers JJ, Bredenbröker D, et al. Reduction in sputum neutrophil and eosinophil numbers by the PDE4 inhibitor roflumilast in patients with COPD. Thorax. 2007 Dec;62(12):1081–7.

148. Kubo S, Kobayashi M, Iwata M, Miyata K, Takahashi K, Shimizu Y. Anti-neutrophilic inflammatory activity of ASP3258, a novel phosphodiesterase type 4 inhibitor. Int Immunopharmacol. 2012 Jan 1;12(1):59–63.

149. Buenestado A, Grassin-Delyle S, Guitard F, Naline E, Faisy C, Israël-Biet D, et al. Roflumilast inhibits the release of chemokines and TNF-α from human lung macrophages stimulated with lipopolysaccharide. Br J Pharmacol. 2012 Mar;165(6):1877–90.

150. Gianello V, Salvi V, Parola C, Moretto N, Facchinetti F, Civelli M, et al. The PDE4 inhibitor CHF6001 modulates pro-inflammatory cytokines, chemokines and Th1- and Th17-polarizing cytokines in human dendritic cells. Biochem Pharmacol. 2019 May 1;163:371–80.

151. Seldon PM, Giembycz MA. Suppression of granulocyte/macrophage colony-stimulating factor release from human monocytes by cyclic AMP-elevating drugs: role of interleukin-10. Br J Pharmacol. 2001 Sep;134(1):58–67.

152. Aoki M, Fukunaga M, Kitagawa M, Hayashi K, Morokata T, Ishikawa G, et al. Effect of a novel anti-inflammatory compound, YM976, on antigen-induced eosinophil infiltration into the lungs in rats, mice, and ferrets. J Pharmacol Exp Ther. 2000 Dec;295(3):1149–55.

153. Lazaros IS, Athanasios M, Dimitrios PB. Phosphodiesterase 4 Inhibitors in Immune-mediated Diseases: Mode of Action, Clinical Applications, Current and Future Perspectives. Curr Med Chem. 2017 Jul 31;24(28):3054–67.

154. Schafer PH, Parton A, Capone L, Cedzik D, Brady H, Evans JF, et al. Apremilast is a selective PDE4 inhibitor with regulatory effects on innate immunity. Cell Signal. 2014 Sep;26(9):2016–29.

155. Baroja ML, Cieslinski LB, Torphy TJ, Wange RL, Madrenas J. Specific CD3ε Association of a Phosphodiesterase 4B Isoform Determines Its Selective Tyrosine Phosphorylation After CD3 Ligation. J Immunol. 1999 Feb 15;162(4):2016–23.

156. Essayan DM, Kagey-Sobotka A, Lichtenstein LM, Huang SK. Differential regulation of human antigen-specific Th1 and Th2 lymphocyte responses by isozyme selective cyclic nucleotide phosphodiesterase inhibitors. J Pharmacol Exp Ther. 1997 Jul;282(1):505–12.

157. Peter D, Jin SLC, Conti M, Hatzelmann A, Zitt C. Differential Expression and Function of Phosphodiesterase 4 (PDE4) Subtypes in Human Primary CD4+ T Cells: Predominant Role of PDE4D. J Immunol. 2007 Apr 15;178(8):4820–31.

158. Chen W, Wang J, Xu Z, Huang F, Qian W, Ma J, et al. Apremilast Ameliorates Experimental Arthritis via Suppression of Th1 and Th17 Cells and Enhancement of CD4+Foxp3+ Regulatory T Cells Differentiation. Front Immunol. 2018;9:1662.

159. Edwards MR, Facchinetti F, Civelli M, Villetti G, Johnston SL. Anti-inflammatory effects of the novel inhaled phosphodiesterase type 4 inhibitor CHF6001 on virus-inducible cytokines. Pharmacol Res Perspect. 2016 Feb;4(1):e00202.

160. Van Ly D, De Pedro M, James P, Morgan L, Black JL, Burgess JK, et al. Inhibition of phosphodiesterase 4 modulates cytokine induction from toll like receptor activated, but not rhinovirus infected, primary human airway smooth muscle. Respir Res. 2013 Nov 15;14(1):127.

161. Leclerc O, Lagente V, Planquois J-M, Berthelier C, Artola M, Eichholtz T, et al. Involvement of MMP-12 and phosphodiesterase type 4 in cigarette smoke-induced inflammation in mice. Eur Respir J. 2006 Jun 1;27(6):1102–9.

162. Martorana PA, Beume R, Lucattelli M, Wollin L, Lungarella G. Roflumilast Fully Prevents Emphysema in Mice Chronically Exposed to Cigarette Smoke. Am J Respir Crit Care Med. 2005 Oct 1;172(7):848–53.

163. Gamble E, Grootendorst DC, Brightling CE, Troy S, Qiu Y, Zhu J, et al. Antiinflammatory effects of the phosphodiesterase-4 inhibitor cilomilast (Ariflo) in chronic obstructive pulmonary disease. Am J Respir Crit Care Med. 2003 Oct 15;168(8):976–82.

164. Rabe KF, Bateman ED, O'Donnell D, Witte S, Bredenbröker D, Bethke TD. Roflumilast--an oral anti-inflammatory treatment for chronic obstructive pulmonary disease: a randomised controlled trial. Lancet Lond Engl. 2005 Aug 13;366(9485):563–71.

165. Rennard SI, Calverley PMA, Goehring UM, Bredenbröker D, Martinez FJ. Reduction of exacerbations by the PDE4 inhibitor roflumilast--the importance of defining different subsets of patients with COPD. Respir Res. 2011 Jan 27;12:18.

166. Mokry J, Joskova M, Mokra D, Christensen I, Nosalova G. Effects of Selective Inhibition of PDE4 and PDE7 on Airway Reactivity and Cough in Healthy and Ovalbumin-Sensitized Guinea Pigs. In: Pokorski M, editor. Respiratory Regulation - The Molecular Approach. Dordrecht: Springer Netherlands; 2013. p. 57–64. (Advances in Experimental Medicine and Biology).

167. Mokrý J, Urbanová A, Medvedová I, Kertys M, Mikolka P, Kosutová P, et al. Effects of Selective Inhibition of PDE4 by YM976 on Airway Reactivity and Cough in Ovalbumin-Sensitized Guinea Pigs. In: Pokorski M, editor. Allergy and Respiration [Internet]. Cham: Springer International Publishing; 2016 [cited 2021 Dec 5]. p. 61–70. (Advances in Experimental Medicine and Biology). Available from: https://doi.org/10.1007/5584_2016_237

168. Jin S-LC, Goya S, Nakae S, Wang D, Bruss M, Hou C, et al. Phosphodiesterase 4B is essential for TH2-cell function and development of airway hyperresponsiveness in allergic asthma. J Allergy Clin Immunol. 2010 Dec 1;126(6):1252-1259.e12.

169. Gauvreau GM, Boulet L-P, Schmid-Wirlitsch C, Côté J, Duong M, Killian KJ, et al. Roflumilast attenuates allergen-induced inflammation in mild asthmatic subjects. Respir Res. 2011 Dec 1;12(1):140.

170. Kosutova P, Mikolka P, Kolomaznik M, Rezakova S, Calkovska A, Mokra D. Effects of roflumilast, a phosphodiesterase-4 inhibitor, on the lung functions in a saline lavage-induced model of acute lung injury. Physiol Res. 2017 Sep 22;66(Suppl 2):S237–45.

171. Cortijo J, Iranzo A, Milara X, Mata M, Cerdá-Nicolás M, Ruiz-Saurí A, et al. Roflumilast, a phosphodiesterase 4 inhibitor, alleviates bleomycin-induced lung injury. Br J Pharmacol. 2009;156(3):534–44.

172. Rocco PRM, Momesso DP, Figueira RC, Ferreira HC, Cadete RA, Légora-Machado A, et al. Therapeutic potential of a new phosphodiesterase inhibitor in acute lung injury. Eur Respir J. 2003 Jul 1;22(1):20–7.

173. Imam F, Al-Harbi NO, Al-Harbi MM, Qamar W, Aljerian K, Belali OM, et al. Apremilast ameliorates carfilzomib-induced pulmonary inflammation and vascular injuries. Int Immunopharmacol. 2019 Jan 1;66:260–6.

174. Yang D, Yang Y, Zhao Y. Ibudilast, a Phosphodiesterase-4 Inhibitor, Ameliorates Acute Respiratory Distress Syndrome in Neonatal Mice by Alleviating Inflammation and Apoptosis. Med Sci Monit Int Med J Exp Clin Res. 2020 Mar 31;26:e922281-1-e922281-8.

175. Sharma G, Sharma DC, Fen LH, Pathak M, Bethur N, Pendharkar V, et al. Reduction of influenza virus-induced lung inflammation and mortality in animals treated with a phosophodisestrase-4 inhibitor and a selective serotonin reuptake inhibitor. Emerg Microbes Infect. 2013 Jan 1;2(1):1–9.

176. Armani E, Amari G, Rizzi A, Fanti RD, Ghidini E, Capaldi C, et al. Novel Class of Benzoic Acid Ester Derivatives as Potent PDE4 Inhibitors for Inhaled Administration in the Treatment of Respiratory Diseases. J Med Chem. 2014 Feb 13;57(3):793–816.

177. Moretto N, Caruso P, Bosco R, Marchini G, Pastore F, Armani E, et al. CHF6001 I: a novel highly potent and selective phosphodiesterase 4 inhibitor with robust anti-inflammatory activity and suitable for topical pulmonary administration. J Pharmacol Exp Ther. 2015 Mar;352(3):559–67.

178. Singh D, Nandeuil MA, Pigeon-Francisco C, Emirova A, Santoro D, Biondaro S, et al. Efficacy and safety of four doses of CHF6001, a novel inhaled phosphodiesterase-4 inhibitor (PDE4i), in patients with moderate-to-severe COPD. Eur Respir J [Internet]. 2019 Sep 28 [cited 2021 May 4];54(suppl 63). Available from: https://erj.ersjournals.com/content/54/suppl_63/OA262

179. Facchinetti F, Civelli M, Singh D, Papi A, Emirova A, Govoni M. Tanimilast, A Novel Inhaled Pde4 Inhibitor for the Treatment of Asthma and Chronic Obstructive Pulmonary Disease. Front Pharmacol. 2021;12:3262.

180. Ponce-Gallegos MA, Ramírez-Venegas A, Falfán-Valencia R. Th17 profile in COPD exacerbations. Int J Chron Obstruct Pulmon Dis. 2017 Jun 22;12:1857–65.

181. Chung KF. Cytokines in chronic obstructive pulmonary disease. Eur Respir J. 2001 Jul 2;18(34 suppl):50s–9s.

182. Lea S, Metryka A, Li J, Higham A, Bridgewood C, Villetti G, et al. The modulatory effects of the PDE4 inhibitors CHF6001 and roflumilast in alveolar macrophages and lung tissue from COPD patients. Cytokine. 2019 Nov;123:154739.

183. Villetti G, Carnini C, Battipaglia L, Preynat L, Bolzoni PT, Bassani F, et al. CHF6001 II: a novel phosphodiesterase 4 inhibitor, suitable for topical pulmonary administration--in vivo preclinical pharmacology profile defines a potent anti-inflammatory compound with a wide therapeutic window. J Pharmacol Exp Ther. 2015 Mar;352(3):568–78.

184. Marass F, Upton C. Sequence Searcher: A Java tool to perform regular expression and fuzzy searches of multiple DNA and protein sequences. BMC Res Notes. 2009 Jan 30;2(1):14.

185. Salvi V, Vaira X, Gianello V, Vermi W, Bugatti M, Sozzani S, et al. TLR Signalling Pathways Diverge in Their Ability to Induce PGE2. Mediators Inflamm. 2016;2016:5678046.

186. Salvi V, Scutera S, Rossi S, Zucca M, Alessandria M, Greco D, et al. Dual regulation of osteopontin production by TLR stimulation in dendritic cells. J Leukoc Biol. 2013;94(1):147–58.

187. Salvi V, Gianello V, Busatto S, Bergese P, Andreoli L, D'Oro U, et al. Exosome-delivered microRNAs promote IFN-**α** secretion by human plasmacytoid DCs via TLR7. JCI Insight [Internet]. 2018 May 17 [cited 2021 Dec 12];3(10). Available from: https://insight.jci.org/articles/view/98204

188. Chow KT, Gale M, Loo Y-M. RIG-I and Other RNA Sensors in Antiviral Immunity. Annu Rev Immunol. 2018 Apr 26;36:667–94.

189. Kim SJ, Kim G, Kim N, Chu H, Park B-C, Yang JS, et al. Human CD141+ dendritic cells generated from adult peripheral blood monocytes. Cytotherapy. 2019 Oct 1;21(10):1049–63.

190. Merad M, Martin JC. Author Correction: Pathological inflammation in patients with COVID-19: a key role for monocytes and macrophages. Nat Rev Immunol. 2020 Jul;20(7):448.

191. Lipscomb MF, Masten BJ. Dendritic Cells: Immune Regulators in Health and Disease. Physiol Rev. 2002 Jan 1;82(1):97–130.

192. Meyerowitz EA, Sen P, Schoenfeld SR, Neilan TG, Frigault MJ, Stone JH, et al. Immunomodulation as Treatment for Severe Coronavirus Disease 2019: A Systematic Review of Current Modalities and Future Directions. Clin Infect Dis [Internet]. 2020 Nov 20 [cited 2021 May 4];(ciaa1759). Available from: https://doi.org/10.1093/cid/ciaa1759

193. Giorgi M, Cardarelli S, Ragusa F, Saliola M, Biagioni S, Poiana G, et al. Phosphodiesterase Inhibitors: Could They Be Beneficial for the Treatment of COVID-19? Int J Mol Sci. 2020 Jan;21(15):5338.

194. Dalamaga M, Karampela I, Mantzoros CS. Commentary: Phosphodiesterase 4 inhibitors as potential adjunct treatment targeting the cytokine storm in COVID-19. Metabolism. 2020 Aug;109:154282.

195. Heil F, Hemmi H, Hochrein H, Ampenberger F, Kirschning C, Akira S, et al. Species-specific recognition of single-stranded RNA via toll-like receptor 7 and 8. Science. 2004 Mar 5;303(5663):1526–9.

196. Kuznik A, Bencina M, Svajger U, Jeras M, Rozman B, Jerala R. Mechanism of endosomal TLR inhibition by antimalarial drugs and imidazoquinolines. J Immunol Baltim Md 1950. 2011 Apr 15;186(8):4794–804.

197. Fabbri M, Paone A, Calore F, Galli R, Gaudio E, Santhanam R, et al. MicroRNAs bind to Toll-like receptors to induce prometastatic inflammatory response. Proc Natl Acad Sci U S A. 2012 Jul 31;109(31):E2110-2116.

198. Li Y, Chen M, Cao H, Zhu Y, Zheng J, Zhou H. Extraordinary GU-rich single-strand RNA identified from SARS coronavirus contributes an excessive innate immune response. Microbes Infect. 2013 Feb;15(2):88–95.

199. Moreno-Eutimio MA, López-Macías C, Pastelin-Palacios R. Bioinformatic analysis and identification of single-stranded RNA sequences recognized by TLR7/8 in the SARS-CoV-2, SARS-CoV, and MERS-CoV genomes. Microbes Infect. 2020 Jun;22(4–5):226–9.

200. Scheuplein VA, Seifried J, Malczyk AH, Miller L, Höcker L, Vergara-Alert J, et al. High secretion of interferons by human plasmacytoid dendritic cells upon recognition of Middle East respiratory syndrome coronavirus. J Virol. 2015 Apr;89(7):3859–69.

201. Cervantes-Barragán L, Kalinke U, Züst R, König M, Reizis B, López-Macías C, et al. Type I IFN-mediated protection of macrophages and dendritic cells secures control of murine coronavirus infection. J Immunol Baltim Md 1950. 2009 Jan 15;182(2):1099–106.

202. Dyavar SR, Singh R, Emani R, Pawar GP, Chaudhari VD, Podany AT, et al. Role of toll-like receptor 7/8 pathways in regulation of interferon response and inflammatory mediators during SARS-CoV2 infection and potential therapeutic options. Biomed Pharmacother Biomedecine Pharmacother. 2021 Sep;141:111794.

203. van der Made CI, Simons A, Schuurs-Hoeijmakers J, van den Heuvel G, Mantere T, Kersten S, et al. Presence of Genetic Variants Among Young Men With Severe COVID-19. JAMA. 2020 Aug 18;324(7):663–73.

204. Onodi F, Bonnet-Madin L, Meertens L, Karpf L, Poirot J, Zhang S-Y, et al. SARS-CoV-2 induces human plasmacytoid predendritic cell diversification via UNC93B and IRAK4. J Exp Med [Internet]. 2021 Jan 28 [cited 2021 Apr 16];218(4). Available from: https://www.ncbi.nlm.nih.gov/pmc/articles/PMC7849819/

205. Kouwaki T, Okamoto M, Tsukamoto H, Fukushima Y, Oshiumi H. Extracellular Vesicles Deliver Host and Virus RNA and Regulate Innate Immune Response. Int J Mol Sci. 2017 Mar 20;18(3):E666.

206. Campbell GR, Rawat P, Bruckman RS, Spector SA. Human Immunodeficiency Virus Type 1 Nef Inhibits Autophagy through Transcription Factor EB Sequestration. PLoS Pathog. 2015 Jun;11(6):e1005018.

207. Borges RC, Hohmann MS, Borghi SM. Dendritic cells in COVID-19 immunopathogenesis: insights for a possible role in determining disease outcome. Int Rev Immunol. 2020 Nov 16;0(0):1–18.

208. Sharma NK, Sarode SC, Sarode G, Patil S. Is a COVID-19 vaccine developed by nature already at work? Med Hypotheses. 2020 Dec;145:110335.

209. Zhang Q, Bastard P, Bolze A, Jouanguy E, Zhang S-Y, COVID Human Genetic Effort, et al. Life-Threatening COVID-19: Defective Interferons Unleash Excessive Inflammation. Med N Y N. 2020 Dec 18;1(1):14–20.

210. Merad M, Martin JC. Pathological inflammation in patients with COVID-19: a key role for monocytes and macrophages. Nat Rev Immunol. 2020 Jun;20(6):355–62.

211. Viswanathan T, Arya S, Chan S-H, Qi S, Dai N, Misra A, et al. Structural basis of RNA cap modification by SARS-CoV-2. Nat Commun. 2020 Jul 24;11(1):3718.

212. Rodrigues TS, de Sá KSG, Ishimoto AY, Becerra A, Oliveira S, Almeida L, et al. Inflammasomes are activated in response to SARS-CoV-2 infection and are associated with COVID-19 severity in patients. J Exp Med. 2021 Mar 1;218(3):e20201707.

213. Xiao TS. The nucleic acid-sensing inflammasomes. Immunol Rev. 2015 May;265(1):103–11.

214. Becker CE, O'Neill LAJ. Inflammasomes in inflammatory disorders: the role of TLRs and their interactions with NLRs. Semin Immunopathol. 2007 Sep;29(3):239–48.

215. Salvi V, Nguyen HO, Sozio F, Schioppa T, Gaudenzi C, Laffranchi M, et al. SARS-CoV-2-associated ssRNAs activate inflammation and immunity via TLR7/8. JCI Insight [Internet]. 2021 Aug 6 [cited 2021 Sep 15]; Available from: https://insight.jci.org/articles/view/150542

216. Zayed Y, Barbarawi M, Ismail E, Samji V, Kerbage J, Rizk F, et al. Use of glucocorticoids in patients with acute respiratory distress syndrome: a meta-analysis and trial sequential analysis. J Intensive Care. 2020 Jun 30;8(1):43.

217. Southworth T, Kaur M, Hodgson L, Facchinetti F, Villetti G, Civelli M, et al. Anti-inflammatory effects of the phosphodiesterase type 4 inhibitor CHF6001 on bronchoalveolar lavage lymphocytes from asthma patients. Cytokine. 2019 Jan;113:68–73.

218. Lea S, Metryka A, Li J, Higham A, Bridgewood C, Villetti G, et al. The modulatory effects of the PDE4 inhibitors CHF6001 and roflumilast in alveolar macrophages and lung tissue from COPD patients. Cytokine. 2019 Nov;123:154739.

219. Robinson PC, Liew DFL, Liew JW, Monaco C, Richards D, Shivakumar S, et al. The Potential for Repurposing Anti-TNF as a Therapy for the Treatment of COVID-19. Med. 2020 Dec 18;1(1):90–102.

220. Stone JH, Frigault MJ, Serling-Boyd NJ, Fernandes AD, Harvey L, Foulkes AS, et al. Efficacy of Tocilizumab in Patients Hospitalized with Covid-19. N Engl J Med. 2020 Dec 10;383(24):2333–44.

221. Li L, Li J, Gao M, Fan H, Wang Y, Xu X, et al. Interleukin-8 as a Biomarker for Disease Prognosis of Coronavirus Disease-2019 Patients. Front Immunol [Internet]. 2021 Jan 8 [cited 2021 Apr 28];11. Available from: https://www.ncbi.nlm.nih.gov/pmc/articles/PMC7820901/

222. Buenestado A, Grassin-Delyle S, Guitard F, Naline E, Faisy C, Israël-Biet D, et al. Roflumilast inhibits the release of chemokines and TNF-α from human lung macrophages stimulated with lipopolysaccharide. Br J Pharmacol. 2012 Mar;165(6):1877–90.

223. Li Y, Meng Q, Rao X, Wang B, Zhang X, Dong F, et al. Corticosteroid therapy in critically ill patients with COVID-19: a multicenter, retrospective study. Crit Care. 2020 Dec 18;24(1):698.

224. Keswani A, Dhana K, Rosenthal JA, Moore D, Mahdavinia M. Atopy is predictive of a decreased need for hospitalization for coronavirus disease 2019. Ann Allergy Asthma Immunol. 2020 Oct 1;125(4):479–81.

225. Green I, Merzon E, Vinker S, Golan-Cohen A, Magen E. COVID-19 Susceptibility in Bronchial Asthma. J Allergy Clin Immunol Pract. 2021 Feb 1;9(2):684-692.e1.

226. Kimura H, Francisco D, Conway M, Martinez FD, Vercelli D, Polverino F, et al. Type 2 inflammation modulates ACE2 and TMPRSS2 in airway epithelial cells. J Allergy Clin Immunol. 2020 Jul 1;146(1):80-88.e8.

227. Huang X, Xiu H, Zhang S, Zhang G. The Role of Macrophages in the Pathogenesis of ALI/ARDS. Mediators Inflamm. 2018 May 13;2018:e1264913.

228. Herbert JM, Savi P, Laplace M-C, Lalé A, Dol F, Dumas A, et al. IL-4 and IL-13 exhibit comparable abilities to reduce pyrogen-induced expression of procoagulant activity in endothelial cells and monocytes. FEBS Lett. 1993;328(3):268–70.

229. Subrahmanian S, Borczuk A, Salvatore SP, Laurence J, Ahamed J. Higher Tissue Factor (TF) Expression in the Lungs of COVID-19 Pneumonia Patients Than Patients with Acute Respiratory Distress Syndrome: Association with Thrombi Formation. Blood. 2020 Nov 5;136(Supplement 1):4–4.

230. Kirshner S, Palmer L, Bodor J, Saji M, Kohn LD, Singer DS. Major Histocompatibility Class I Gene Transcription in Thyrocytes: A Series of Interacting Regulatory DNA Sequence Elements Mediate Thyrotropin/Cyclic Adenosine 3′,5′-Monophosphate Repression. Mol Endocrinol. 2000 Jan 1;14(1):82–98.

231. Lira EC, Gonçalves DAP, Parreiras-E-Silva LT, Zanon NM, Kettelhut IC, Navegantes LCC. Phosphodiesterase-4 inhibition reduces proteolysis and atrogenes expression in rat skeletal muscles. Muscle Nerve. 2011 Sep;44(3):371–81.

232. Ganji A, Farahani I, Khansarinejad B, Ghazavi A, Mosayebi G. Increased expression of CD8 marker on T-cells in COVID-19 patients. Blood Cells Mol Dis. 2020 Jul 1;83:102437.

233. Ronit A, Berg RMG, Bay JT, Haugaard AK, Ahlström MG, Burgdorf KS, et al. Compartmental immunophenotyping in COVID-19 ARDS: A case series. J Allergy Clin Immunol. 2021 Jan 1;147(1):81–91.

234. Navarro J, Punzón C, Jiménez JL, Fernández-Cruz E, Pizarro A, Fresno M, et al. Inhibition of Phosphodiesterase Type IV Suppresses Human Immunodeficiency Virus Type 1 Replication and Cytokine Production in Primary T Cells: Involvement of NF-κB and NFAT. J Virol. 1998 Jun;72(6):4712–20.

235. Mata M, Martinez I, Melero JA, Tenor H, Cortijo J. Roflumilast Inhibits Respiratory Syncytial Virus Infection in Human Differentiated Bronchial Epithelial Cells. PLOS ONE. 2013 Jul 23;8(7):e69670.

236. Chemboli R, Kapavarapu R, Deepti K, Prasad KRS, Reddy AG, Kumar AVDN, et al. Pyrrolo[2,3-b]quinoxalines in attenuating cytokine storm in COVID-19: their sonochemical synthesis and in silico / in vitro assessment. J Mol Struct. 2021 Apr 15;1230:129868.

237. Kang S, Yang M, Hong Z, Zhang L, Huang Z, Chen X, et al. Crystal structure of SARS-CoV-2 nucleocapsid protein RNA binding domain reveals potential unique drug targeting sites. Acta Pharm Sin B. 2020 Jul 1;10(7):1228–38.

238. Weiner P, Weiner M, Azgad Y, Zamir D. Inhaled Budesonide Therapy for Patients With Stable COPD. CHEST. 1995 Dec 1;108(6):1568–71.

239. Liu J, Guan X, Tamura T, Ozato K, Ma X. Synergistic Activation of Interleukin-12 p35 Gene Transcription by Interferon Regulatory Factor-1 and Interferon Consensus Sequence-binding Protein*. J Biol Chem. 2004 Dec 31;279(53):55609–17.

240. Zhu C, Rao K, Xiong H, Gagnidze K, Li F, Horvath C, et al. Activation of the Murine Interleukin-12 p40 Promoter by Functional Interactions between NFAT and ICSBP*. J Biol Chem. 2003 Oct 10;278(41):39372–82.

241. Munn DH, Sharma MD, Lee JR, Jhaver KG, Johnson TS, Keskin DB, et al. Potential Regulatory Function of Human Dendritic Cells Expressing Indoleamine 2,3-Dioxygenase. Science. 2002 Sep 13;297(5588):1867–70.

242. Marteau F, Gonzalez NS, Communi D, Goldman M, Boeynaems J-M, Communi D. Thrombospondin-1 and indoleamine 2,3-dioxygenase are major targets of extracellular ATP in human dendritic cells. Blood. 2005 Dec 1;106(12):3860–6.

243. Dai K, Huang L, Chen J, Yang L, Gong Z. Amphiregulin promotes the immunosuppressive activity of intrahepatic CD4+ regulatory T cells to impair CD8+ T-cell immunity against hepatitis B virus infection. Immunology. 2015 Mar;144(3):506–17.

244. Ohm JE, Gabrilovich DI, Sempowski GD, Kisseleva E, Parman KS, Nadaf S, et al. VEGF inhibits T-cell development and may contribute to tumor-induced immune suppression. Blood. 2003 Jun 15;101(12):4878–86.

245. Bles N, Di Pietrantonio L, Boeynaems J-M, Communi D. ATP confers tumorigenic properties to dendritic cells by inducing amphiregulin secretion. Blood. 2010 Oct 28;116(17):3219–26.

246. Bles N, Horckmans M, Lefort A, Libert F, Macours P, Housni HE, et al. Gene Expression Profiling Defines ATP as a Key Regulator of Human Dendritic Cell Functions. J Immunol. 2007 Sep 15;179(6):3550–8.

247. Peng Q, Qiu X, Zhang Z, Zhang S, Zhang Y, Liang Y, et al. PD-L1 on dendritic cells attenuates T cell activation and regulates response to immune checkpoint blockade. Nat Commun. 2020 Sep 24;11(1):4835.

248. Cella M, Döhring C, Samaridis J, Dessing M, Brockhaus M, Lanzavecchia A, et al. A Novel Inhibitory Receptor (ILT3) Expressed on Monocytes, Macrophages, and Dendritic Cells Involved in Antigen Processing. J Exp Med. 1997 May 19;185(10):1743–51.

249. Ito T, Wang Y-H, Duramad O, Hori T, Delespesse GJ, Watanabe N, et al. TSLP-activated dendritic cells induce an inflammatory T helper type 2 cell response through OX40 ligand. J Exp Med. 2005 Nov 7;202(9):1213–23.

250. Planès R, BenMohamed L, Leghmari K, Delobel P, Izopet J, Bahraoui E. HIV-1 Tat Protein Induces PD-L1 (B7-H1) Expression on Dendritic Cells through Tumor Necrosis Factor Alpha- and Toll-Like Receptor 4-Mediated Mechanisms. J Virol. 2014 Jun;88(12):6672–89.

251. Vlad G, Chang C-C, Colovai AI, Vasilescu ER, Cortesini R, Suciu-Foca N. Membrane and Soluble ILT3 Are Critical to the Generation of T Suppressor Cells and Induction of Immunological Tolerance. Int Rev Immunol. 2010 Mar 1;29(2):119–32.

252. Olesch C, Sha W, Angioni C, Sha LK, Açaf E, Patrignani P, et al. MPGES-1-derived PGE2 suppresses CD80 expression on tumor-associated phagocytes to inhibit anti-tumor immune responses in breast cancer. Oncotarget. 2015 Apr 30;6(12):10284–96.

253. Hammad H, Charbonnier A-S, Duez C, Jacquet A, Stewart GA, Tonnel A-B, et al. Th2 polarization by Der p 1–pulsed monocyte-derived dendritic cells is due to the allergic status of the donors. Blood. 2001 Aug 15;98(4):1135–41.

254. Jirapongsananuruk O, Hofer MF, Trumble AE, Norris DA, Leung DY. Enhanced expression of B7.2 (CD86) in patients with atopic dermatitis: a potential role in the modulation of IgE synthesis. J Immunol Baltim Md 1950. 1998 May 1;160(9):4622–7.

255. Kuchroo VK, Prabhu Das M, Brown JA, Ranger AM, Zamvil SS, Sobel RA, et al. B7-1 and B7-2 costimulatory molecules activate differentially the Th1/Th2 developmental pathways: Application to autoimmune disease therapy. Cell. 1995 Mar 10;80(5):707–18.

256. Osterholzer JJ, Ames T, Polak T, Sonstein J, Moore BB, Chensue SW, et al. CCR2 and CCR6, but Not Endothelial Selectins, Mediate the Accumulation of Immature Dendritic Cells within the Lungs of Mice in Response to Particulate Antigen. J Immunol. 2005 Jul 15;175(2):874–83.

257. Lloyd CM, Snelgrove RJ. Type 2 immunity: Expanding our view. Sci Immunol. 2018 Jul 6;3(25):eaat1604.

258. Gagliardi MC, Sallusto F, Marinaro M, Langenkamp A, Lanzavecchia A, Magistris MTD. Cholera toxin induces maturation of human dendritic cells and licences them for Th2 priming. Eur J Immunol. 2000;30(8):2394–403.

259. Gosset P, Bureau F, Angeli V, Pichavant M, Faveeuw C, Tonnel A-B, et al. Prostaglandin D2 Affects the Maturation of Human Monocyte-Derived Dendritic Cells: Consequence on the Polarization of Naive Th Cells. J Immunol. 2003 May 15;170(10):4943–52.

260. Kaliński P, Hilkens CM, Snijders A, Snijdewint FG, Kapsenberg ML. IL-12-deficient dendritic cells, generated in the presence of prostaglandin E2, promote type 2 cytokine production in maturing human naive T helper cells. J Immunol. 1997 Jul 1;159(1):28–35.

261. Sala A la, Ferrari D, Corinti S, Cavani A, Virgilio FD, Girolomoni G. Extracellular ATP Induces a Distorted Maturation of Dendritic Cells and Inhibits Their Capacity to Initiate Th1 Responses. J Immunol. 2001 Feb 1;166(3):1611–7.

262. Salem S, Salem D, Gros P. Role of IRF8 in immune cells functions, protection against infections, and susceptibility to inflammatory diseases. Hum Genet. 2020 Jun;139(6–7):707–21.

263. Yoshida Y, Yoshimi R, Yoshii H, Kim D, Dey A, Xiong H, et al. The transcription factor IRF8 activates integrin-mediated TGF-β signaling and promotes neuroinflammation. Immunity. 2014 Feb 20;40(2):187–98.

264. Baban B, Chandler PR, Sharma MD, Pihkala J, Koni PA, Munn DH, et al. IDO Activates Regulatory T Cells and Blocks Their Conversion into Th17-Like T Cells. J Immunol. 2009 Aug 15;183(4):2475–83.

265. Monticelli LA, Sonnenberg GF, Abt MC, Alenghat T, Ziegler CGK, Doering TA, et al. Innate lymphoid cells promote lung-tissue homeostasis after infection with influenza virus. Nat Immunol. 2011 Nov;12(11):1045–54.

266. Thickett DR, Armstrong L, Millar AB. A Role for Vascular Endothelial Growth Factor in Acute and Resolving Lung Injury. Am J Respir Crit Care Med. 2002 Nov 15;166(10):1332–7.

267. Zhao Y, Xiong Z, Lechner EJ, Klenotic PA, Hamburg BJ, Hulver M, et al. Thrombospondin-1 triggers macrophage IL-10 production and promotes resolution of experimental lung injury. Mucosal Immunol. 2014 Mar;7(2):440–8.

268. Lee CG, Link H, Baluk P, Homer RJ, Chapoval S, Bhandari V, et al. Vascular endothelial growth factor (VEGF) induces remodeling and enhances TH2-mediated sensitization and inflammation in the lung. Nat Med. 2004 Oct;10(10):1095–103.

269. Clark DA, Blois S, Kandil J, Handjiski B, Manuel J, Arck PC. Reduced uterine indoleamine 2,3-dioxygenase versus increased Th1/Th2 cytokine ratios as a basis for occult and clinical pregnancy failure in mice and humans. Am J Reprod Immunol N Y N 1989. 2005 Oct;54(4):203–16.

270. Kanazawa H, Yoshikawa J. Elevated Oxidative Stress and Reciprocal Reduction of Vascular Endothelial Growth Factor Levels With Severity of COPD. CHEST. 2005 Nov 1;128(5):3191–7.

271. Doyen V, Rubio M, Braun D, Nakajima T, Abe J, Saito H, et al. Thrombospondin 1 Is an Autocrine Negative Regulator of Human Dendritic Cell Activation. J Exp Med. 2003 Oct 20;198(8):1277–83.

272. Salvi V, Vermi W, Gianello V, Lonardi S, Gagliostro V, Naldini A, et al. Dendritic cell-derived VEGF-A plays a role in inflammatory angiogenesis of human secondary lymphoid organs and is driven by the coordinated activation of multiple transcription factors. Oncotarget. 2016 May 31;7(26):39256–69.

273. Sunagawa M, Shimada S, Hanashiro K, Nakamura M, Kosugi T. Elevation of intracellular cAMP up-regulated thrombomodulin mRNA in cultured vascular endothelial cells derived from spontaneous type-II diabetes mellitus model rat. Endothel J Endothel Cell Res. 2006 Oct;13(5):325–33.

274. Weiler-Guettler H, Yu K, Soff G, Gudas LJ, Rosenberg RD. Thrombomodulin gene regulation by cAMP and retinoic acid in F9 embryonal carcinoma cells. Proc Natl Acad Sci U S A. 1992 Mar 15;89(6):2155–9.

275. Abeyama K, Stern DM, Ito Y, Kawahara K, Yoshimoto Y, Tanaka M, et al. The N-terminal domain of thrombomodulin sequesters high-mobility group-B1 protein, a novel antiinflammatory mechanism. J Clin Invest. 2005 May 2;115(5):1267–74.

276. Van de Wouwer M, Plaisance S, De Vriese A, Waelkens E, Collen D, Persson J, et al. The lectin-like domain of thrombomodulin interferes with complement activation and protects against arthritis. J Thromb Haemost JTH. 2006 Aug;4(8):1813–24.

277. Takagi T, Taguchi O, Toda M, Ruiz DB, Bernabe PG, D'Alessandro-Gabazza CN, et al. Inhibition of Allergic Bronchial Asthma by Thrombomodulin Is Mediated by Dendritic Cells. Am J Respir Crit Care Med. 2011 Jan 1;183(1):31–42.

278. Kelly A, Fahey R, Fletcher JM, Keogh C, Carroll AG, Siddachari R, et al. CD141+ myeloid dendritic cells are enriched in healthy human liver. J Hepatol. 2014 Jan 1;60(1):135–42.

279. Kerkhoff N, Kordasti S, Seidl T, Van de Loosdrecht AA, Mufti GJ. Expansion of CD141int Dendritic Cells in Myelodysplastic Syndrome (MDS). Blood. 2012 Nov 16;120(21):3856–3856.

280. Leeuwen-Kerkhoff N van, Westers TM, Poddighe PJ, Gruijl TD de, Kordasti S, Loosdrecht AA van de. Thrombomodulin-expressing monocytes are associated with low-risk features in myelodysplastic syndromes and dampen excessive immune activation. Haematologica. 2020 Apr 1;105(4):961–71.

281. Savill J, Dransfield I, Gregory C, Haslett C. A blast from the past: clearance of apoptotic cells regulates immune responses. Nat Rev Immunol. 2002 Dec;2(12):965–75.

282. Toda M, Shao Z, Yamaguchi KD, Takagi T, D'Alessandro-Gabazza CN, Taguchi O, et al. Differential Gene Expression in Thrombomodulin (TM; CD141)+ and TM− Dendritic Cell Subsets. PLoS ONE [Internet]. 2013 Aug 23 [cited 2019 Aug 23];8(8). Available from: https://www.ncbi.nlm.nih.gov/pmc/articles/PMC3751914/

283. Toda M, D'Alessandro-Gabazza CN, Takagi T, Chelakkot-Govindalayathila A-L, Taguchi O, Roeen Z, et al. Thrombomodulin Modulates Dendritic Cells via Both Antagonism of High Mobility Group Protein B1 and an Independent Mechanism. Allergol Int. 2014 Jan 1;63(1):57–66.

284. Undas A, Jankowski M, Kaczmarek P, Sladek K, Brummel-Ziedins K. Thrombin generation in chronic obstructive pulmonary disease: dependence on plasma factor composition. Thromb Res. 2011 Oct;128(4):e24–8.

285. Zhang Y, Li S, Wang G, Han D, Xie X, Wu Y, et al. Changes of HMGB1 and sRAGE during the recovery of COPD exacerbation. J Thorac Dis [Internet]. 2014 Jun [cited 2021 Nov 19];6(6). Available from: https://jtd.amegroups.com/article/view/2508

286. Allen JE, Wynn TA. Evolution of Th2 Immunity: A Rapid Repair Response to Tissue Destructive Pathogens. PLOS Pathog. 2011 May 12;7(5):e1002003.

PARTICIPATION TO CONGRESS

1. "5th International Conference of translational medicine on pathogenesis and therapy of immunomediated diseases". Milan, Italy, 16-18/5/2019. *Poster presentation*

2. International Retreat of PhD students 2019. Camogli, Italy, 5-6/12/2019. *Oral presentation*

3. The SIICA School of Immunology 2020. Online meeting, 14/4 - 4/5/2020. *Auditor*

4. SIICA 2021 – XII National Congress. Online congress, 26-28/5/21. *Poster presentation*

5. Day of Immunology 2021 Virtual Public Lecture - COVID-19 Vaccines. Online meeting, 30/4/2021. *Auditor*

6. VaxInLive2021 – eSymposium. Online symposium, 19/5/2021. *Auditor*

7. 6th European Congress of Immunology. Online congress, 1-4/9/2021. *Poster presentation*

PUBLICATIONS

SARS-CoV-2–associated ssRNAs activate inflammation and immunity via TLR7/8

Valentina Salvi, Hoang Oanh Nguyen, Francesca Sozio, Tiziana Schioppa, Carolina Gaudenzi, Mattia Laffranchi, Patrizia Scapini, Mauro Passari, Ilaria Barbazza, Laura Tiberio, Nicola Tamassia, Cecilia Garlanda, Annalisa Del Prete, Marco A. Cassatella, Alberto Mantovani, Silvano Sozzani, and Daniela Bosisio.

The journal of Clinical Investigation insight. Impact factor: 8.315

2021 Sep 22;6(18):e150542. DOI: 10.1172/jci.insight.150542.

ACKNOWLEDGMENTS

First and foremost, I am extremely grateful to my supervisor, Prof. Daniela Bosisio for her invaluable advice, continuous support, and patience during my PhD study. I would also like to thank Dr. Valentina Salvi and Dr. Laura Tiberio for their great advice and technical support on my study. Their immense knowledge and plentiful experience have encouraged me in all the time of my academic research and daily life.

I would like to thank all the members in the Lab of Immunology, especially my thanks to Ms. Carolina Gaudenzi. It is their kind help and attentive support that have made my study and life in Italy wonderful time.

Finally, I would like to express my gratitude to my parents. Without their understanding and encouragement, it would be impossible for me to complete my study.